
**ARIZONA DEPARTMENT OF WATER RESOURCES
3550 North Central Avenue, Second Floor
PHOENIX, ARIZONA 85012-2105
(602) 771-8500**

DRAFT TECHNICAL MEMORANDUM

TO: FILE

FROM : KEITH NELSON

SUBJECT: DRAFT TECHNICAL MEMO AND APPENDICES DESCRIBING NEW
ADWR NATURAL RECHARGE ANALYSIS FOR PRESCOTT AMA AND
PRESCOTT AMA GROUNDWATER FLOW MODEL

DATE: DECEMBER 18, 2012

EXECUTIVE SUMMARY

The Arizona Department of Water Resources (ADWR) developed a groundwater flow model of the Prescott Active Management Area (PrAMA) in 1995. The model domain covers portions of the Upper Agua Fria (UAF) and Little Chino (LIC) sub-basins, and simulates groundwater flow conditions in the Upper Alluvial Unit (UAU) and the Lower Volcanic Unit (LVU) aquifers. The model has been used to gain a better understanding of the hydrologic system and to explore alternative water management strategies. The model was updated in 2002, 2006 and is currently being modified to represent the latest available hydrologic information. Some of the more significant modifications include 1.) the expansion of the aquitard between the UAU and LVU aquifers, and 2.) the redistribution of natural recharge such that, with respect to previous model versions, higher rates of long-term episodic natural recharge are simulated along major stream channels including Granite and Lynx Creeks, while comparatively lower rates of long-term natural recharge are simulated along peripheral mountain front recharge (MFR) areas. The importance of fluctuations in natural groundwater recharge over time are amplified in this update because observation data indicate that a larger percentage of overall natural recharge originates from episodic streamflow recharge events along major surface water tributaries including Granite and Lynx Creeks. In particular, relatively high rates of natural seasonal recharge were simulated between the mid-1970's and the mid-1990's, while comparatively low rates of natural recharge were simulated from the early 1940's to the mid-1960's, and again from the mid-1990's through mid-2012.

Independent of the model calibration, stream recharge was analyzed to support the higher rates of simulated natural recharge. Furthermore, aquifer test data was analyzed for comparison to estimated values. Where applicable, leaky aquifer test solutions were compared with confined solutions. Non-linear regression was used to help calibrate horizontal and vertical hydraulic conductivity, natural recharge and underflow at model boundaries.

Applying non-linear regression techniques also enabled the efficient evaluation of alternative conceptual models (ACMs). The following ACMs were tested and included in ADWR's evaluation:

- (1) different initialization conditions;
- (2) assignment of varying ratios of peripheral mountain front recharge (MFR)-to-stream/flood recharge along major tributaries;
- (3) different prior-information weighting assignments in the non-linear regression for a few key Lower Volcanic Unit (LVU) aquifer zones;
- (4) different plausible weighting criteria associated with head and flow targets associated with inverse models;
- (5) assigning underflow as an independent variable in steady and transient inverse models; and
- (6) exploration of other plausible estimates of historical pumping and incidental agricultural-related recharge.

Based on available data and estimated by non-linear regression for steady and transient conditions, the lowest model bias and error consistently tended towards toward a common solution, as documented in this Technical Memorandum. Results of selected ACM's and associated inversion statistics are presented in the Appendix B. Important byproducts of non-linear regression include statistical information about the reliability of each estimated parameter. ADWR's presentation of the testing and disclosure of various ACM's, combined with the presentation of inversion statistics, is designed to provide transparency to its model calibration. While it is impossible to develop a perfect groundwater flow model, model solutions with the lowest error tended toward similar parameters, thus narrowing the range of plausible viable groundwater flow models.

Introduction and Background, Prescott AMA Groundwater Flow Model

The Arizona Department of Water Resources (ADWR) developed the Prescott AMA Groundwater Flow Model in 1995 (Corkhill and Mason, 1995). The model simulates groundwater flow conditions in the Little Chino (LIC) and Upper Agua Fria (UAF) sub-basins within the Prescott Active Management Area (AMA) and consists of two layers including a heterogeneous upper alluvial unit (UAU) aquifer (layer 1) and a lower volcanic unit (LVU) aquifer, surrounded by less transmissive materials (layer 2). The first model update (Nelson, 2002) added a confined LVU aquifer zone in the northern UAF sub-basin and modified natural recharge to include episodic recharge along Lynx Creek and the Agua Fria River. The model was updated further in 2006 to incorporate hydrogeologic information from exploratory test wells, and extend the model domain to include portions of Williamson Valley and Mint Wash, an area experiencing significant groundwater level declines (Timmons and Springer, 2006). Over the years, the Prescott Model has been used evaluate different water management strategies, including predictive groundwater levels, predictive groundwater discharge to stream channels and different components of the water budget.

Model Development

Model development consisted of testing alternative conceptual models and calibrating associated parameters with observed data. The initialization period for steady state flow was 1939. The steady state solution was constrained to head (measured water levels) and flow data collected from the late 1930's to early 1940's. The transient simulation period covers 72 years from 1939 to 2011. Fundamental parameters including horizontal and vertical hydraulic conductivity and distributions, K_x and K_y , and K_z , respectively (collectively referred to as "K") and natural recharge and natural underflow in the LIC and UAF sub-basins were estimated using inverse modeling techniques. Inverse models calculate model parameter values that minimize a weighted least-squares objective function using non-linear regression (Hill, 1998). A key feature - and byproduct - of inverse modeling is the calculation of model parameter statistics, providing information about the sensitivity and reliability of the model parameters. Inversing modeling was used better understand model parameters over steady and transient state conditions.

Because all natural recharge (stream recharge as well as MFR) effectively occurs along losing reaches, it is assumed that the natural steady recharge rate is consistent with the long-term natural recharge rate estimated between 1939 and 2011. Accordingly, ADWR employed non-linear regression to independently derive estimates of (1) steady state and (2) long-term transient (1939-2011) natural recharge at annualized rates between 9,000 to 10,000 AF/yr. Lowest residual model errors (observed minus simulated heads and flows) result when the majority of natural recharge is applied along major tributaries, including Granite Creek, Lynx Creek and along tributaries in the Bradshaw Mountain Foothills. However, data indicates significant variations in recharge occurring over time. For example, relatively low rates of annualized natural recharge occurred during the dry periods between mid-1941 and mid-1965 and again between mid-1995 and mid-2012 (time of this writing). Conversely, relatively high rates of annualized natural recharge occurred during the wetter period experienced between 1978 and mid-1995. Again, based on available data constraining the inverse model, the lowest residual model errors occurred when natural recharge was applied during significant streamflow events, and omitted during "dry" periods.

Previous model versions simulated vertical gradients in the vicinity of the Town of Chino Valley (Corkhill and Mason, 1995) and further south in the UAF sub-basin near the Town of Prescott Valley (Nelson, 2002). Disparate groundwater levels measured in neighboring wells screened across different aquifer intervals indicate that the aquitard separating the UAU and LVU is more extensive than previously thought. Inspection of available groundwater data collected adjacent to Granite Creek indicates that vertical flow of water originating as stream recharge is impeded by fine-grain materials (aquitard). Well hydrographs illustrate observed and simulated groundwater levels in neighboring wells adjacent to northern Granite Creek, (B-16-01)20cdb and (B-16-01) 20cac and middle Granite Creek, (B-15-01)19dcd1 and (B-15-01)19dcd2 (See

Appendix A) . Well data shows that the UAU aquifer has a direct response to Granite Creek recharge as compared to the attenuated response of the LVU aquifer. Recent water levels in LAU completed wells are on the order of 200 feet lower than UAU heads.

All K zones, long-term natural steady recharge, and LIC and UAF underflow rates were calibrated by non-linear regression (inverse model). Due to insensitivity, some parameters such as K_y , K_z and peripheral recharge were either tied or fixed at ratios to master parameters. However, all spatial K zones and natural recharge (tied to one master zone), as well as two underflow zones, were included in the regression in order to minimize model bias. That is, all fundamental hydraulic model parameters (K , S natural recharge and natural underflow) whether tied to a master parameter or independent, were included in the non-linear regression in order to calculate sensitivities and thus obtain information about the reliability of model parameters. If a parameter was not included as a variable in the regression, the exclusion may affect (or bias) parameters that are being estimated, which in turn, may impact sensitivity calculations and resultant model statistics (“posterior” statistics). The idea is that if a model parameter is fixed in the regression, yet others remain adjustable, the fixed parameter will influence or bias the adjustable variables as the inverse model attempts to minimize the objective function to available target data.

Many different ACM’s were tested, including alternative K and recharge zonation schemes, different boundary condition assumptions, and different initialization assumptions. Some of the alternative initializations tested include: (1) pre-development steady conditions, posed by Corkhill and Mason (1995); (2) post-development steady as described by Nelson (2002) and Timmons and Springer (2006); (3) assumptions employed by the recent USGS NARGFM (Pool et al, 2011); as well as (4) different variations of the above-described conditions.

Model-assigned weights are inversely proportional to the standard deviation of the target (WinPEST, 2003). The assigned weight reflects the reliability of the target. Thus, the difference between a model simulated head and a target head (i.e., residual error in units of feet) is multiplied by the assigned head weight (inverse of model unit elevation) to yield a unitless value for each target. Likewise, the difference between the model simulated flow and the target flow (residual error in units cubic-feet-per-day (CFD) is multiplied by the assigned flow weight (inverse of model-unit flow) to yield a unitless value. The unitless components, representing head, flow and prior information errors are then squared and summated to yield the objective function, Φ ; hence Φ , is the sum of weighted square residuals and is an important measure model error and bias. For the steady flow solution, the standard deviation for Layer 1 heads (61 targets) and Layer 2 heads (43 targets) were assigned at 20 feet and 10 feet, respectively. Only Layer 1 heads assumed to be in long-term dynamic equilibrium (i.e., not adversely impacted by groundwater development) were assigned as Layer 1 targets. Nonetheless, Layer 1 head targets were given a lower reliability weight than the readily available pre-development or early-post development LVU heads. For transient conditions, the standard deviation for Layer 1 and Layer 2 heads was 20 feet; thus the assigned weight associated with each transient head target was 0.05 ft⁻¹. For more information about model weighting, see Appendix E.

Groundwater discharge targets for steady mean flow and associated standard deviation were assigned at 6 cfs and 0.5 cfs, respectively, for Del Rio Springs; and 4 cfs and 1 cfs, respectively, for Agua Fria baseflow. Available steady flow data from the early 1940’s recorded at Del Rio Springs (Schwalen, 1967) provide confidence for the calibration-target weighting; thus the coefficient-of-variation (σ/μ) associated with the flow during steady state conditions at Del Rio Springs is a low 0.0833. For the Agua Fria River, the assigned steady groundwater discharge target rate and variance (i.e., weight) was based on baseflow-separated measurements taken after 1939, combined with the understanding that groundwater discharge along the river is subject to long-term dynamic equilibrium conditions. That is, available head and flow data adjacent to the Agua Fria River (valley) in the Dewey-Humboldt area show seasonal and multi-year fluctuations based on pumping and recharge patterns. However observed water levels and baseflow have not shown significant long-term (decadal) decreases or increases, and tend to fluctuate about mean values. See Figures C.5, C19-22. Thus, the coefficient-of-variation (σ/μ) associated with the Agua Fria River flow target is 0.25, and is subject to greater uncertainty. For transient flow, weighting was based on an assumed standard deviation of 1 cfs for

both Del Rio Springs and Agua Fria baseflow. For most ACM's, including the Base model, prior information was assigned to three LVU K aquifer zones to moderate estimated K values. Without prior information assigned in the non-linear regression, estimates of K tended to be significantly larger than previous model versions; see Corkhill and Mason (1995); Nelson (2002); Timmons and Springer (2006). With respect to previous model versions, lower model error is simulated when higher values of LVU K (K23 and K25) are assigned; thus *available data* suggests that previous model versions were under-estimating the transmissivity in layer two in the central LIC Sub-basin. Prior information weighting for most ACM's was based on: 1) available aquifer test data; 2) past model calibrated values; and 3) inspection of the standard error of weighted residuals. All estimated K zones were log-transformed in the non-linear regression. For additional information on parameter weighting see Table 1, below, Appendix E, WinPEST (2003), and Hill (1998).

TABLE 1.

A-Priori K Zone	Target K (ft/d)	Approximate a-priori, 95 % CI (ft/d)*
LVU Zone 23 (North LIC)	166	75 – 370
LVU Zone 25 (Central LIC)	100	25 – 390
LVU Zone 26 (Northwest UAF)	100	45 – 215

*Log-normal distribution based on available aquifer test data and previous model-calibrated values. These statistics were used as criteria to assign prior information weights. Note that without the assignment of prior information “anchoring” the LVU K’s, inverse model estimates of the LVU K’s were higher and more uncertain than the posterior estimates provided below. No other K zones employed prior information in the regression.

For transient conditions, all time-dependant stresses were either assigned previously-estimated or recorded values, or were manually calibrated to observed target data. Transient-based PEST solutions were also evaluated to gain a better understanding of individual parameter sensitivity, including natural recharge. The storage parameter distribution was simplified in this update as follows: Sy for Layers 1 and 2 was assigned a uniform value of 0.09 with the exception of a coarse gravel UAU zone along upper and middle Lynx Creek, which gravity-water level relations infer are about on the order of 0.16. The Ss was uniformly assigned a value of 1E-5 ft⁻¹. Compared to the K and recharge distributions, storage is a relatively insensitive parameter.

The extension of the aquitard (Kz3) separating the UAU and LVU necessitated an updated natural recharge distribution. The steady state (post-development steady ACM3) natural recharge rate was consistent with the long-term calibrated transient recharge; in other words, along *losing reaches* steady state (post-development steady) recharge is approximately equal to long-term transient recharge rates.

Other model updates include: (1) adding transient evapotranspiration (ET) near Del Rio Springs and the Agua Fria River; (2) assigning simulated pumpage-per-layer based on estimated or recorded screened-interval and estimated layer transmissivity -- resulting in a modification of the original Q2:Q1 ratio of 3:1 to 3.6:1; that is with respect to previous model versions, slightly higher rates of simulated pumpage was assigned to model layer 2 and slightly less were assigned to Layer 1. (3) generally deepening the LVU bottom by 100 feet in order to reduce the likelihood of encountering dry cells during long-term, predictive simulations; and (4) adding an underflow component to the UAF sub-basin. As with LIC underflow, less model bias results when underflow is simulated from the UAF sub-basin because the flux facilitates baseflow variation with more accuracy than the previously-assigned no-flow boundary. Although the southern model boundary was extended to the west with respect to the previous model boundaries, the exact hydraulic/physical mechanism responsible for the UAF underflow remains unclear at the time of this writing (See Appendix F).

Model results show that significant recharge enters the groundwater flow system along major streams including Granite and Lynx Creeks, the Agua Fria River and along the Bradshaw Mountain foothills. During periods of significant streamflow high rates of recharge occur (i.e., 1993; 2004-05), while over extended dry periods

(1941-1965; 1995-2004) water tables decline due, in part, to limited streamflow recharge. During the 1939-2009 simulation, over 70% of all natural recharge occurred during only 11% of the total 69-year transient period. For provisional simulated water budget information associated with the “base” model, see Appendix G.

Inverse Model Statistics, Discussion and Conclusion

The steady state inverse model solutions resulting in low model error and bias consequently led to transient solutions with low model error and bias for most tested ACMs. All K zones were log-transformed in the regression. Consequently, the posterior statistics including the 95% CIs shown in the appendices are based on log-normal K distributions. Normal distributions are assumed for estimated underflow and recharge. An excerpt from the PEST record file is shown in Appendix E. All $K_x=K_y$. All K_z 's were tied to K_{z3} except for the following tied ratios of $K_{x26}:K_{z26}=1E7:1$; $K_{x25}:K_{z25}=100:1$; $K_{x2}:K_{z2}=2.5:1$; and K_{z13} and K_{z14} , $K_x:K_z=10:1$. See WinPEST (2003) for linearity assumptions associated with 95% CIs. See Appendix E for more detailed information on weighting.

Figures 1 and 2 below show the model cross section along Row 7, near Road 4 North in the LIC Sub-basin within the Town of Chino Valley. Figure ## represents simulated 1940 flow conditions, shows downward hydraulic gradients below Granite Creek (east) and the transition to upward gradients below Chino Valley (middle). Figure ## represents simulated early 2009 flow conditions, showing the impact of nearly seven decades of groundwater pumping and the subsequent reversal of hydraulic gradient and flow direction under the LIC Sub-basin after an approximate 100 feet decline in pressure head.

Much about the collective state of the PrAMA hydrologic system can be summarized by evaluating groundwater discharge patterns at Del Rio Springs and baseflow along the Agua Fria River. Groundwater discharge at Del Rio Springs reflects composite stresses (pumping and natural and artificial recharge) imposed to the UAU and LVU aquifers in the LIC sub-basin over long periods of time. Note how the groundwater discharge decline rate at Del Rio Springs mirrors the LVU pressure head decline in the LIC sub-basin. See figure C.4.

Because of streamflow capture, induced stream recharge and bank storage, groundwater discharge signals along the lower Agua Fria River are believed to represent long-term dynamic equilibrium conditions, where the magnitude of the time-varying baseflow (groundwater discharge) reflects the influences of seasonal pumpage, artificial recharge, ET and episodic stream recharge. Along the Agua Fria River baseflow reach, relatively high rates of groundwater discharge are directly observed following major stream recharge events. Note how the baseflow trends for the convergent stream-aquifer system along the Agua Fria River differ from the regional-scale decline rates observed at Del Rio Springs, where impacts from stresses are much more indirect (see Appendix C, Figures C.3 and C.4).

FIGURE 1. Cross-section of Simulated Groundwater Flow Directions in Chino Valley, Arizona *SEE FIGURE 3 for location*

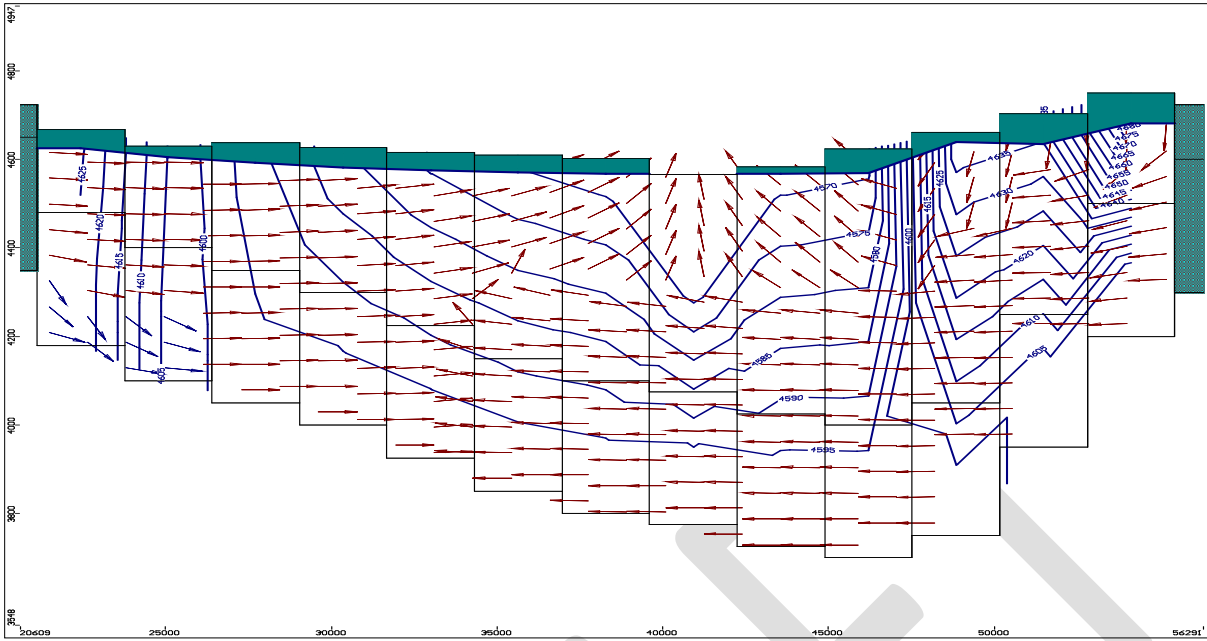


FIGURE 2. Groundwater Flow Directions in Chino Valley 2009; *SEE FIGURE 3 for location*

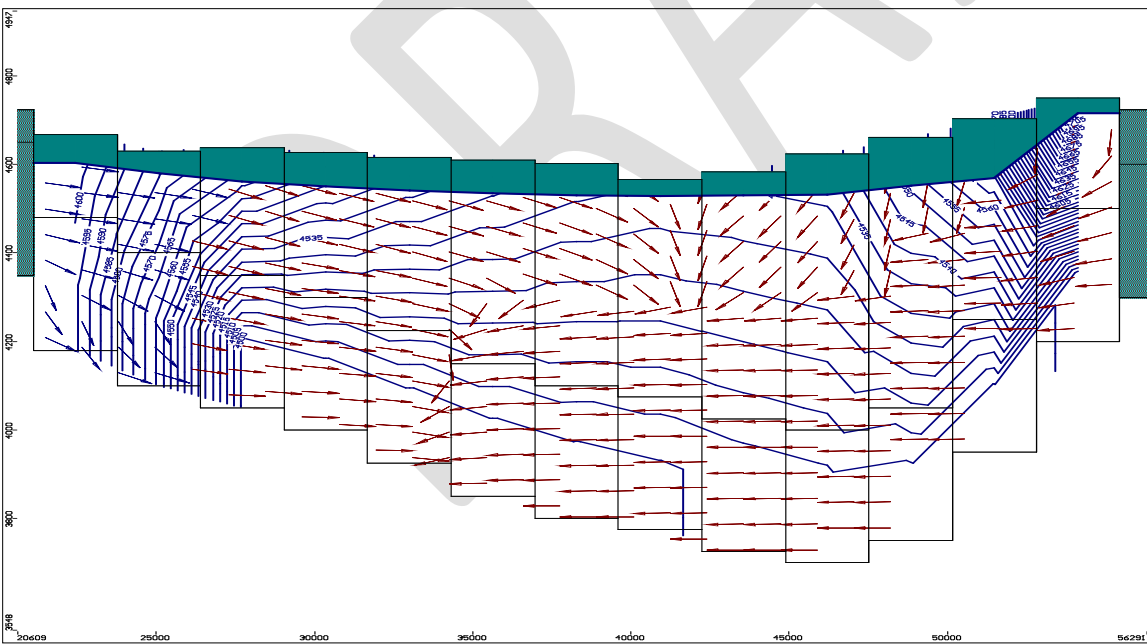
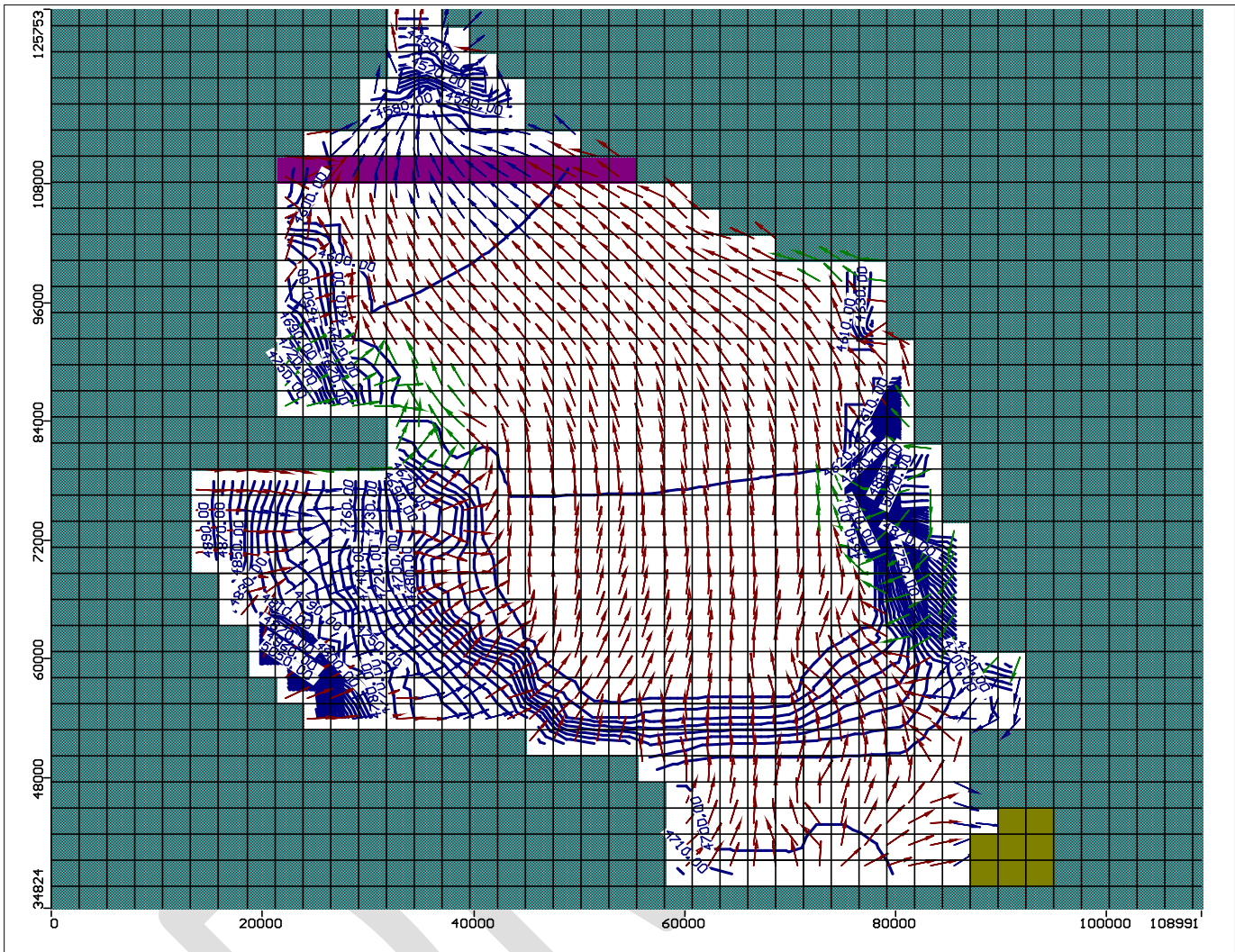


FIGURE 3. Cross-section (purple) showing simulated flow in Model Layer 2, Row 7 in 1940



ADWR is updating the Prescott AMA groundwater flow model with the latest available hydrologic information and employing emerging modeling methodologies. Non-linear regression was used to calibrate all horizontal and vertical hydraulic conductivity zones, steady (long-term) state recharge and steady underflow from the LIC and UAF sub-basins. The regression includes statistical information about the reliability of estimated model parameters, providing an additional layer of transparency to the calibration. Significant modifications to the model include the expansion of the aquitard between the UAU and LVU aquifers and the spatial and temporal redistribution of natural recharge such that, with respect to previous model versions, higher rates of episodic recharge are simulated along major stream channels including Granite and Lynx Creeks, while comparatively lower rates of recharge are simulated along peripheral MFR areas. Both observation data and ADWR's model results suggest that special consideration may be required for simulating natural recharge when using the model to evaluate water management planning scenarios.

Relation between Streamflow Magnitude and Stream Recharge

This section discusses the physical processes that can result in groundwater recharge in the Prescott AMA. Although most precipitation falling as either rain or snow ultimately evaporates, some water can percolate down to the water table and result in groundwater recharge. In areas where the unsaturated zone is thick, or in areas where there is significant hydraulic resistance to vertical flow, natural recharge rates from ground cover moisture is relatively low. Precluding stream channels, most precipitation that falls in valley areas (i.e., Chino Valley) results in very low rates of natural groundwater recharge. However along losing, ephemeral stream channels where water (runoff from direct precipitation events; snowmelt, etc.) is concentrated for weeks or months, significant recharge can occur due to stage-driven infiltration. Observation data, as well as, recent provisional modeling in the Prescott AMA, indicate that most natural recharge occurs along losing reaches of major stream channels and tributaries such as Granite Creek, Lynx Creek and Agua Fria River; thus most natural recharge occurs during and following periods of significant precipitation. Data shows that in the Prescott AMA, the winter and early spring period has consistently had the highest rates of natural recharge. In some cases, rain-on-snow events can result in significant streamflow and subsequent stream-driven recharge. See Figures A1 through A.4.

Groundwater recharge is driven by streamflow magnitude, frequency and streamflow duration. When streamflow rates are high over extended periods (seasonal), the flowing water can infiltrate the stream bed and, if storage space is available, replenish the underlying aquifer. Conversely, during extended “dry” periods near stream groundwater levels are subject to decline in the absence of stream recharge.

The USGS streamflow gauge on the Agua Fria River near Mayer (USGS 09512500) is located roughly 12 miles southeast of the southern Prescott AMA boundary. Approximately 30% of its contributing watershed is within the Prescott AMA. The balance of its watershed is subject to similar forcing patterns as the UAF sub-basin of the PrAMA. USGS 09512500 has the longest continuous record in streamflow in general vicinity and includes invaluable records dating back to 1940. ADWR assumed that the streamflow patterns recorded at USGS 09512500 between 1940 and mid-2012 provide a reasonable surrogate for recharge potential and variability over time. Figures ## and ##, below, chart (1) annualized streamflow rates and (2) the five-year moving-average annualized streamflow rates at the Agua Fria River near Mayer and demonstrate streamflow trends over time. These data include a period of relatively low streamflow from the early 1940’s to mid-1960’s and again from the mid-1990’s to 2011; and a period of relatively high stream flow from the mid-1970’s to the mid-1990’s. Similar regional trends were observed in other regions of the State including near Tucson, where groundwater recharge between 1977 and 1998 was three times higher than recharge between 1941–1957 period (Stonestron, et al, 2007).

Both observed head and streamflow data, as well as groundwater flow modeling, demonstrate the large temporal fluctuations in natural recharge, driven by prevailing weather conditions weather conditions and storage potential in the near stream aquifer system. Integrating groundwater level and streamflow data, ADWR’s recent modeling efforts indicates that approximately half of all long-term (1939-2011) natural recharge occurred during the relatively “wet” period between 1973 and 1995.

The steady state and long-term transient state natural recharge rates are reasonably consistent, suggesting that the model is congruent with respect to the treatment of natural recharge and the conditioning of model parameters. That is, the initializing steady state recharge rate and the long-term transient recharge rate (minus induced recharge – see below) were consistent and resulted in a balanced model calibration. Long-term simulated natural recharge (in transient model) is slightly higher than the steady state recharge rate. ADWR attributes this difference to induced recharge, which occurs along losing reaches where water tables are shallow and groundwater pumping “creates” storage space for subsequent (induced) stream recharge.

By example, the “Base” model (i.e., the primary conceptual model used for presenting model results herein), resulted in a steady state natural recharge of 9,170 AF/yr, while the long-term transient recharge rate for the

same base model resulted in a long-term rate of 9,920 AF/yr. Because most natural recharge occurs along predominately losing reaches, the steady state and transient natural recharge rates are similar. Along extended stream reaches where water tables are shallow, southwest streams typically transition between gaining, losing and hydrostatic conditions (hydrostatic conditions occur when water table elevations are equal to stream stage elevations, resulting in no flow to-or-from the stream and aquifer. Under these conditions, the “long-term” transient natural recharge rate is subject to near stream aquifer head elevations changes over time (flood stage recharge; capture and induced recharge). Thus “steady” flow for the aforementioned conditions (typically inner valley areas), would only be a temporary, conditional (seasonal) state. As such, this steady condition is generally not applicable - or assumed - for the Prescott model area.

FIGURE 4. Average Annualized Streamflow Agua Fria near Mayer

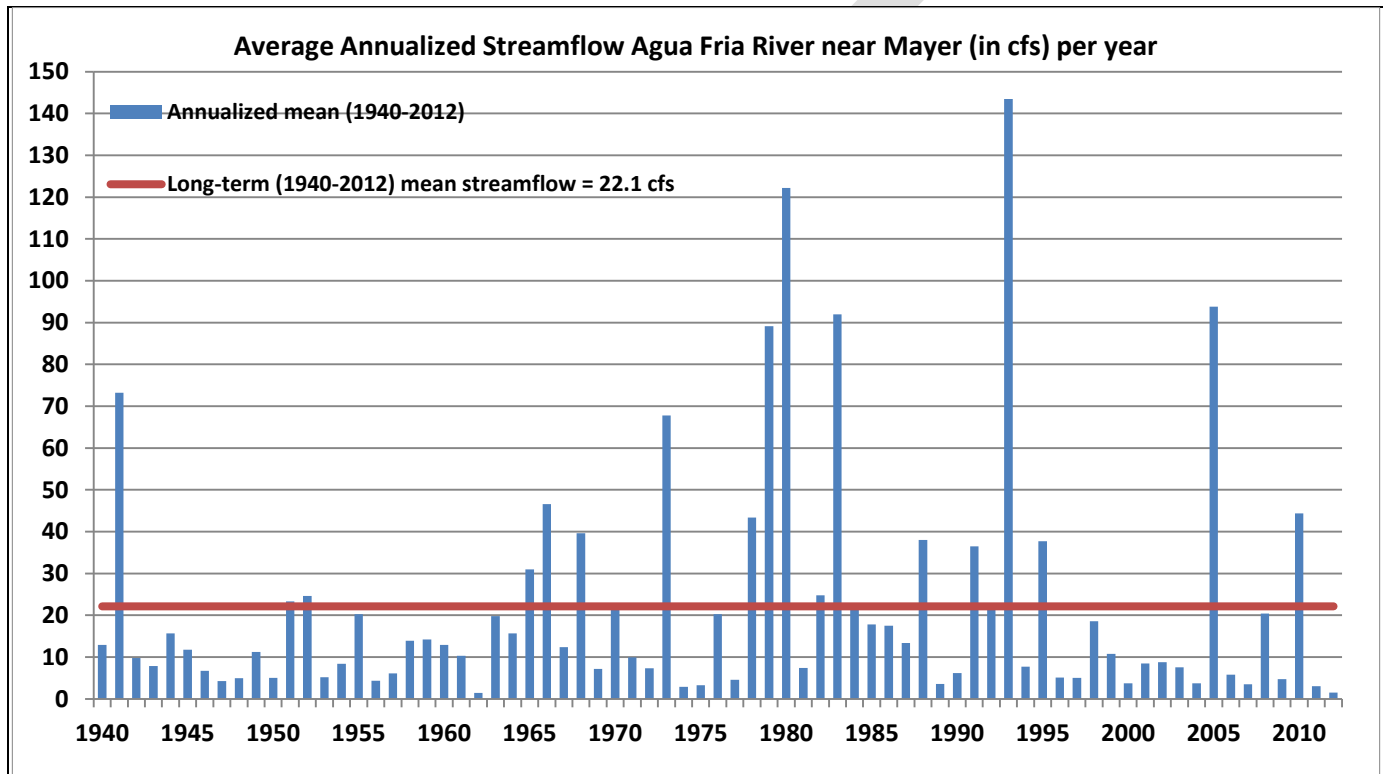


FIGURE 5. 5-year Moving Annualized Average Streamflow Agua Fria River near Mayer

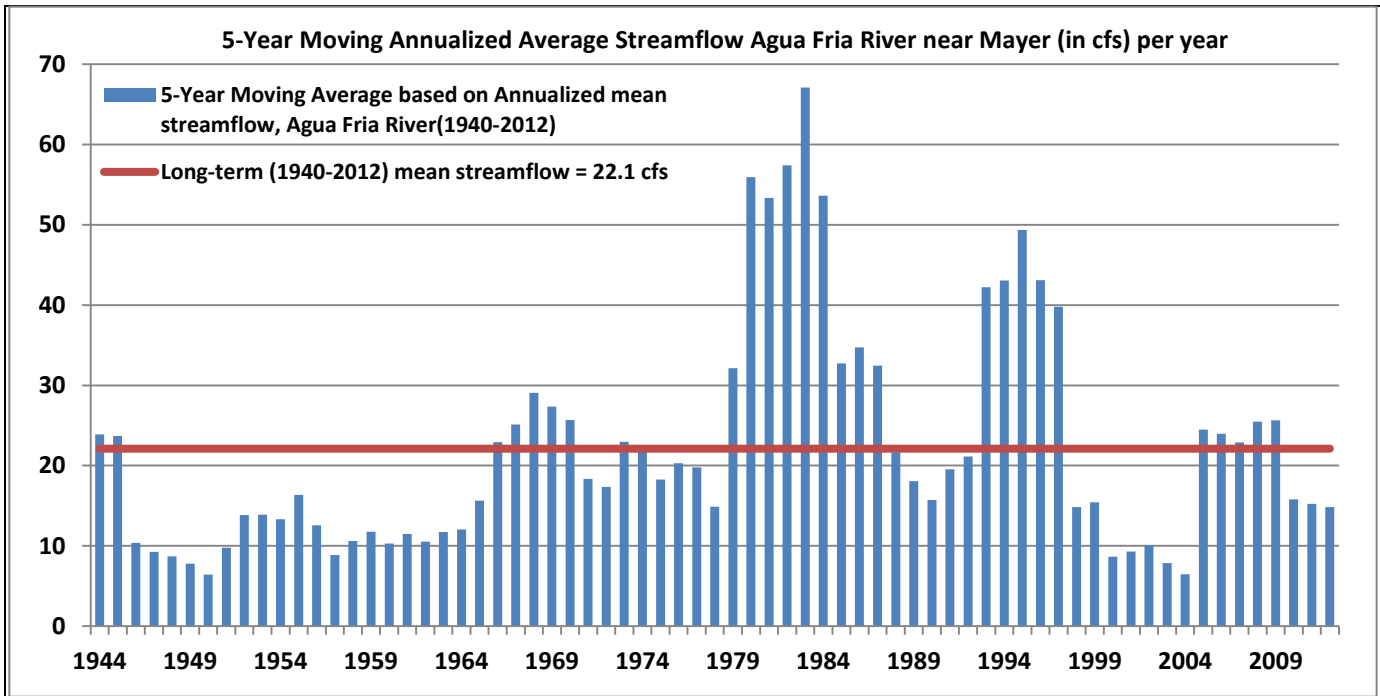
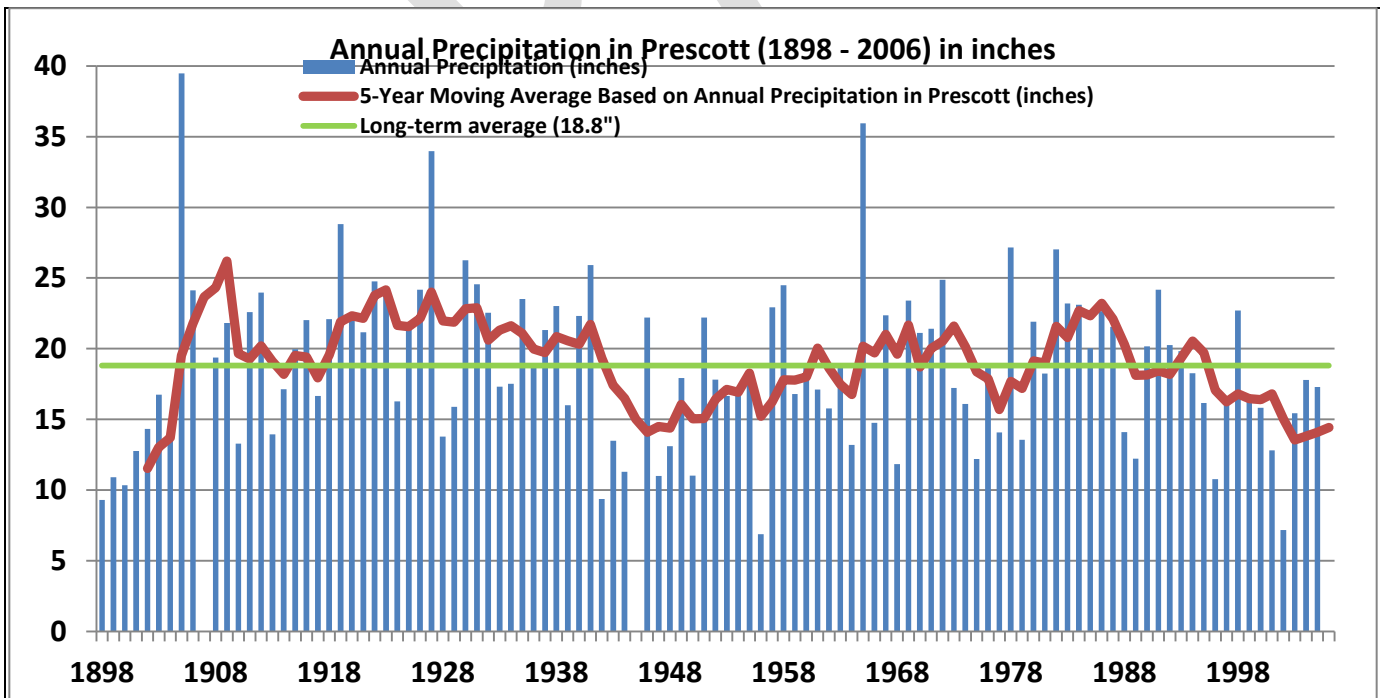


FIGURE 6. Annual Precipitation in Prescott (1898-2006)



Estimation of Streamflow for the Granite Creek and Upper Agua Fria Contributing Areas

ADWR estimated streamflow for the Granite Creek (LIC Sub-basin) and Upper Agua Fria (UAF) Sub-basin contributing areas during periods of relatively high flow and used these estimates as a basis for evaluating streamflow *recharge* potential along portions of Granite Creek, Lynx Creek and the Agua Fria River. Streamflow estimates for contributing areas were then compared to simulated stream recharge. In this context the contributing area streamflow would represent the rate defined at the downstream boundary, with runoff contributions originating from upstream areas. For example the Granite Creek contributing area (229 miles²) includes: Upper Granite Creek (45 miles²), Willow Creek (25 miles²), Lower Granite Creek (61 miles²), and Lonesome Valley (98 miles²) contributing areas,

Streamflow estimates for the Granite Creek and Upper Agua Fria contributing areas are based solely on scaling properties as described below. Where relevant, all baseflow components were removed prior to scaling. It is understood that, within semi-arid and arid regions there may be other factors impacting streamflow estimates besides scale, such as precipitation patterns (orographic; elevation, urbanization; impounds; diversions, etc.), topography, soil type, etc. (Vogel and Sankarasubramanian, 2000). However, establishing multiple regression (MR) equations have additional complicating assumptions and the development of MR relations were beyond the scope of this modeling effort. In general, years having higher annualized rates of streamflow had higher coefficient-of-determination (R^2) values, and were thus deemed more reliable. *Years having modest rates of annualized flood flow streamflow (i.e., 1998, 2008) had poor regression fits and results, for those years, should be used with caution.* Dry years having low annualized rates of streamflow (above baseflow) were assigned natural recharge rates of zero along the main stems of the GC and UAF contributing areas.

Granite Creek contributing area (228.5 miles²)

For the Granite Creek contributing area (229 miles²), six streamflow gauges were used in the scaling process, based on log-linear relations discussed in Vogel et al., (2000). For more information about the GC sub-contributing areas, see Table 1, below. The six gauges have contributing areas inclusive to - and above - the Verde River near Clarkdale watershed. These include, from smallest contributing area to largest: Granite Creek at Prescott, AZ (09502960), Granite Creek near Prescott, AZ (09503000), Granite Creek below Watson Lake, AZ (09503300), Williamson Valley Wash near Pauldin, AZ (09502800), Verde River near Pauldin, AZ (09503700) and Verde River near Clarkdale, AZ (09504000). All baseflow components were removed as determined by the USGS (see Blasch et al, 2005) prior to scaling, such that only high-flow events having flood recharge and/or bank storage potential were included in the scaling process. For example, the annualized streamflow rate for the 1995 “water year” (October 1, 1994 to September 30, 1995) at the Verde Pauldin gauge (USGS 09502800) was 55.6 cfs. However, for *high-flow* scaling purposes, the period-of-record baseflow component of 24.4 cfs - determined by Blach at al. (2005) - was removed to yield an assumed “high” streamflow rate of 31.2 cfs (55.6 cfs minus 24.4 cfs) for that year. Thus, the “high” flow stream rate of 31.2 was used in the analysis.

TABLE 2.

Gauge	Contributing Area miles ²	Period-of-Record
Granite Creek at Prescott	30	1996-2011
Granite Creek near Prescott	36.3	1932-1947; 1995-2011
Granite Creek below Watson Lake*	47.2	1999 (1 month); 2000-2011
Williamson Valley Wash near Pauldin	255	1965-1985; 2001-2011
Verde River near Pauldin	2150	1963-2011
Verde River near Clarkdale	3124	1915-1921; 1965-2011
*Measured discharge on Granite Creek below Watson Lake is problematic to use for regression purposes since it measures flow immediately downstream of a reservoir capable of impounding flows. That said, including flows from this gauge in the regression may act to “down-weight” scaled flows; thus inclusion of this site - for regression purposes - is assumed to yield more conservative scaled rates for years where the gage was included/active (i.e., 2000-2011).		

It is important to note that the common-year (1965-85; 2001-2011) average annualized streamflow rate at Williamson Valley Wash (baseflow removed) and Verde Pauldin (baseflow removed) was 13.5 cfs and 19.3 cfs, respectively. However the contributing area for the Williamson Valley Wash site is 255 miles², while the contributing area associated with the Verde Pauldin site is 2,150 miles². Thus, with respect to Verde Pauldin gauge, Williamson Valley Wash yields 70% of the streamflow from only 12% of the contributing area. The proportional differences between averaged annualized streamflow and contributing area suggests that significant flood recharge occurs upstream of the Verde Pauldin gauge along major tributaries. However, paucity of streamflow data along individual tributaries such as Williamson Valley Wash (downstream from USGS 09502800), Granite Creek (downstream from USGS 09503300), Big Chino Wash, Walnut Creek etc., preclude identifying the spatial recharge distribution above the Verde Pauldin site along these reaches.

To better understand the distribution of streamflow (baseflow removed) and recharge potential along major streams and tributaries in north-central Arizona, the ratio of streamflow-to-contributing area for ten different locations, having common - or similar - periods-of-record were evaluated.

TABLE 3.

Stream Gauge Name/Location	USGS Ref	Contributing Area (in miles ²)	¹ Flow (in cfs)	Ratio of Streamflow-to-Contributing Area
Dry Beaver Creek	09505350 ¹	142	46.8	0.330
West Clear Creek	09505800 ^{1,2}	241	46.5	0.193
Williamson Valley	09502800 ^{1,5}	255	13.2	0.052
Oak Creek Cornville	09504500 ^{1,2}	355	55.1	0.155
Agua Fria Mayer	09512500 ^{1,5}	585	26.6	0.045
Agua Fria Rock Springs	09512800 ³	1111	82.0	0.074
Santa Maria River	09424900 ^{4,7}	1129	54.6	0.048
Verde Pauldin	09503700^{1,2}	2150	19.7	0.00918
Big Sandy River	09424450 ^{1,6}	2732	93.2	0.0341
Verde Clarkdale	09504000 ^{1,2}	3124	93.3	0.0299
¹ Unless otherwise indicated, common period of record (POR) is 1965-1985; 2001-2011; ² Streamflow with baseflow removed at rate defined by USGS (Blasch et al. 2005). ³ POR 1971-73; 1975-1985; 2001-2011. ⁴ POR 1967-85; 2001-2011; ⁵ Baseflow removed, 1.5cfs. ⁶ Baseflow removed, 3 cfs; ⁷ Baseflow removed, 2 cfs				

Similar ratios between contributing area and streamflow (defined as “runoff” in Tables 6 and 7 in Blasch et al, 2006) were computed for different reaches of the Verde and major tributaries for their complete respectively POR. Note that the POR, for the different stream data listed in Blasch et al (2006), are not common. Data generally shows higher streamflow-to-contributing area ratios among smaller watersheds. However, the Verde Pauldin site has a disproportionately small streamflow-to-contributing area ratio compared to all the other sites. Although there are many factors which influence transmission losses along stream channels, available data suggests that, over long-term periods, relatively high rates of recharge occur along major stream channels upstream of the Verde Pauldin site that would otherwise contribute runoff to the Verde Pauldin site.

UAF Sub-basin contributing area (175 miles²)

Three stream gauges were used to estimate flow for the Agua Fria Sub-basin. Three gauges have contributing areas inclusive to the Agua Fria River near Rock Springs and include (smallest contributing area to largest): Agua Fria near Humboldt, AZ (09512450), Agua Fria River near Mayer (09512500) and Agua Fria River near Rock Springs (09512800). Where relevant, baseflow was removed prior to scaling, such that only high flow events (with flood recharge and/or bank storage potential) were employed in the scaling process.

TABLE 4.

USGS Streamflow Gauge	Contributing Area (miles ²)	Period-of-Record
Agua Fria River near Humboldt	175	2000-2011
Agua Fria River near Mayer	585	1940-2011
Agua Fria River near Rock Springs	1,111	1970-1973; 1975-2011

Average Annualized Estimated Streamflow Using Log-Linear Scaling Method (1973-2011)

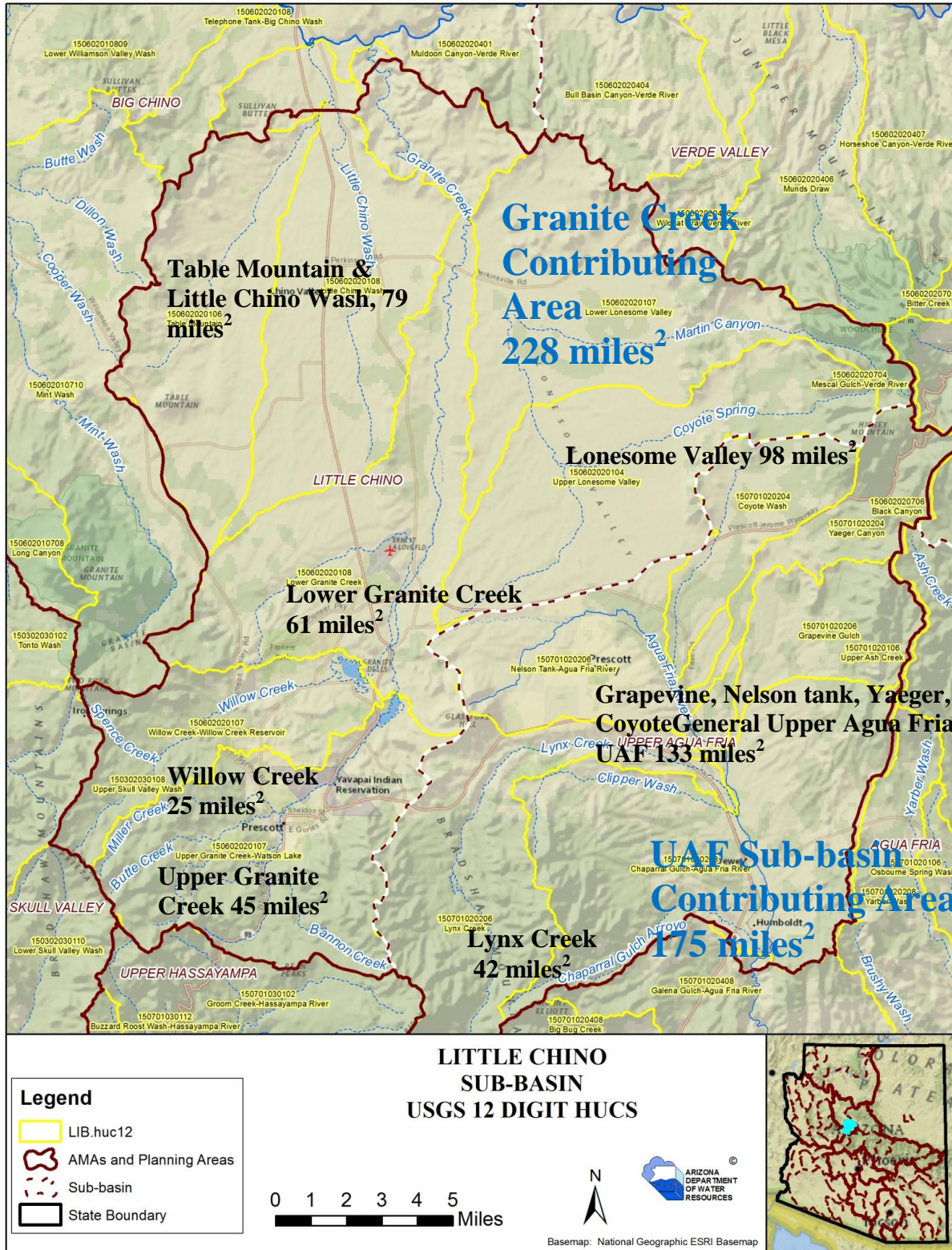
Table 5, below, shows streamflow estimates (1973-2011) for both the Granite Creek contributing area (228 miles²) and the UAF sub-basin contributing area (175 miles²). For variable definitions and regression details, assumptions and limitations, see the Appendices and table footnotes below.

TABLE 5. Estimated Streamflow Recharge Using Log-Linear Regression (1973-2011)

Estimated Streamflow Recharge Using Log-Linear Regression (1973-2011); all units in AF/yr			
Contributing Area	$\ln(Q)=a+b\ln(A)$	$\ln(Q)=0+b\ln(A)$	$\ln(Q)=0+b\ln(A)$; 2005=20,000 AF/yr
Granite Creek 228 miles²	7,500	7,000	6,520 ¹
Contributing Area	$\ln(Q)=a+b\ln(A)$	$\ln(Q)=0+b\ln(A)$	Mean: $\ln(Q)=a+b\ln(A)$; $\ln(Q)=\ln(A)$
UAF 175 miles²	2,310 ³	9,400	5,850 ²

¹Considered a conservative estimate. For example, in the Granite Creek 228 miles² contributing area, streamflow for 2005 was limited 20,000 AF/yr, or the rate recorded at USGS 09503300, and does not include other potential contributing ungauged sources. ³For the UAF 175 miles² contributing area the “Y” (a) intercept was exclusively negative, resulting in low Q bias; see Table B.3. It is assumed that the lack of streamflow data s upstream of USGS 09512450 , resulted in low streamflow estimates for the UAF 175 miles².contributing area ²Used average annualized natural streamflow rate for UAF 175 miles²contributing areas between 1973 and 2011.

FIGURE 5. Little Chino Sub-basin

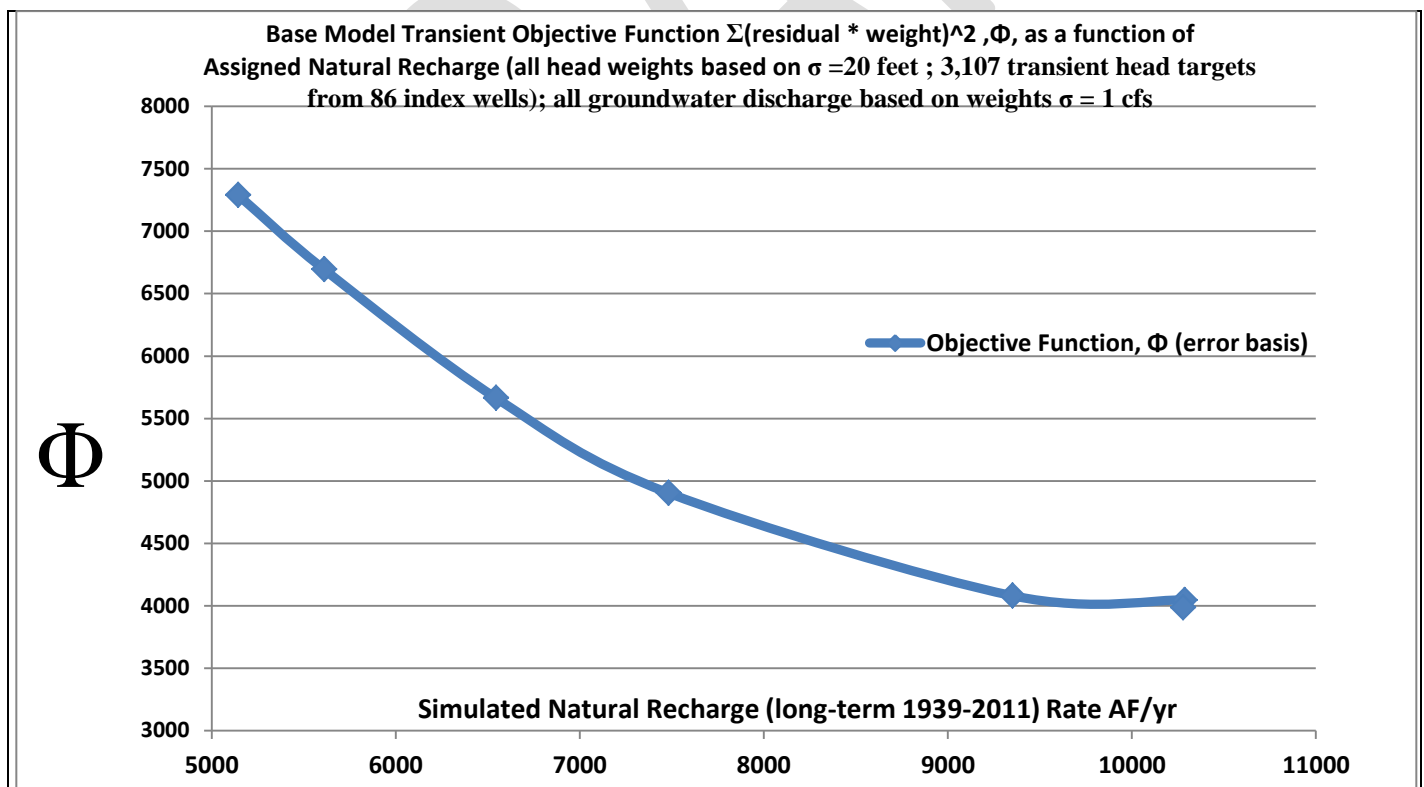


Estimated Streamflow Recharge using the Prescott AMA Groundwater Flow Model

A synopsis of model-estimated recharge rates and associated model error for the “base” model is provided below. For technical details about model development, calibration, evaluation of alternative conceptual models (ACM’s), parameter sensitivity, simulated and observed hydrographs, etc., see Appendices C, D and E .

A concise and effective measure of model error and bias is defined by the objective function, Φ , which is the sum of the weighted-square residual error (i.e., the difference between simulated and observed heads, flows and for some models, a-priori information is assigned to a few LVU K-zones). Thus $\Phi = \sum_i^m (w_i r_i)^2$, where w is the weight, r is the residual of the i th observation. Because different units comprise Φ (i.e., feet, CFD; K in ft/d), assigned target weights can be cross checked for appropriateness by evaluating the error variance and/or the standard error of weighted residuals (SE), which should approximate 1.0 (Hill, 1998). For the Base Model the steady state and transient SE were 1.35 and 1.14, respectively, indicating that the weights were in general properly assigned. Other measures of model fit and bias include evaluating the mean residual error (in alternative formats including numerical totals, histograms and X-Y plots), as well as, evaluating the absolute residual error; these measures of model fit are presented in Appendices C and D. However unlike evaluating Φ , because different kinds of calibration targets are included (i.e., different units), the relative magnitude of error associated with the raw residuals cannot be directly compared between different units. For more details about the Φ , PEST and associated inversion statistics, see WinPEST, and Appendices D and E. Note how the transient-simulated model error and bias decrease as the rate of simulated, long-term (1939-2011) annualized natural recharge increases from 5,000 AF/yr to about 10,000 AF/yr. Other plausible ACM’s show similar Φ -natural recharge rate trends.

FIGURE 6. Base Model Transient Objective Function Φ



Comparison between Estimated Streamflow and Simulated Recharge (1973-2011)

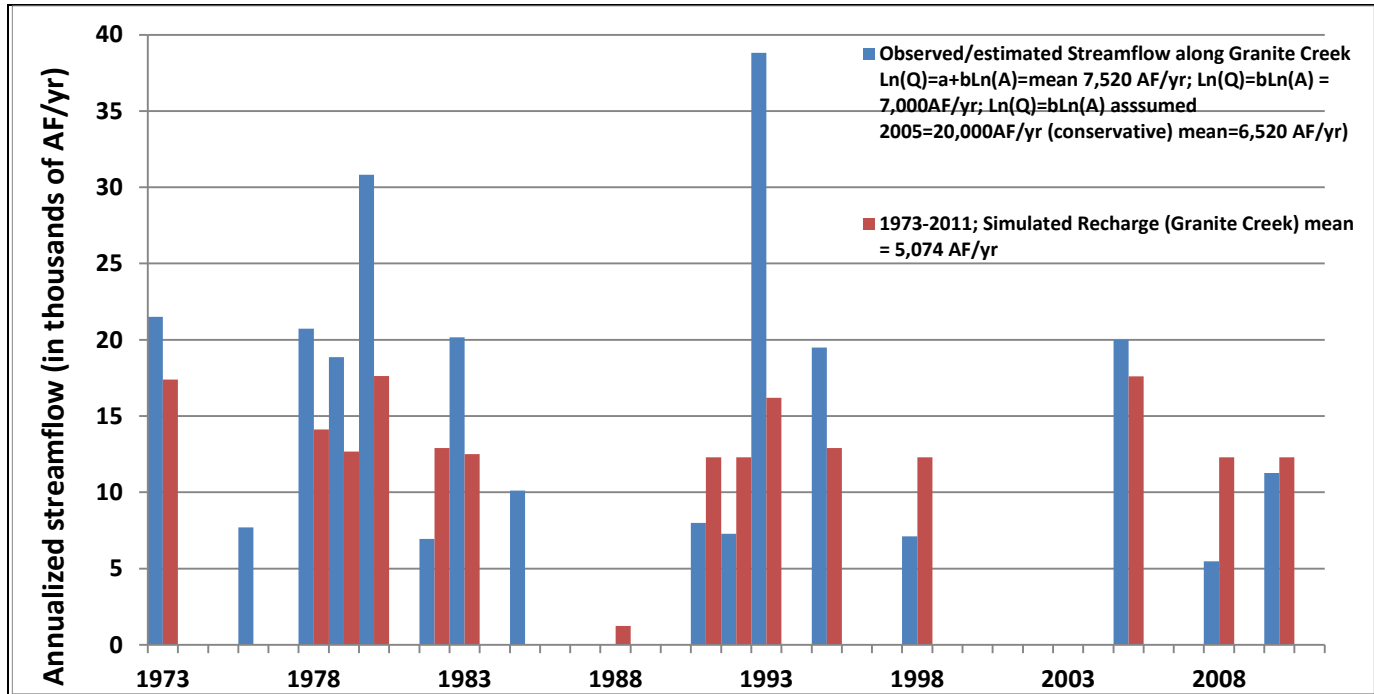
Estimated annualized streamflow for (1) the Granite Creek contributing area (228 miles²) and (2) the Upper Fria Sub-basin contributing area (175 miles²) are compared with model-simulated recharge rates along portions of Granite Creek and Lynx Creek/Agua Fria River, respectively. For simplicity, simulated recharge along Granite Creek represents all other possible streamflow recharge locations within valley areas inclusive to the Granite Creek contributing area (228 miles²); for example any runoff occurring along Lonesome Valley is simulated along Granite Creek.

The comparison focuses on the 1973 to 2011 period because there was less data available prior to 1973, and there were relatively fewer significant stream recharge events before 1973. Estimates of streamflow provide a basis for comparing streamflow recharge *potential* with simulated recharge. , streamflow estimates were determined by using least squares analysis employing a Log-Linear regression function based on Vogel, et al. (2000). For both the Granite Creek and Lynx/Agua Fria contributing areas, both (1) $\ln(Q)=a+b\ln(A)$ and (2) the zero-intercept version, $\ln(Q)=0+b\ln(A)$, were evaluated; see Appendix B, where Q is the annualized streamflow (baseflow removed) rate in cfs; A is the contributing area in miles²; the number a, and the coefficient b, are solved to yield the minimum model error based on a least-squares approach. When the number “a” (i.e., “Y” intercept) is assigned a value of zero, the solution forces y to equal zero when x is equal to zero. Ln is the base of the natural logarithm.

Estimates of streamflow for the Granite Creek contributing area using both (1) $\ln(Q)=a+b\ln(A)$ and (2) the zero-intercept version, $\ln(Q)=0+b\ln(A)$, resulted in long-term (1973-2011) average streamflow means of 7,520 AF/yr and 7,000 AF/yr, respectively. In addition, a more conservative long-term streamflow estimate was calculated using the assumption that the 2005 streamflow event was consistent with flows recorded from Upper Granite Creek (47.2 miles²), or 6,510 AF/yr (1973-2011) (see Figure 7, below). Constraining USGS 09503300 (the 47.2 miles² contributing area) for Water Year 2005, to an annualized flow rate of 20,000 AF/yr, would represent the lowest possible annualized flow rate.

The average annualized simulated recharge rate along Granite Creek (1973-2011) was 5,070 AF/yr. Although some years indicate higher annualized rates of recharge, with respect to streamflow estimates, this typically occurred in years (i.e., 1991; 1998; 2008) preceded by relatively “dry” periods, and were likely subject to higher rates of induced recharge.

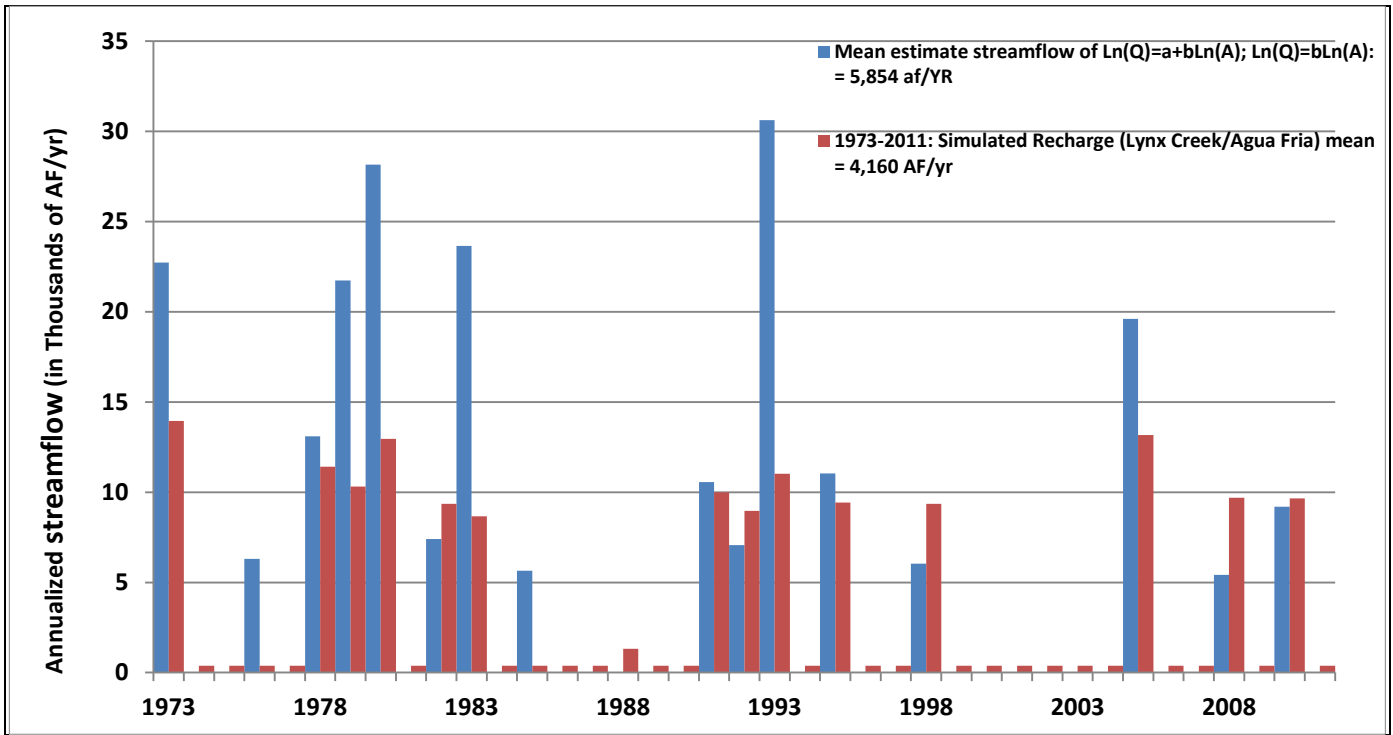
FIGURE 7. Comparison of estimated streamflow and simulated stream recharge along Granite Creek



Estimates of streamflow for the Lynx Creek UAF contributing area using the mean of (1) $\ln(Q)=a+b\ln(A)$ and (2) the zero-intercept version, $\ln(Q)=0+b\ln(A)$, resulted in a long-term (1973-2011) annualized streamflow estimate of 5,854 AF/yr (See Figure 8, below). The average annualized simulated recharge rate along portions of Lynx Creek and the Agua Fria River (1973-2011) was 4,160 AF/yr.

Evidence of induced recharge is seen when comparing simulated recharge in 1973 (14,000 AF/yr), 1993 (11,000 AF/yr) and 2005(13,170 AF/yr). Water Years of 1973 and 2005 were preceded by a relatively “dry” period, while 1993 was preceded by a relatively “wet” period, resulting in higher water tables. In the model, stream-aquifer parameters were assigned in a categorical manner based on relative estimates streamflow. For 1973, 1993 and 2005, the same stream-aquifer parameters (*i.e.*, conductance; stage, input streamflow rate, etc.) were assigned, based on similar high flow estimates. However, the stream-aquifer boundary operates as a head-dependent boundary in the model. As such, when water tables are high, less stream recharge occurs. Conversely, when water tables are lower, more stream recharge (induced recharge) can occur for comparable surface water flow events.

FIGURE 8. Comparison of estimated streamflow and simulated stream recharge along Lynx Creek and Agua Fria River



Conclusion

Using a Log-Linear LSE model and available streamflow data (baseflow removed), the average annualized (1973-2011) streamflow rate for the Granite Creek contributing area was estimated at 6,500 AF/yr. The average annualized streamflow rate for the Lynx Creek/Agua Fria contributing area over that same timeframe was estimated at about 5,800 AF/yr. Simulated recharge along portions of Granite Creek and Lynx Creek/Agua Fria River between 1973 and 2011 were 5,070 AF/yr and 4,160 AF/yr, respectively. Based on annualized streamflow estimates and simulated recharge for the 1973 to 2011 period, physical streamflow volumes were theoretically possible based on the analysis presented for portions of Granite Creek, Lynx Creek and the Agua Fria River. This available data, analysis and model calibration provide strong support for estimating long-term annualized natural recharge in the range of 7,500 to 12,000 AF/yr in these two sub-basins that comprise the Prescott AMA.

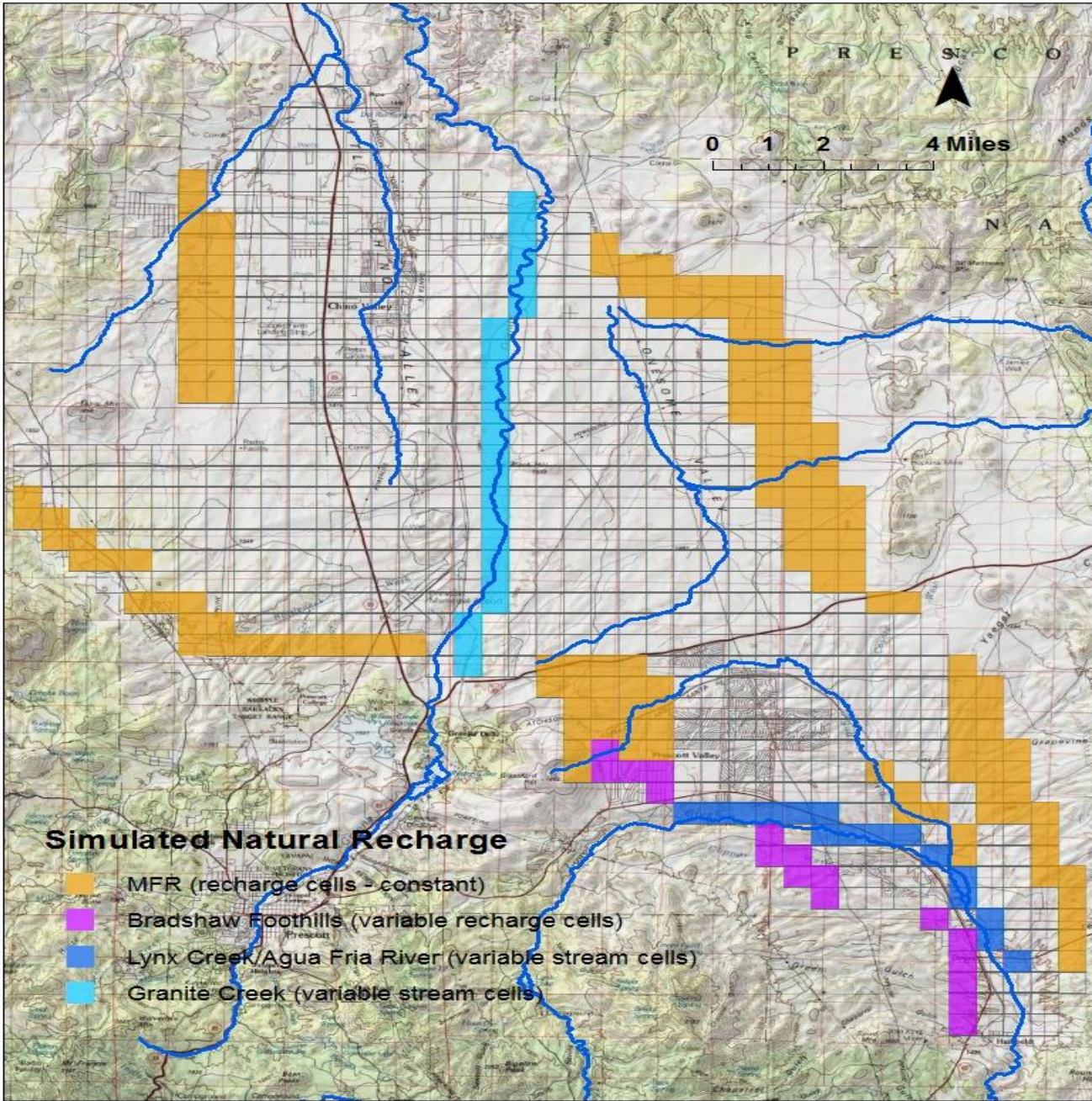
Both the streamflow and model analyses indicate that episodic flood events along major drainages in the AMA contribute significant amounts of recharge to the groundwater system. ADWR's analysis indicates that the stream-to-MFR ratio is approximately 70:30 over both the transient period from 1939-2011 and steady flow conditions(See Figure 9). However, due to the lack of comprehensive stream gaging data for various years and locations, the estimation of stream recharge for major drainages in specific years carries an inherent (and sometimes significant) levels of uncertainty. **Therefore, the overall long-term natural recharge for the AMA is probably a more reasonable overall estimate than any recharge estimated for a specific year.**

Available historical data suggests that developing time-varying estimates of natural recharge is important to: understand how the PrAMA hydrologic system functions; develop a comprehensive understanding of the AMAs overall safe-yield status; and also comprehend, in a more general way, how significant climatic variability may impact natural recharge in the future. As discussed above, placing additional stream gauges in key locations along major tributaries will improve spatial and temporal estimates of natural recharge.

In conclusion, based on available data and analysis of numerous alternative conceptual models (ACM), the most plausible estimates of total long-term (1939-2011) annualized natural recharge range from about 7,500 to 12,000 AF/yr, with central tendencies around 10,000 AF/yr. However, it is important to note that there is significant year-to-year natural recharge variability. For example, during "dry" years, the natural recharge rate may be less than 3,000 AF/yr (i.e., 2002). While during "wet" periods, the natural recharge rate may exceed 25,000 AF/yr (i.e., 2005). Recharge is not entirely streamflow dependent as antecedent hydrologic conditions, including near stream water table elevation, can impact stream recharge rates (streamflow capture and induced recharge).

Significant changes in natural recharge can also occur over extended periods. For example, ADWR simulated natural recharge between 1941 and 1965 at an *annualized* rate of only about 4,000 AF/yr, while between 1965 and 1995 natural recharge was simulated at an *annualized* rate of about 15,000 AF/yr (See Appendix G). Different weather regimes along with other significant water budget components, such as pumping, incidental and artificial recharge, can have significant impacts on groundwater levels, baseflow and water budgets. A better understanding and quantification of the natural recharge distribution over space and time will allow for improved planning with respect to water management in the Prescott AMA.

FIGURE 9. Simulated Natural Recharge



Information contained in this technical memo is draft, and is subject to future revision. The development and evaluation of the groundwater flow model discussed herein is a highly technical process. Specific details of the model development, calibration, and testing process are provided in the appendices for interested readers. In addition, data collected in the future - or data not currently available - are anticipated to result in further refinement or modification of natural recharge estimates in the Prescott AMA. Any questions regarding the contents of this memo should be directed to Keith Nelson knelson@azwater.gov (602) 771-8558.

References

- Anderson, M.P. and Woessner W.W., 1992. Applied groundwater modeling: Simulation of flow and advective transport, Academic Press Inc., Harcourt Brace Jovanovich Publishers, 382 p.
- Barnett et al., 2009. Reconnaissance Watershed and hydrologic Analysis on the Upper Agua Fria Watershed
- Blasch et al., 2005. Hydrogeology of the Upper and Middle Verde River Watersheds, Central Arizona, Scientific Investigations Report 2005-5198.
- Corkhill E.F. and Mason D.A., 1995. Hydrogeology and Simulation of Groundwater Flow, Prescott Active Management Area, Yavapai County, Arizona: Arizona Department of Water Resources, Modeling Report No. 9.
- Hill, M. 1998. Methods and Guidelines for Effective Model Calibration. USGS, WRIR 98-4005.
- Nelson, K., 2002. Application of the Prescott Active Management Area Groundwater Flow Model Planning Scenario 1999-2025: Arizona Department of Water Resources Model Report No. 12.
- Southwest Ground-water Consultants, Inc. (SWGC), 1998. Hydrogeology and groundwater modeling report for the Prescott Active Management Area Yavapai County, Arizona. Prepared in association with Hydro Research for Shamrock Water Company. Vol I, II and III.
- Stonestrom, et al., 2007. Ground-water Recharge in the Arid and Semiarid Southwestern United States. USGS Profesional Paper 1703.
- Timmons D., and Springer, A., 2006. Prescott AMA Groundwater Flow Model Update Report. Prepared for Arizona Department of Water Resources, contract # 2005-2592.
- Vogel, R., Sankarasubramanian, A., 2000. Spatial scaling properties of annual streamflow in the United States. Hydrological Sciences Journal 45(3) June 2000, Pp 465-476.
- Wilson, R.P., 1988. Water Resources of the Northern Part of the Agua Fria Area Yavapai County, Arizona. Prepared by the U.S. Geologic Survey Department of the Interior.
- WinPEST, 2003. Users Manual for WinPEST, Watermark Numerical Computing & Waterloo Hydrogeologic Inc.
- Woessner, William W., 1998. Evaluation of Two Groundwater Models of the Prescott Active Management Area: ADWR Model (1995) and Southwest Ground-water Consultants, Inc. Model (1998).

APPENDIX A:

Observed Groundwater Levels Showing Response to Stream Recharge

DRAFT

Appendix A

Observed Groundwater Levels Showing Response to Stream Recharge

Inspection of groundwater level data also provides revealing information about the frequency, magnitude and variability of natural recharge. Streamflow data shows that high-magnitude flow events occurred at higher frequencies between the mid-1970's and mid-1990's, with respect to earlier (early-1940's to mid-1960's) or later (mid-1995 to mid-2012) periods. Likewise, groundwater levels stabilized (or even increased) between the mid 1970's and 1990's. Higher rates of natural recharge had to be imposed along major drainages, with respect to previous model versions, in order to reduce model bias and error to acceptable levels. (More about natural recharge will be discussed in the model calibration section of the report.) The impact of natural recharge, in combination with other factors, is shown below in selected hydrographs. Data also shows groundwater level rises in response to streamflow (recharge) patterns and decline in absences of recharge, especially in aquifers in direct hydraulic contact with major streams and tributaries.

FIGURE A.1. Groundwater Level Data LIC Sub-basin (UAU Aquifer, shallow well) adjacent to Granite Creek, (B-16-01)20cbd1 (1940-2012). The underlying LVU Aquifer [neighboring well, (B-16-01)20cac, not shown] has an attenuated response to recharge.

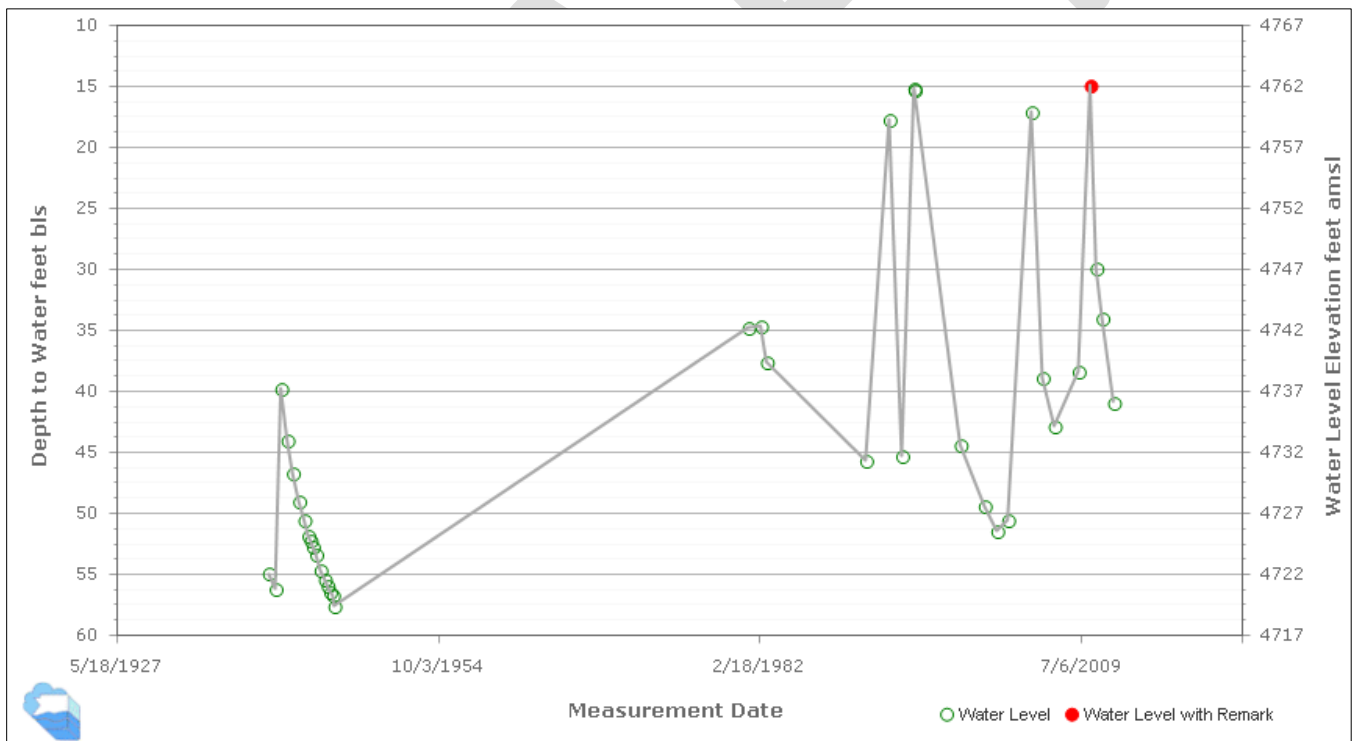


FIGURE A.2. Groundwater Level Data LIC Sub-basin (UAU Aquifer, shallow well) adjacent to Granite Creek, (B-15-01)19dcd1 (1992-2012). The underlying LVU Aquifer [neighboring well, (B-15-01)19dcd2, not shown] has an attenuated response to recharge.

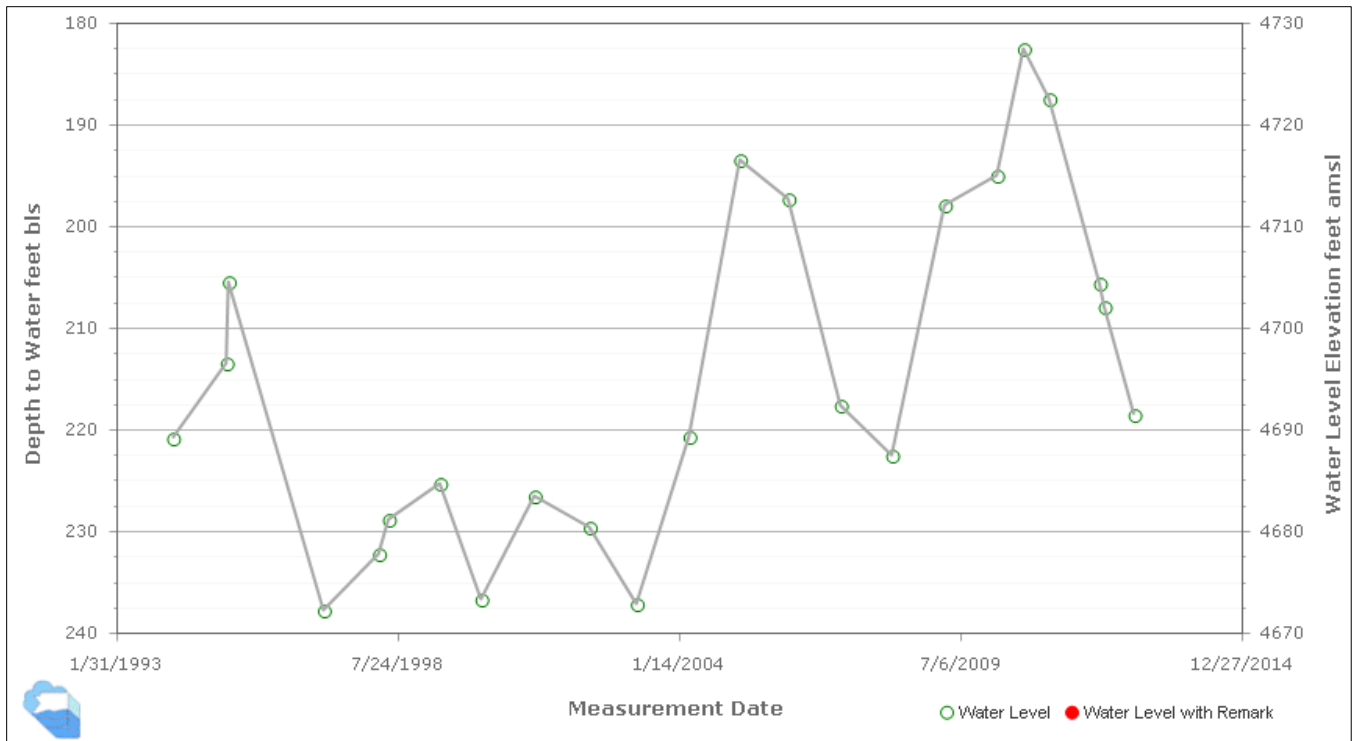


FIGURE A.3. Groundwater Level Data UAF Sub-basin adjacent to Lynx Creek, (B-14-01)22ada (1971-2012).

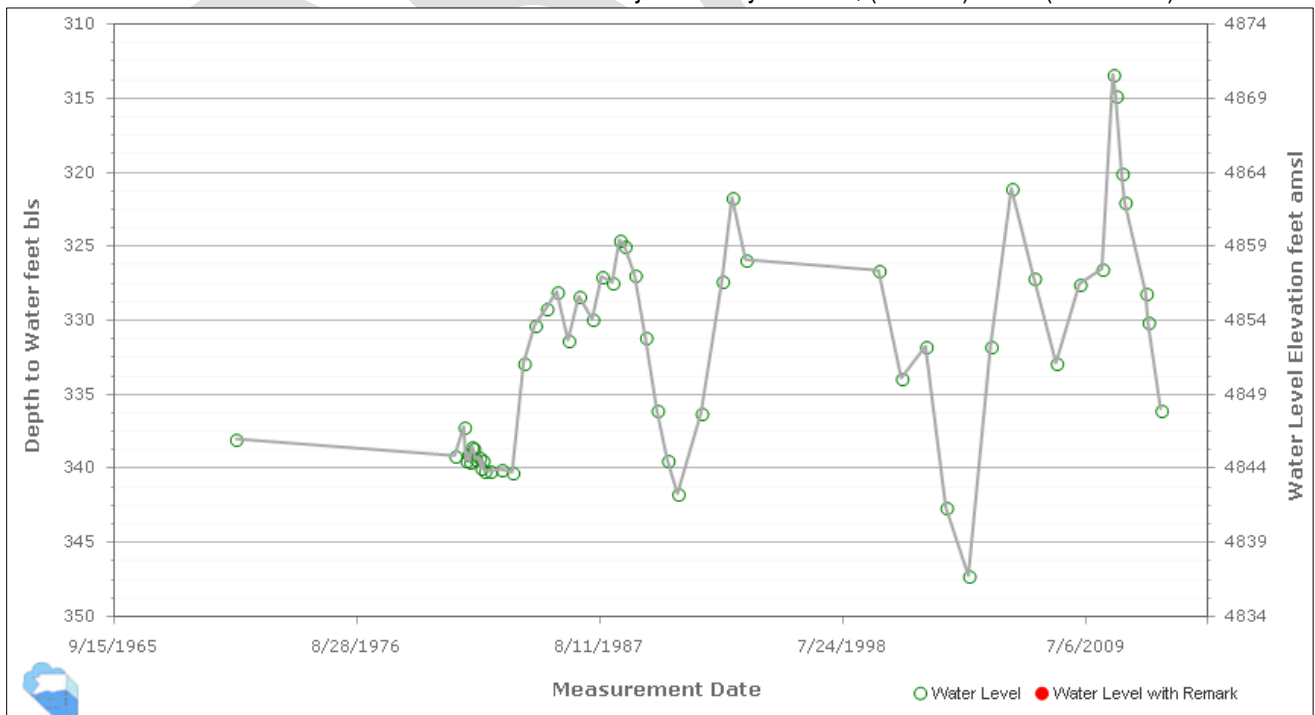
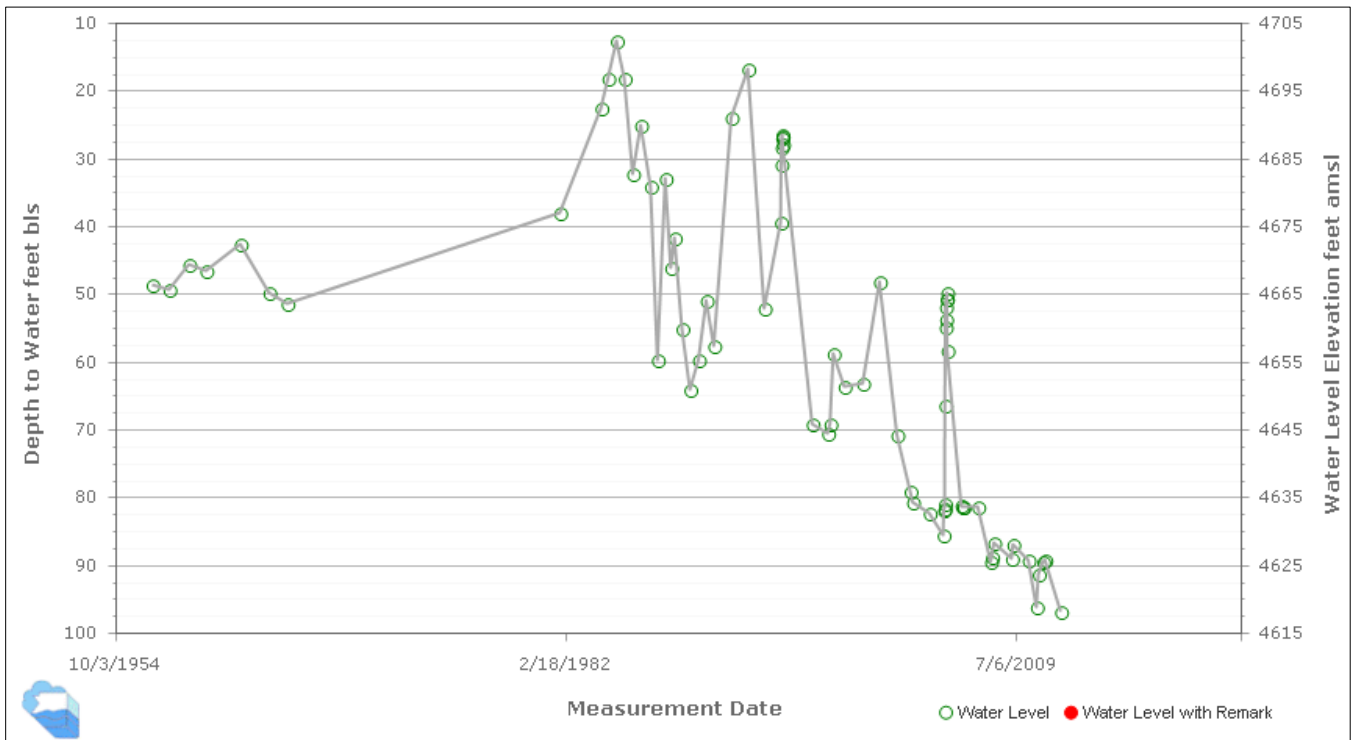


FIGURE A.4. Groundwater Level Data in the UAF Sub-basin adjacent to Lynx Creek, (A-14-01)28bbb (1956-2008). Groundwater level data shows the impacts of significant and frequent recharge in the 1980's and 1990's.



Examples of Attenuated Recharge Responses in the LVU Aquifer (Layer 2) in the LIC Sub-basin

FIGURE A.5. Observed Groundwater Level Data Chino Valley Area, (B-16-02)01cbd (1938-2012).

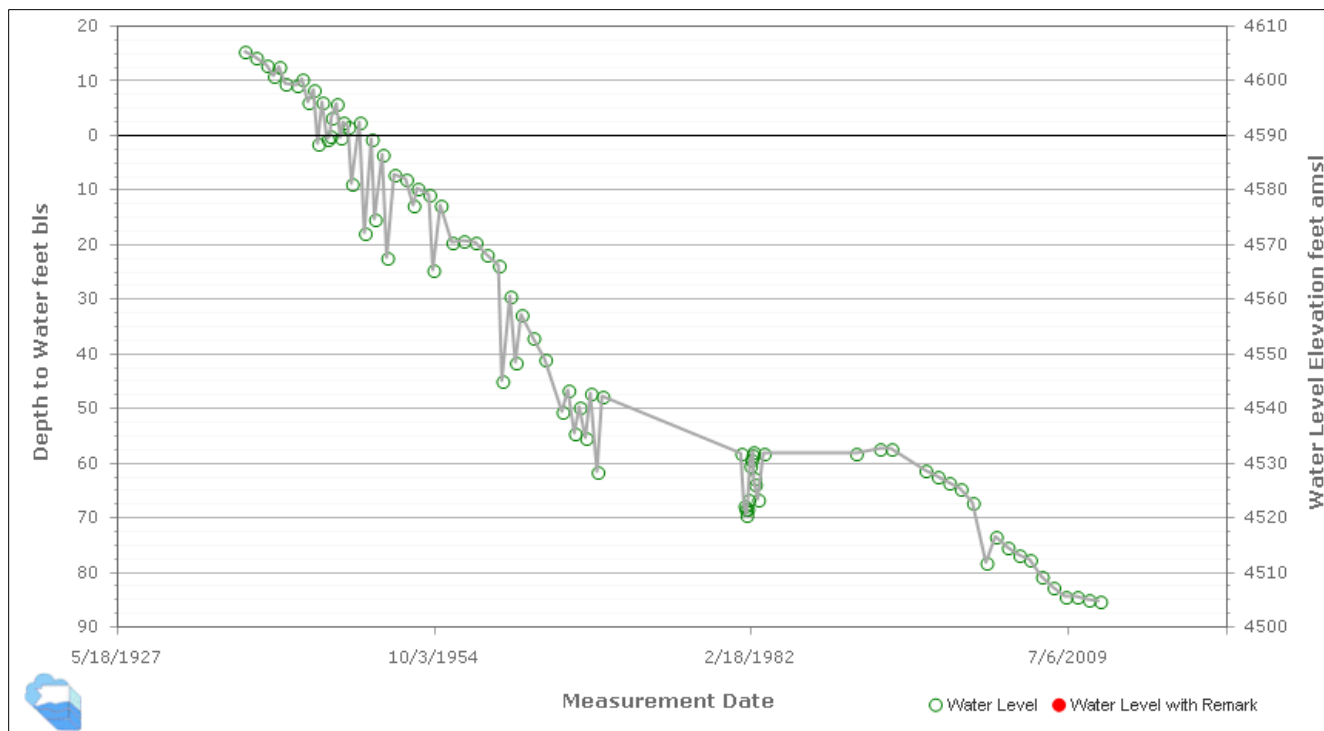


FIGURE A.6. Observed Groundwater Level Data Chino Valley, Lonesome Valley area (B-16-02)12add.

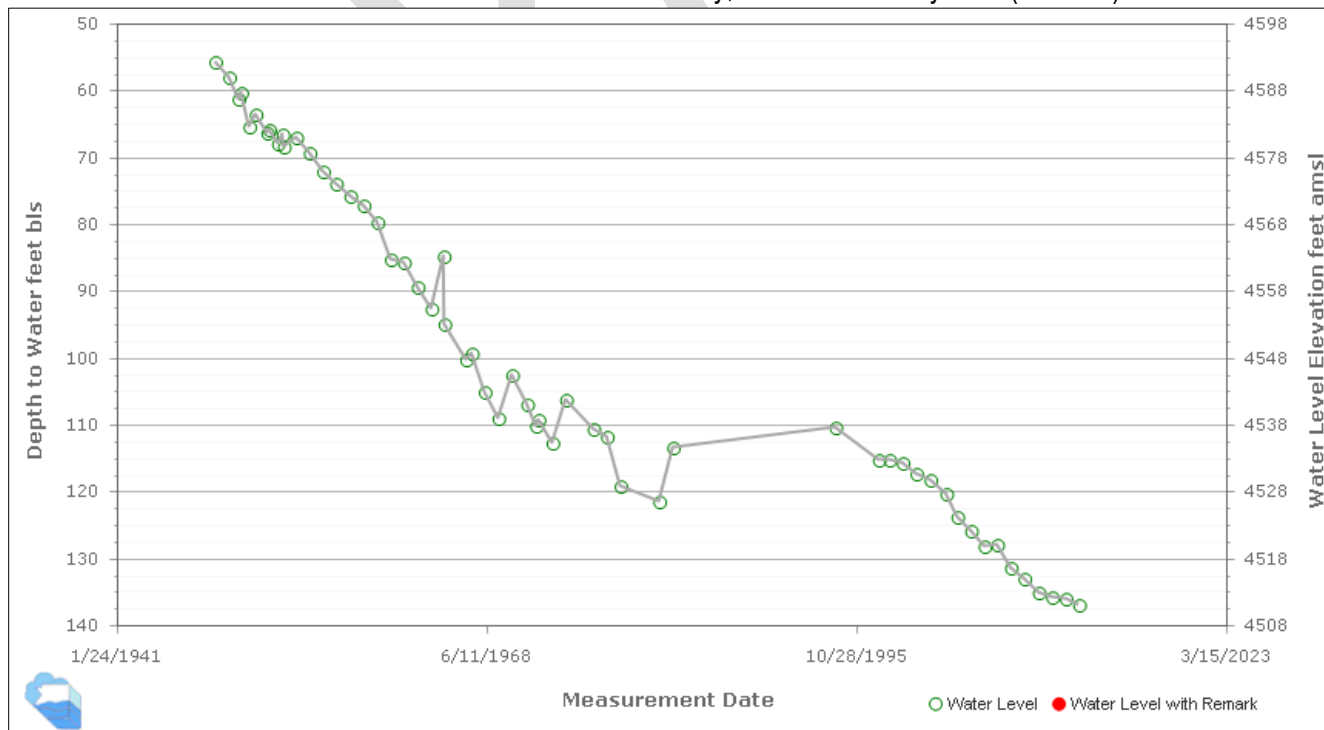
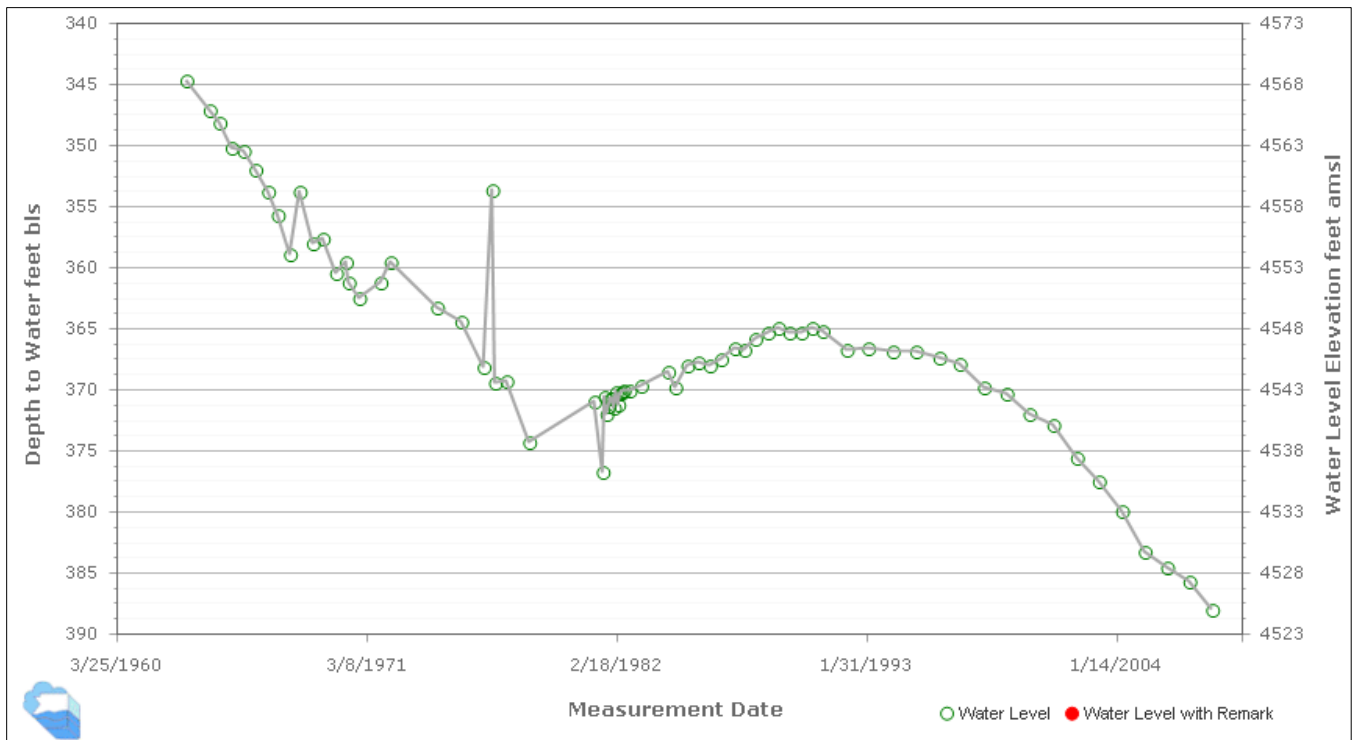


FIGURE A.7. Observed Groundwater Level Data Chino Valley – Lonesome Valley area, (B-15-01)01cdc (1963-2008).



During relatively “wet” climatic conditions including the period from the mid-1970’s into early-1995, late 2004 into mid-2005, and early 2010, significant rates of natural recharge occurred in northern Arizona. Photo below left shows streamflow along Granite Creek in response to significant precipitation events in January-March 2010.



Left: Photo courtesy of the Chino Valley Review. Right: Photo shows Streamflow along Granite Creek, circa 1995.

APPENDIX B:

Log-Linear Least-Squares Regression Analysis

DRAFT

Appendix B

Log-Linear Least-Squares Regression Analysis

Log-linear LSE regression was used to estimate streamflow (baseflow removed) for the 228.5 miles² and 175 miles² contributing areas. For details, see Vogel, 2000. Prior to 1973 there was less quantitative streamflow data available for regression analysis; thus the comparison between estimated streamflow (potentially available for recharge) and simulated stream recharge were limited to the 1973-2011 period.

TABLE B.1. Estimated Streamflow for the 228.5 miles² Granite Creek Contributing Area

Year 1973-2011	Estimated Streamflow for the 228.5 miles ² Granite Creek Contributing Area			
	Log-Linear Relation Least Squares Regression Fit (see Vogel et al (2000))			
	Ln(Q)=a+bLn(A) solved for 228.5 miles ²		Ln(Q)=bLn(A) solved for 228.5 miles ²	
	Estimated Streamflow in cfs (AF/yr)	R ²	Estimated Streamflow cfs (AF/yr)	R ²
1973	30.1 (21,760)	0.55	29.7 (21,500)	0.58
1974	0		0	
1975	0		0	
1976	11.17 (8,085)	----	10.7 (7,710)	----
1977	0		0	
1978	34.6 (25,400)	0.56	28.6 (20,720)	0.59
1979	26.3 (19,070)	0.59	26.0 (18,854)	0.62
1980	57.1 (41,320)	0.82	42.6 (30,820)	0.75
1981	0		0	
1982	4.2 (3,034)	----	9.60 (6,951)	----
1983	39.1 (28,310)	0.54	27.8 (20,160)	0.53
1984	0		0	
1985	17.3 (12,492)	----	13.96 (10,110)	---
1986	0		0	
1987	0		0	
1988	0		0	
1989	0		0	
1990	0		0	
1991			11.0 (7,989)	---
1992			10.1 (7,287)	---
1993			54.0 (38,820)	0.55
1994	0		0	
1995	34.1 (24,693)	0.64	26.9 (19,495)	0.33
1996	0		0	
1997	0		0	
1998	12.53 (9,068)	----	9.81 (7,103)	---
1999	0		0	
2000	0		0	
2001	0		0	
2002	0		0	
2003	0		0	
2004	0		0	
2005	81.0 (58,000)	0.95	64.7 (46,800)	0.71
2006	0		0	
2007	0		0	
2008	9.04 (6,547)	----	7.56 (5,472)	----
2009	0		0	
2010	19.3 (14,000)	0.3	15.6 (11,260)	-0.31
2011	0		0	
1973-2011 mean	(7,518 AF/yr)		(7,002 AF/yr)	

Water years having significant streamflow are shown in **bold print**. Null place indicates that data were not available, or not used, in the regression analysis. Some values have been rounded. Ln(Q)=a+bLn(A), where Q is in units of cfs and A is in units of miles².

FIGURE B.1. Estimated Streamflow for Granite Creek Contributing Area Using: $\ln(Q)=a+b\ln(A)$

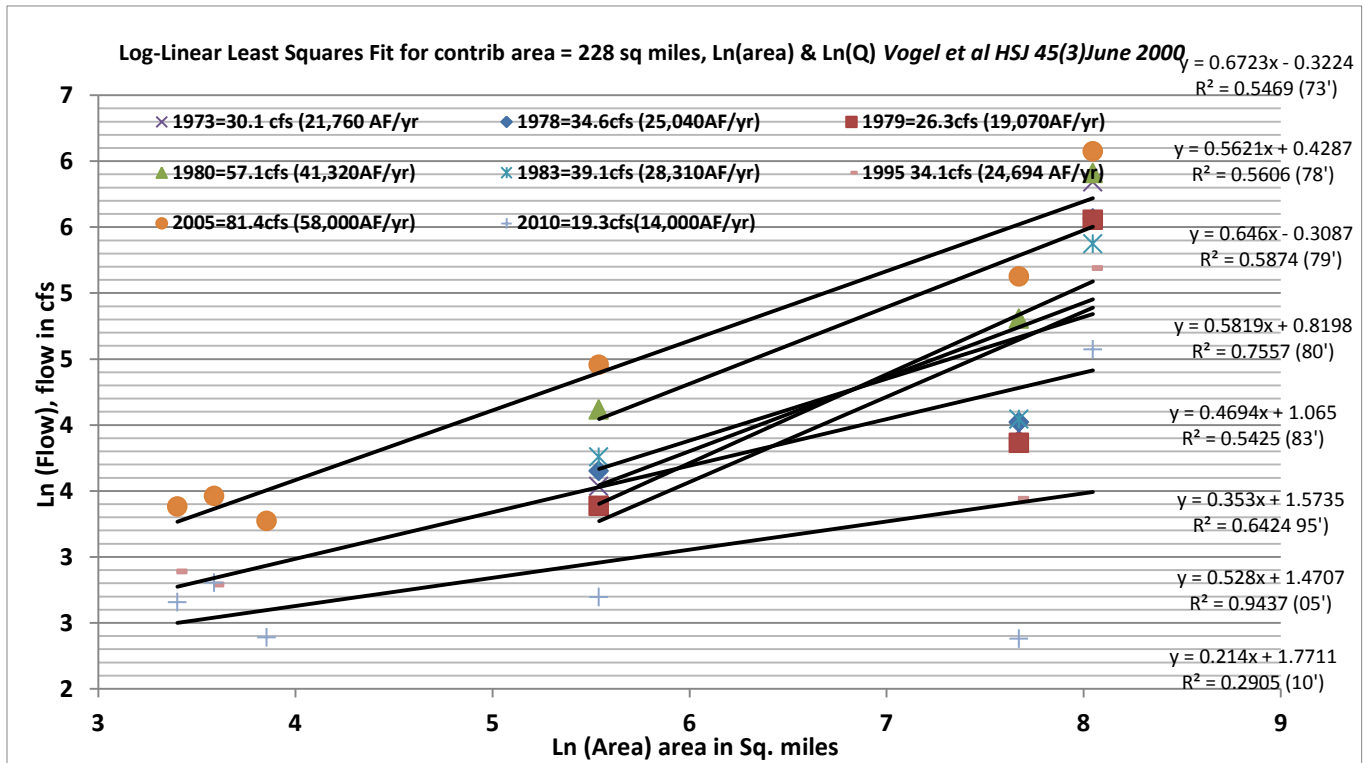


FIGURE B.2. Estimated Streamflow for Granite Creek Contributing Area Using: $\ln(Q)=b\ln(A)$

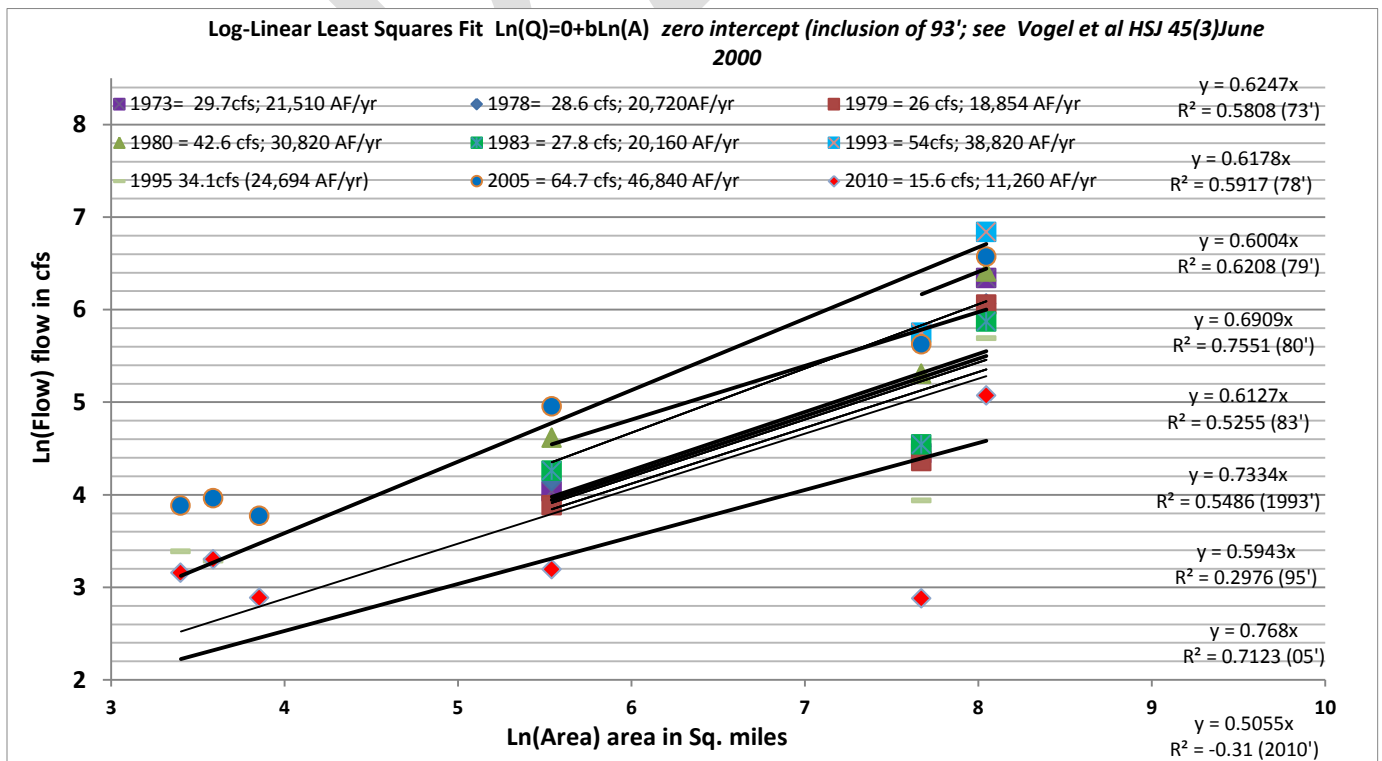


TABLE B.2. Estimated Streamflow for the 175 miles² Upper Agua Fria Contributing Area

Year 1973-2011	Estimated Streamflow for the 175 miles ² Upper Agua Fria Contributing Area					
	Log-Linear Relation Least Squares Regression Fit (see Vogel et al (2000))					
	Ln(Q=a+bLn(A) solved for 175 miles ²)			Ln(Q)=bLn(A) solved for 175 miles ²		
	Estimated Streamflow in cfs (AF/yr)		R ²	Estimated Streamflow cfs (AF/yr)		R ²
1973	23.3	(16,892)	N/A	39.5	(28,581)	0.65
1974	0			0		
1975	0			0		
1976	2.13	(1,539)	N/A	15.3	(11,061)	0.50
1977	0			0		
1978	1.95	(1,431)	N/A	34.2	(24,784)	0.47
1979	12.6	(9,150)	N/A	47.4	(34,333)	0.71
1980	15.8	(11,454)	N/A	62.0	(44,865)	0.72
1981	0			0		
1982	3.64	(2,636)	N/A	16.82	(12,177)	0.58
1983	21.7	(15,730)	N/A	43.6	(31,560)	0.85
1984	0			0		
1985	1.70	(1,230)		13.93	(10,080)	0.47
1986	0			0		
1987	0			0		
1988	0			0		
1989	0			0		
1990	0			0		
1991	3.01	(2,181)	N/A	26.16	(18,940)	0.52
1992	1.18	(852)	N/A	18.33	(13,270)	0.42
1993	13.3	(6,660)	N/A	75.4	(54,590)	0.67
1994	0			0		
1995	2.58	(1,870)	N/A	27.9cfs	(20,220)	0.50
1996	0			0		
1997	0			0		
1998	1.35	(980)	N/A	15.3	(11,100)	0.43
1999	0			0		
2000	0			0		
2001	0			0		
2002	0			0		
2003	0			0		
2004	0			0		
2005	15.22	(11,020)	0.99	38.9	(28,190)	0.69
2006	0			0		
2007	0			0		
2008	3.16	(2,290)	0.99	11.8	(8,530)	
2009	0			0		
2010	5.94	(4,300)	1.0	19.5	(14,090)	0.57
2011	0			0		
1973-2011 mean	(2,313 AF/yr)			(9,394 AF/yr)		

Water years having significant streamflow are shown in **bold print**. Streamflow estimates prior to 1999 applied two data points when solving for $\ln(Q=a+b\ln(A))$, where $A = \ln(175 \text{ miles}^2)$; in these cases R^2 is not applicable – hence N/A. For UAF Sub-basin contributing area streamflow estimates (175 miles²), there are no data available for contributing areas above – or less than the 175 miles²; it is unclear if/how the paucity of data less than 175 miles² may impact the Log-linear regression estimates. Note that the estimates in the right column are typically much smaller than those estimated in the left column; this difference is attributed to the regression solution allowing the “Y” intercept to be negative number, due to the lack of stream flow data for contributing areas less than 175 miles². Some values have been rounded. $\ln(Q)=a+b\ln(A)$, where Q is in units of cfs and A is in units of miles².

TABLE B.3. Estimated Streamflow for the 175 miles² Upper Agua Fria Contributing Area

Estimated Streamflow for the 175 miles ² Upper Agua Fria Contributing Area			
Year 1973-2011	$\ln(Q)=a+b\ln(A)$ solved for 175 miles ² ; Estimated Streamflow shown in AF/yr	$\ln(Q)=b\ln(A)$ solved for 175 miles ² ; Estimated Streamflow shown in (AF/yr	Mean estimated strm $\ln(Q)=a+b\ln(A)$ & $\ln(Q)=b\ln(A)$ shown in AF/yr
1973	16,892	28,581	22,737
1974	0	0	0
1975	0	0	0
1976	1,539	11,061	6,300
1977	0	0	0
1978	1,431	24,784	13,108
1979	9,150	34,333	21,742
1980	11,454	44,865	28,160
1981	0	0	0
1982	2,636	12,177	7,407
1983	15,730	31,560	23,645
1984	0	0	0
1985	1,230	10,080	5,655
1986	0	0	0
1987	0	0	0
1988	0	0	0
1989	0	0	0
1990	0	0	0
1991	2,181	18,940	10,561
1992	852	13,270	7,061
1993	6,660	54,590	30,625
1994	0	0	0
1995	1,870	20,220	11,045
1996	0	0	0
1997	0	0	0
1998	980	11,100	6,040
1999	0	0	0
2000	0	0	0
2001	0	0	0
2002	0	0	0
2003	0	0	0
2004	0	0	0
2005	11,020	28,190	19,605
2006	0	0	0
2007	0	0	0
2008	2,290	8,530	5,410
2009	0	0	0
2010	4,300	14,090	9,195
2011	0	0	0
1973-2011 mean	2,313 AF/yr	9,394 AY/yr	5,854AF/yr

Water years having significant streamflow are shown in **bold print**. Null place indicates that data were not available for regression analysis. Due to a paucity of data, solution prior to 1999 used only two data points when solving for $\ln(Q)=a+b\ln(A)$, where $A = \ln(175 \text{ miles}^2)$; this frequently resulted in $a < 0$. Some values have been rounded. $\ln(Q)=a+b\ln(A)$, where Q is in units of cfs and A is in units of miles².

FIGURE B.3. Estimated Streamflow for UAF Sub-basin Contributing Area Using: $\ln(Q)=a+b\ln(A)$

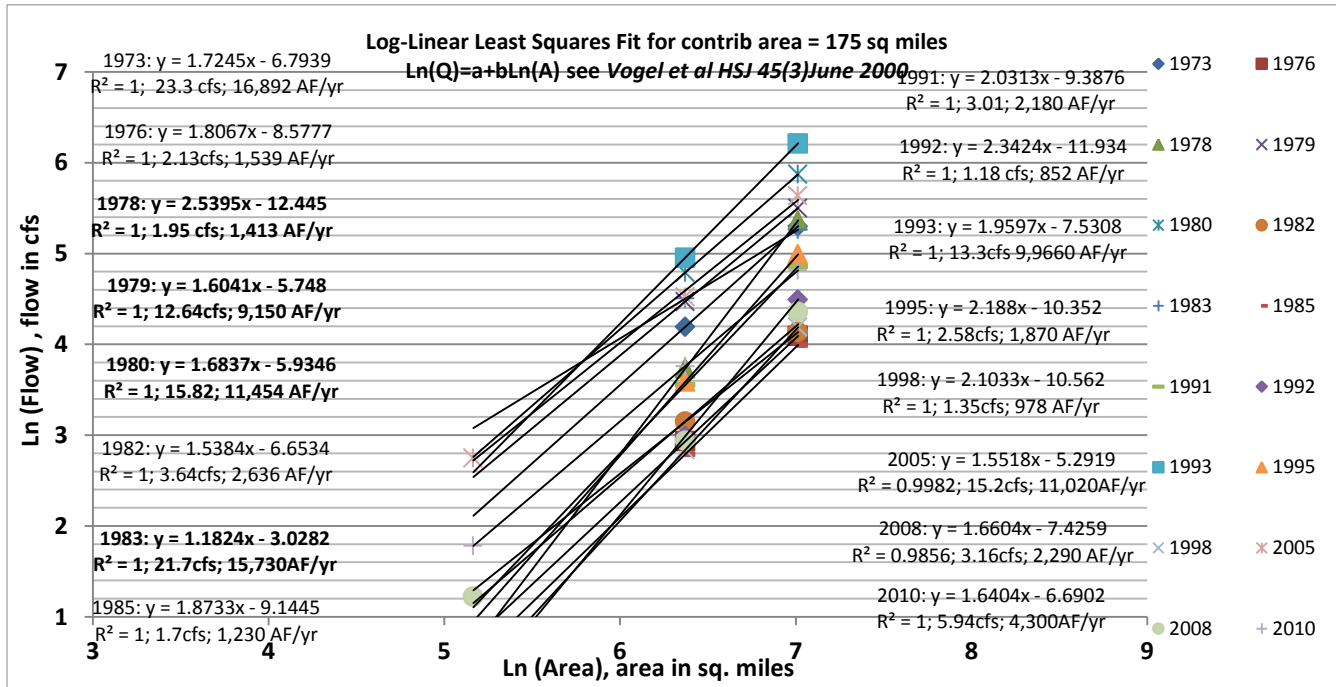


FIGURE B.4. Estimated Streamflow for UAF Sub-basin Contributing Area Using: $\ln(Q)=b\ln(A)$

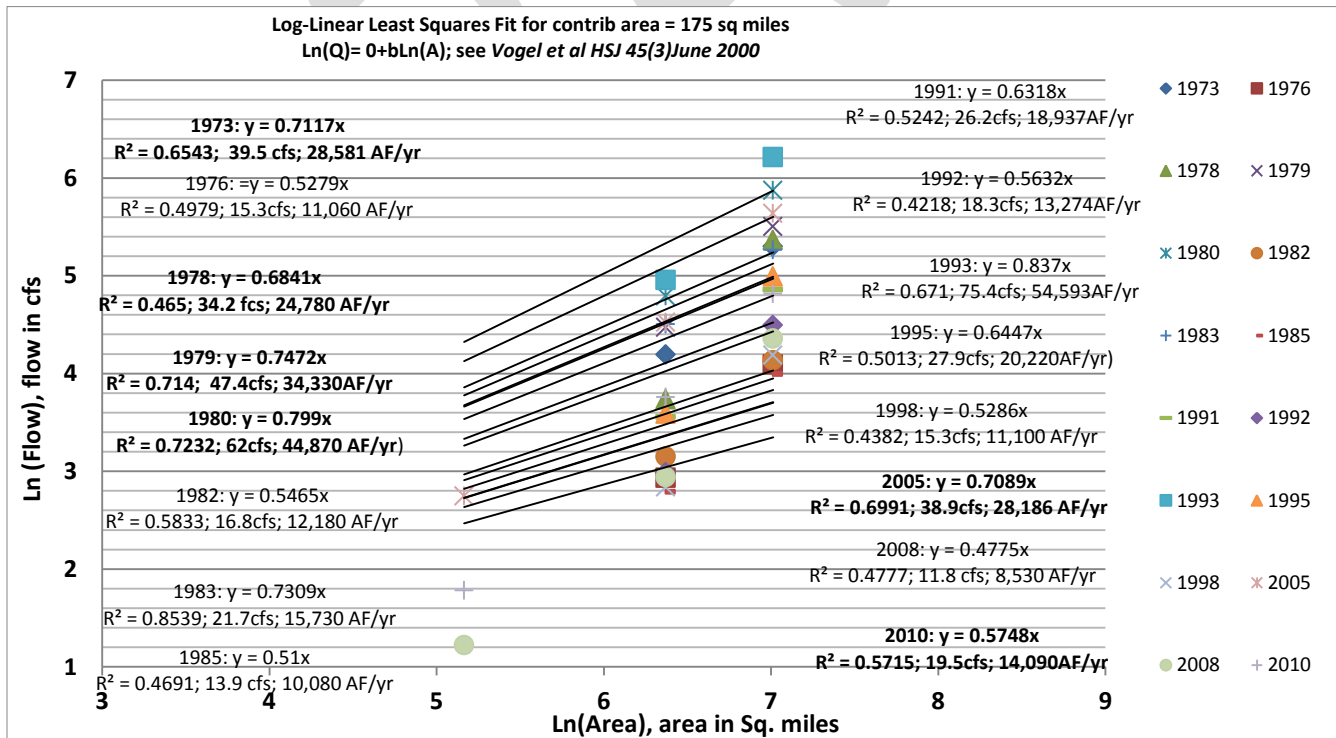


TABLE B.4. Comparison of Simulated Recharge and Estimated Streamflow with Number Days having Streamflow above Baseflow Rates (>10 cfs); Note that model simulated stream recharge during 155-day stress period

Year	Days of base flow above base (10 cfs) Agua Fria River near Mayer	Days of base flow above base (10 cfs) Agua Fria River near Humboldt	Simulated Recharge Lynx Creek and Agua Fria River AF/yr	Estimated Streamflow Lynx Creek/Agua Fria River in AF/yr
1973	162		13951	22736.5
1974	11		379	0
1975	11		379	0
1976	29		379	6300
1977	13		379	0
1978	56		11409	13107.5
1979	163		10316	21741.5
1980	140		12949	28159.5
1981	22		379	0
1982	66		9352	7406.5
1983	165		8668	23645
1984	127		379	0
1985	120		379	5655
1986	67		379	0
1987	44		379	0
1988	70		1314	0
1989	5		379	0
1990	19		379	0
1991	44		9993	10560.5
1992	69		8971	7061
1993	170		11026	30625
1994	37		379	0
1995	115		9419	11045
1996	11		379	0
1997	23		379	0
1998	89		9347	6040
1999	26		379	0
2000	25	4	379	0
2001	38	4	379	0
2002	6	4	379	0
2003	36	4	379	0
2004	15	9	379	0
2005	135	85	13172	19605
2006	23	8	379	0
2007	8	5	379	0
2008	37	24	9696	5410
2009	27	19	379	0
2010	64	43	9664	9195
2011	4	8	379	0
Mean			4,061 AF/yr	5,854 AF/yr

TABLE B.5.

	Days above baseflow at Williamson Valley (10 cfs)	Days above baseflow at Williamson Valley (10 cfs) Inferred	Days above baseflow at Granite Creek (cfs)	Simulated Recharge Granite Creek	Estimated Streamflow Granite Creek
1973	92			17389	21500
1974	3			0	0
1975	2			0	0
1976	15			0	7710
1977	6			0	0
1978	35			14129	20720
1979	92			12665	18854
1980	84			17623	30820
1981	0			0	0
1982	19			12906	6951
1983	66			12495	20160
1984	14			0	0
1985	65			0	10110
1986		34		0	0
1987		22		0	0
1988		35		1230	0
1989		3		0	0
1990		10		0	0
1991		22		12298	7989
1992		35		12298	7287
1993		86		16205	38820
1994		19		0	0
1995		58		12895	19495
1996		6		0	0
1997		12		0	0
1998		45		12298	7103
1999		13	3	0	0
2000		13	0	0	0
2001	3		8	0	0
2002	2		1	0	0
2003	9		9	0	0
2004	3		0	0	0
2005	108		98	17609	20000*
2006	1		2	0	0
2007	2		0	0	0
2008	24		42	12298	5472
2009	15		7	0	0
2010	51		72	12289	11260
2011	0		0	0	0
Mean				5,041 AF/yr	6,519 AF/yr

APPENDIX C:

Base Model Calibration Comparing Simulated Heads and Flows

DRAFT

Appendix C

Base Model Calibration Comparing Simulated Heads and Flows where Natural Recharge was applied at about 1) 10,000 AF/yr and at 2) 5,100 AF/yr with Observed Heads and Flows

FIGURE C.1: Long-term transient recharge \approx 5,100 AF/yr 10,000 Mean residual = -13.3 feet (under simulation)

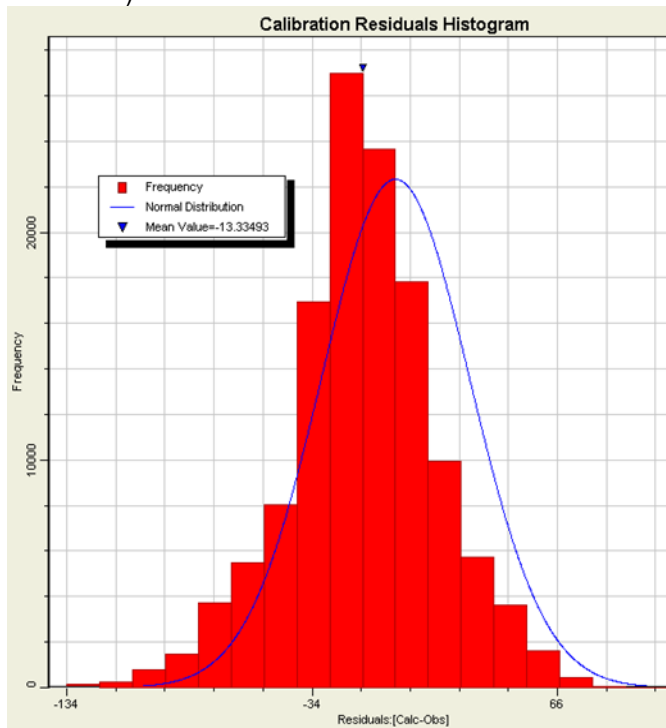
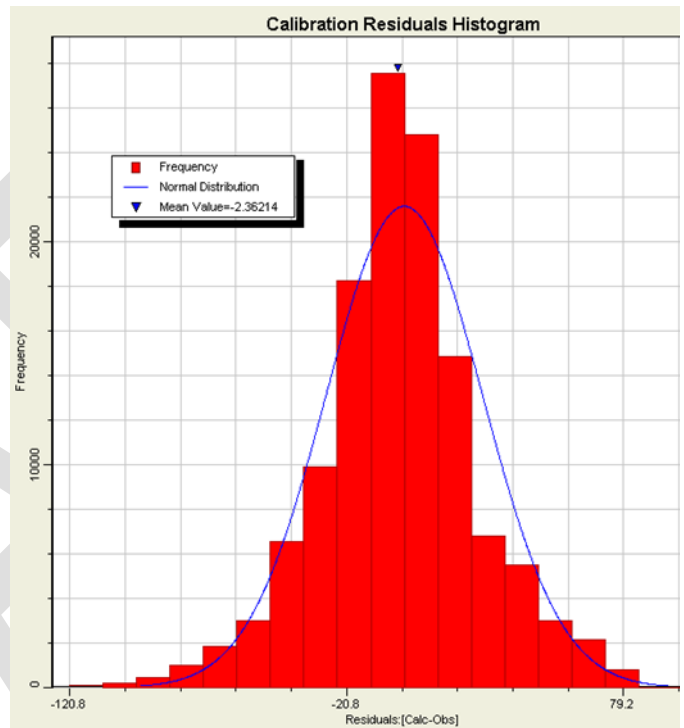


FIGURE C.2: Long-term transient recharge \approx AF/yr Mean residual = -2.36 feet



Observed and Simulated Heads and Flows for Selected PrAMA Model Locations Associated with the “Base” Model Comparing Long-Term (1939-2011): 1) Calibrated Natural Recharge Rates (\sim 10,000 AF/yr); and 2) Arbitrarily Low Natural Recharge Rates (\sim 5,100 AF/yr)

For comparison of observed and simulated heads and flows, see Figures C.3 to C.21. Simulated heads associated with the calibrated “Base” model are shown in cool colors. The “Base” model is associated with long-term (1939-2011) natural recharge rates of about 10,000 AF/yr. Note that for calibration purposes, stream-aquifer parameters associated with simulated recharge were categorically applied, based on five generalized magnitudes of recharge; thus little effort was expended to “tweak” the model calibration for individual events. Simulated heads and flows associated with lower (non-calibrated) natural recharge rates (5,100 AF/yr) are shown in warm colors. Note that the non-calibrated, long-term natural recharge rate of 5,100 AF/yr was arbitrarily selected to represent “low” natural recharge rates, and slightly lower than previous PrAMA model versions (Nelson, 2002; Timmons et al, 2005). See Figure C.3. for location of observed and simulated groundwater levels, and groundwater discharge at Del Rio Springs and baseflow along the Agua Fria River. Note

evapotranspiration (ET) is also simulated in the same cells assigned to Del Rio Springs and the Agua Fria River.

FIGURE C.3. Location of selected observe and simulated groundwater levels and groundwater discharge

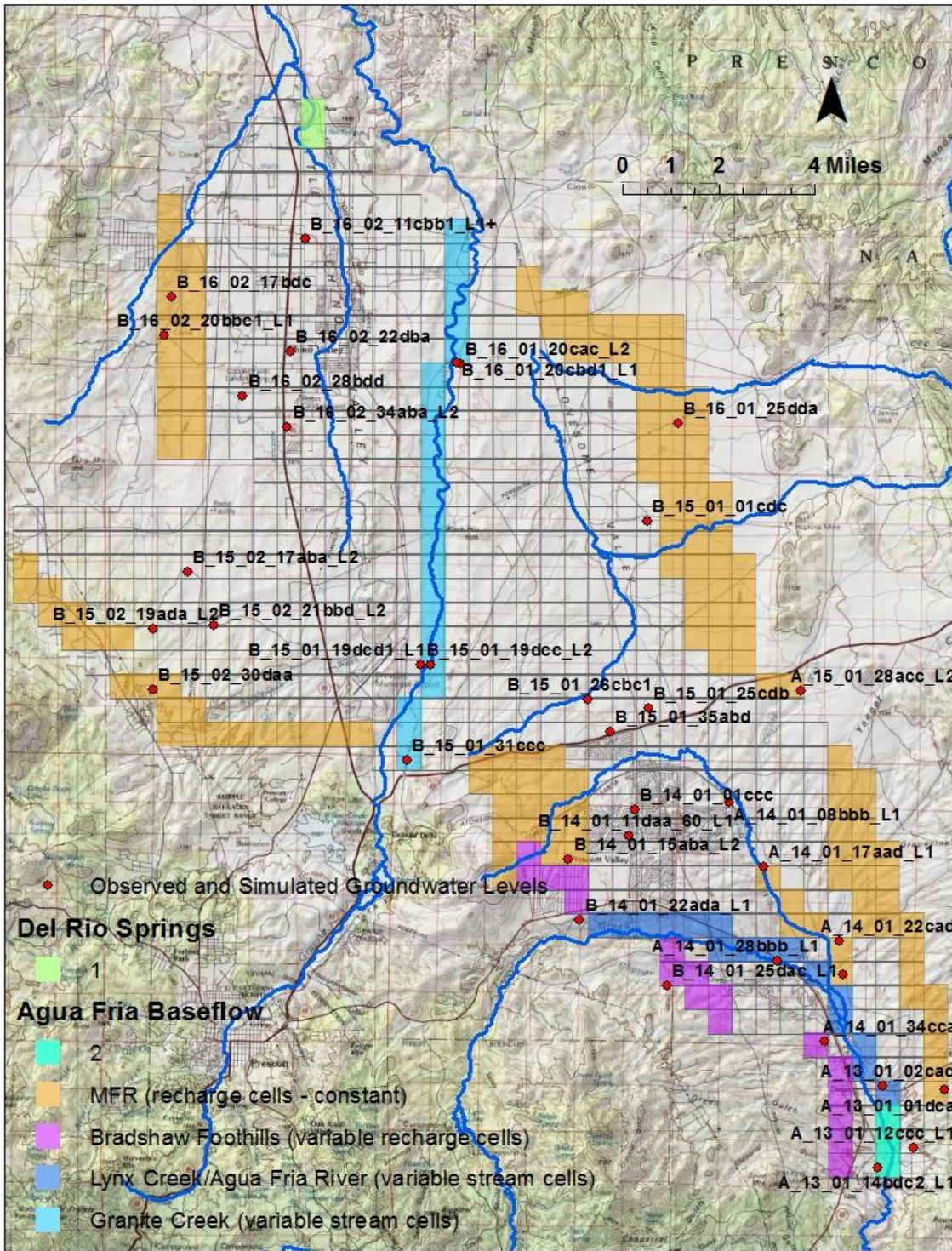


FIGURE C.4. Simulated and Observed Groundwater Discharge, Del Rio Springs

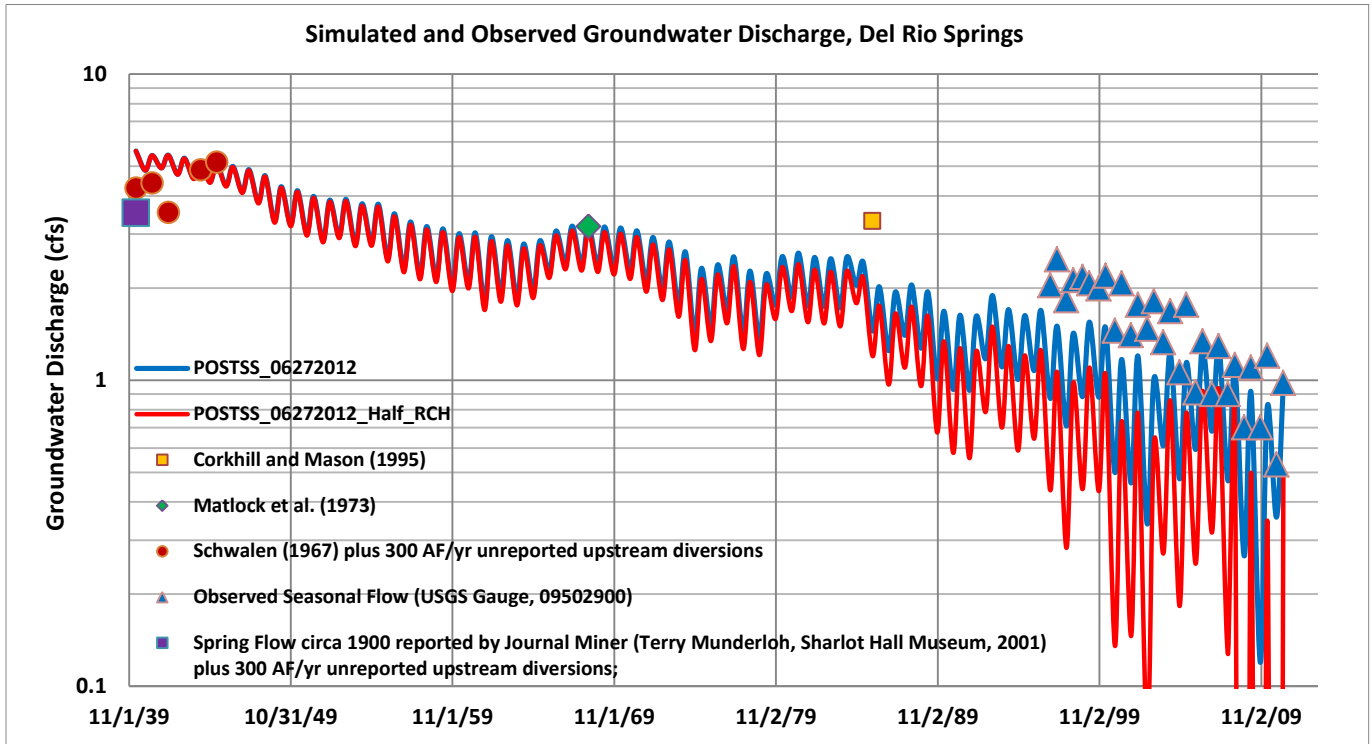


FIGURE C.5. Simulated and Observed Groundwater Discharge, Agua Fria River

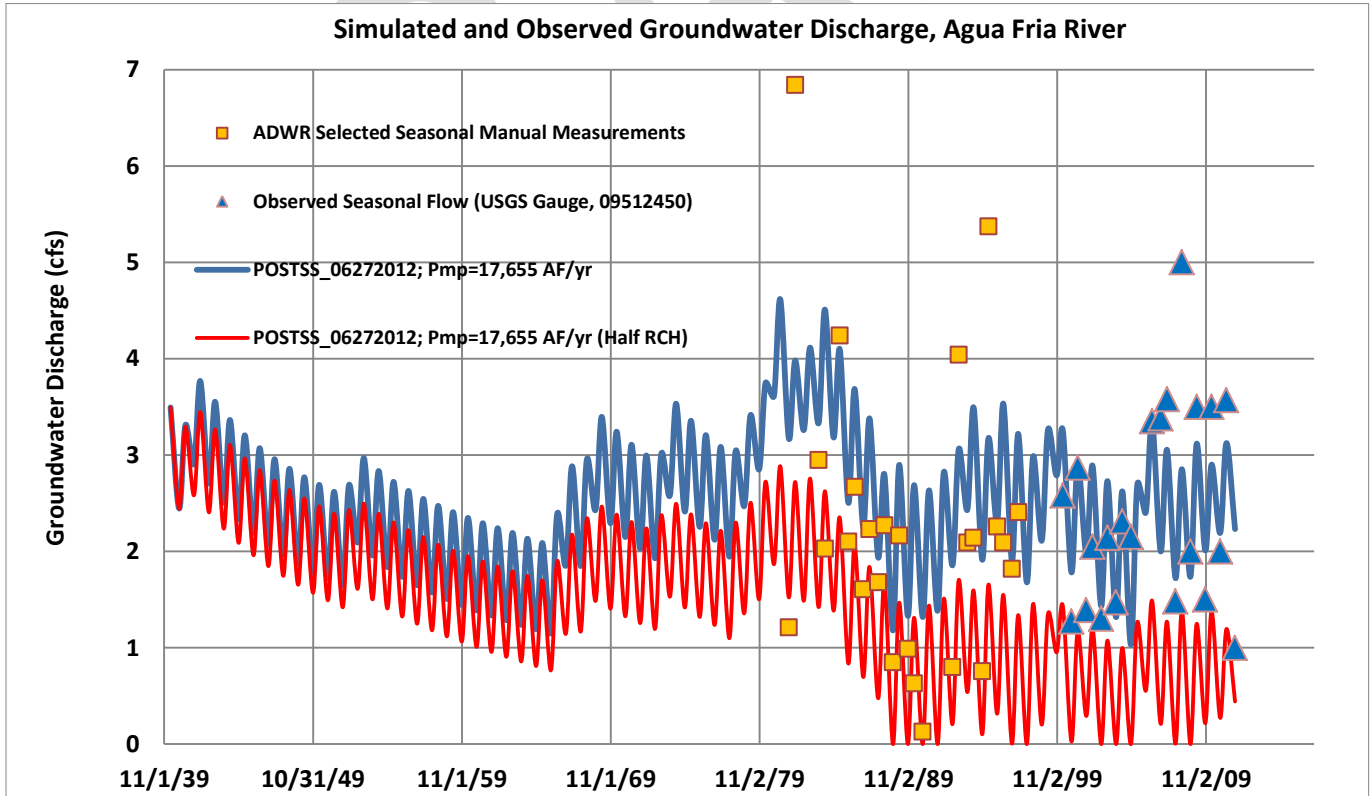


FIGURE C.6. Simulated and Observed Heads Central LIC Sub-basin

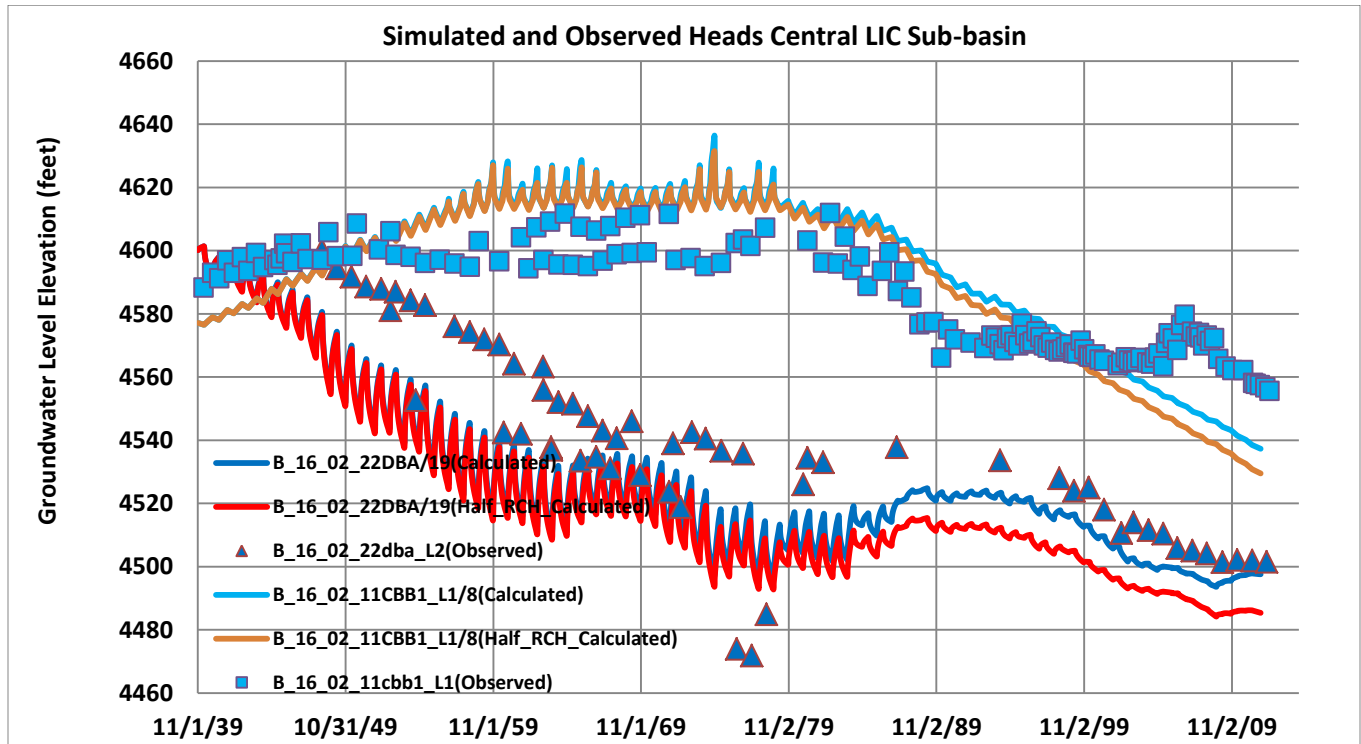


FIGURE C.7. Simulated and Observed Heads Western LIC Sub-basin

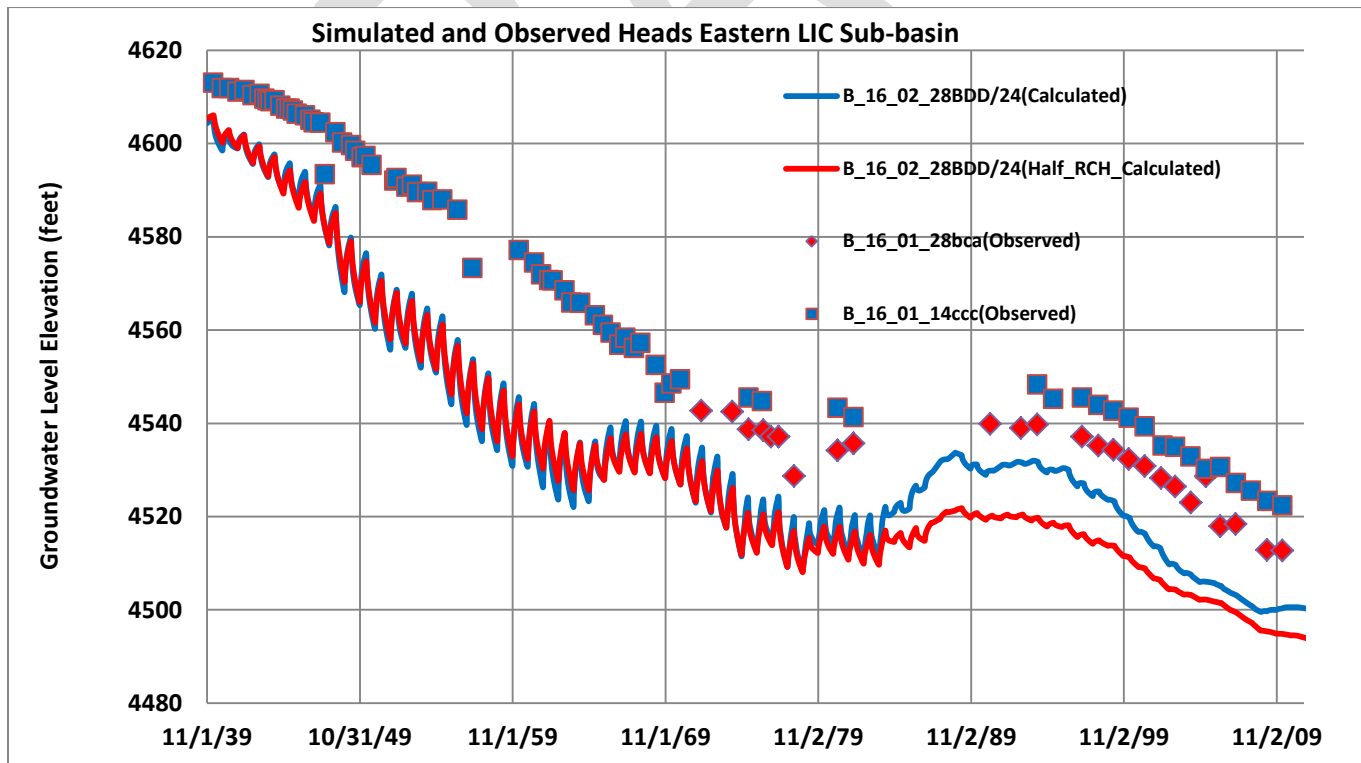


FIGURE C.8. Simulated and Observed Heads Eastern LIC Sub-basin

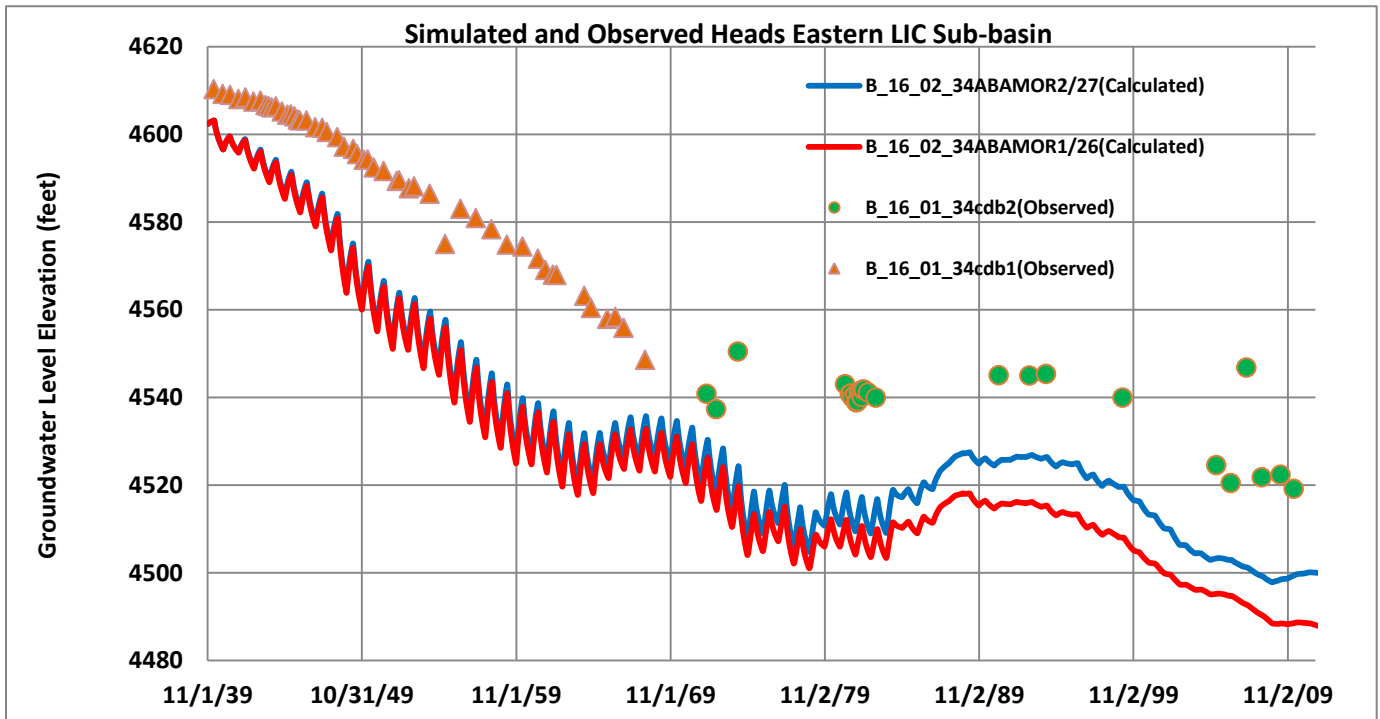


FIGURE C.9. Simulated and Observed Heads Far Eastern LIC Sub-basin

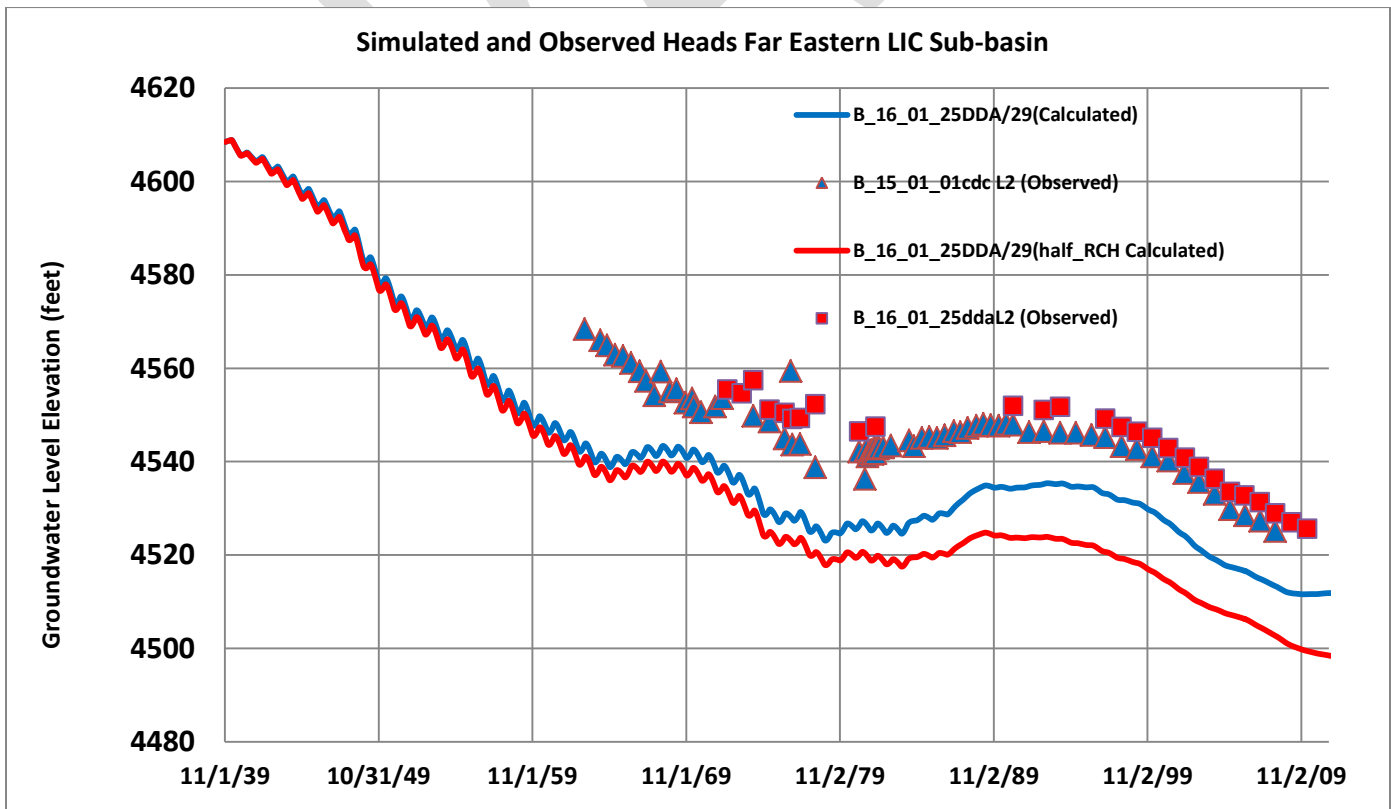


FIGURE C.10. Simulated and Observed Heads near Granite Creek – North LIC Sub-basin

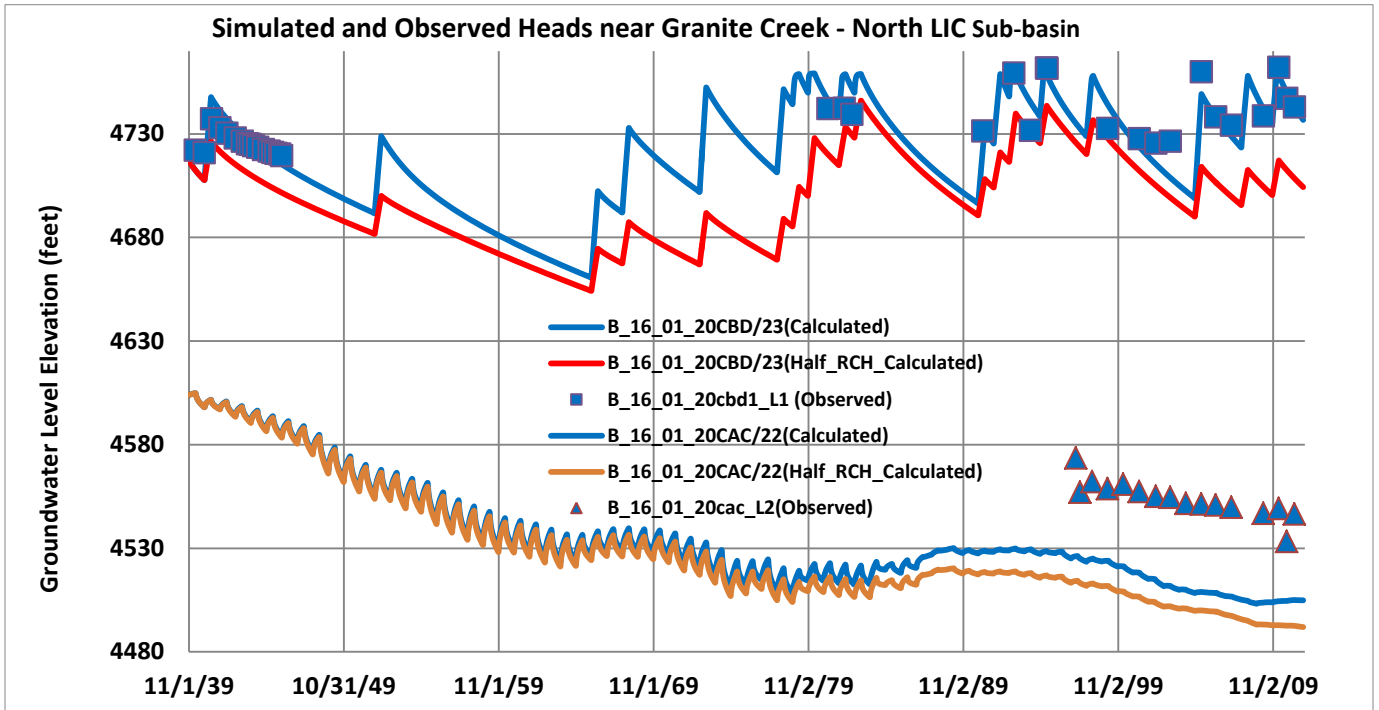


FIGURE C.11. Simulated and Observed Heads near Granite Creek- North LIC Sub-basin

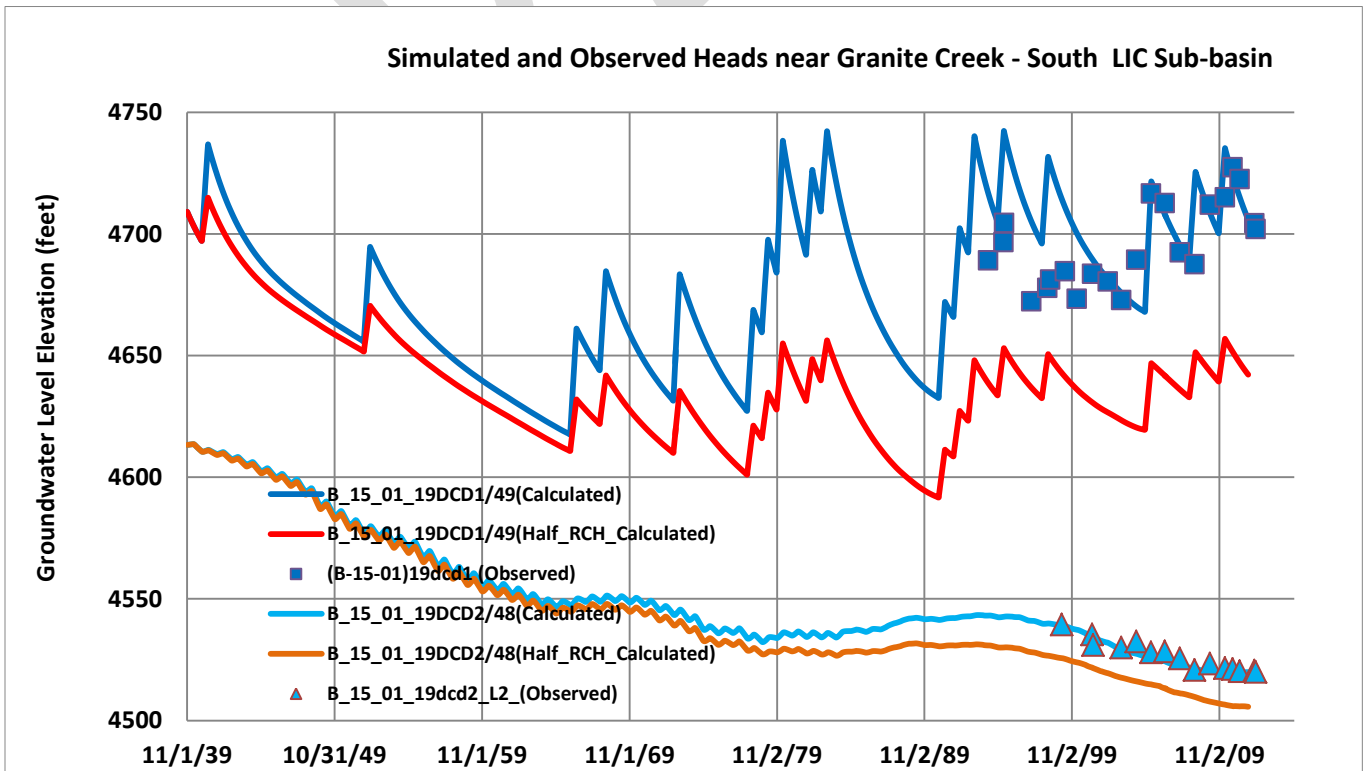


FIGURE C.12. Simulated and Observed Heads Northwest LIC

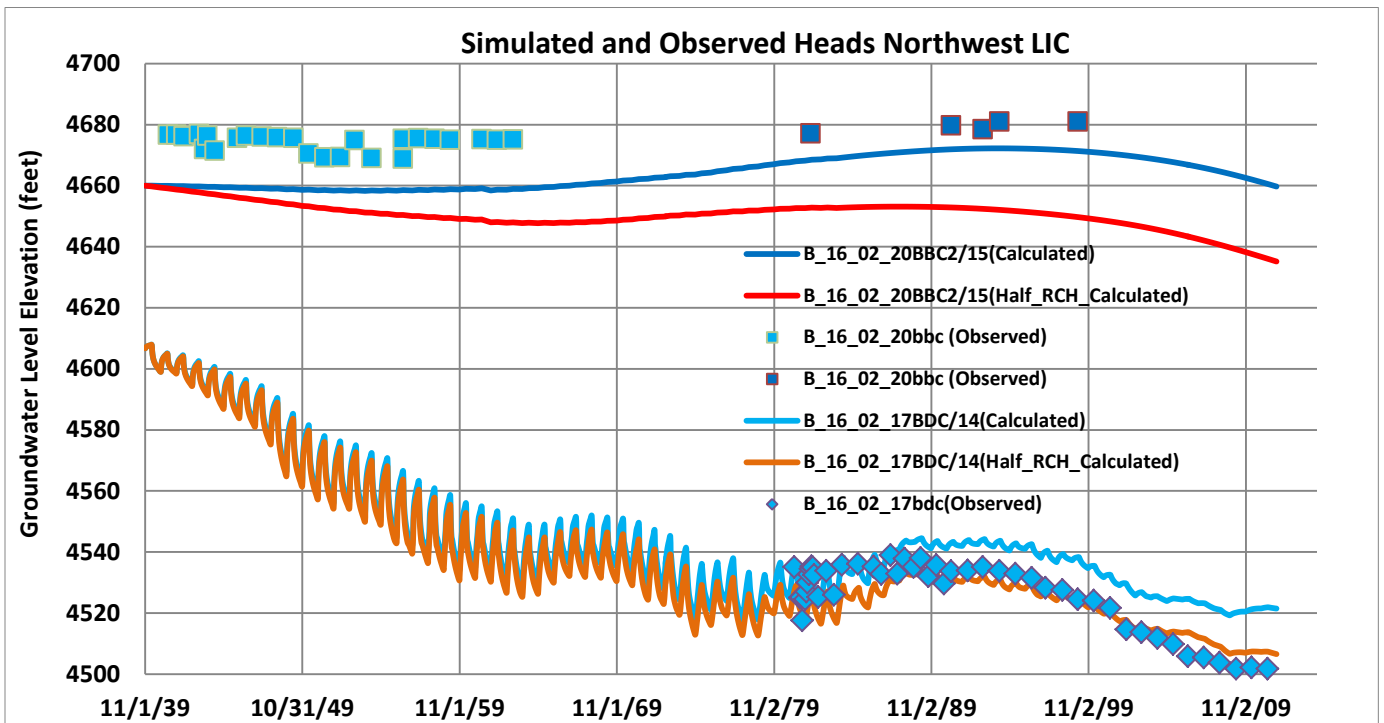


FIGURE C.13. Simulated and Observed Heads Mint Wash/Williamson Valley- Western PrAMA

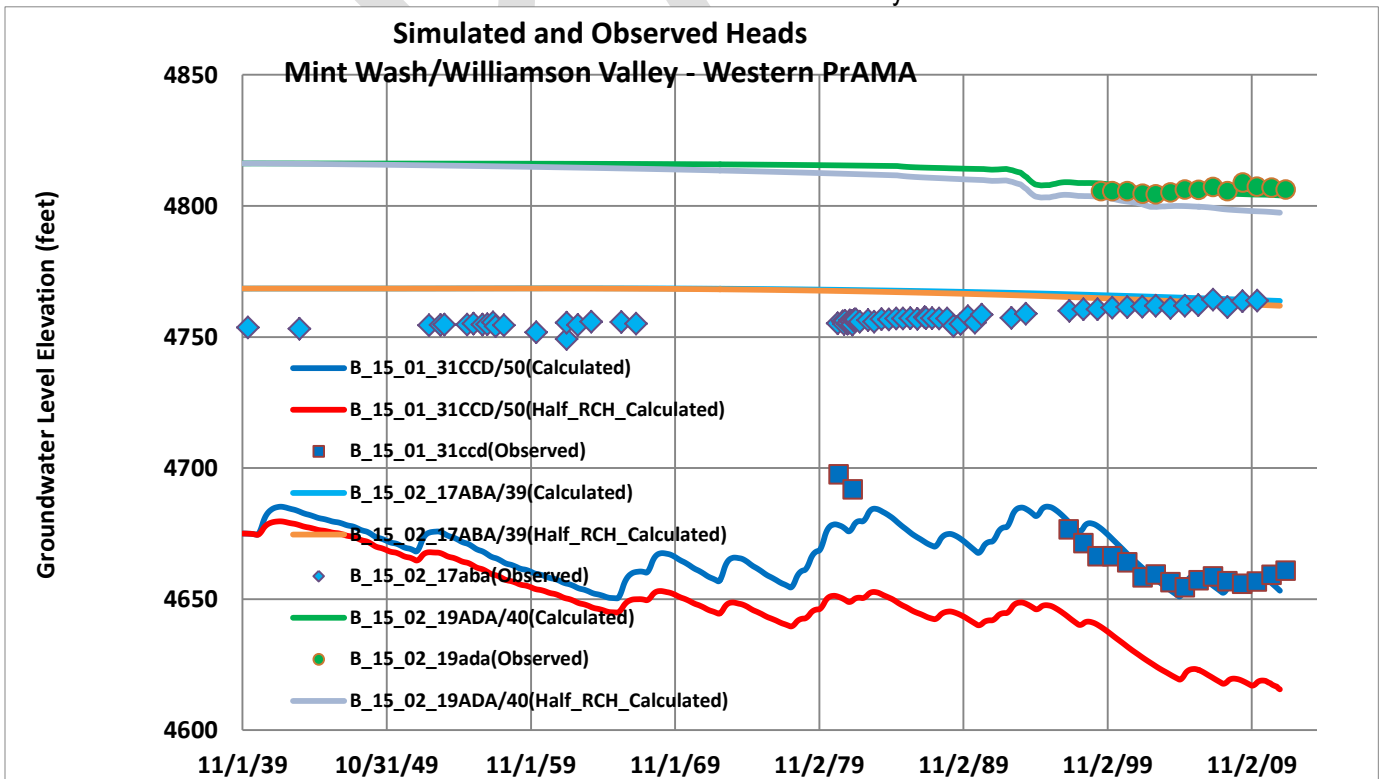


FIGURE C.14. Simulated and Observed Heads Mint Wash/Williamson Valley- Western PrAMA

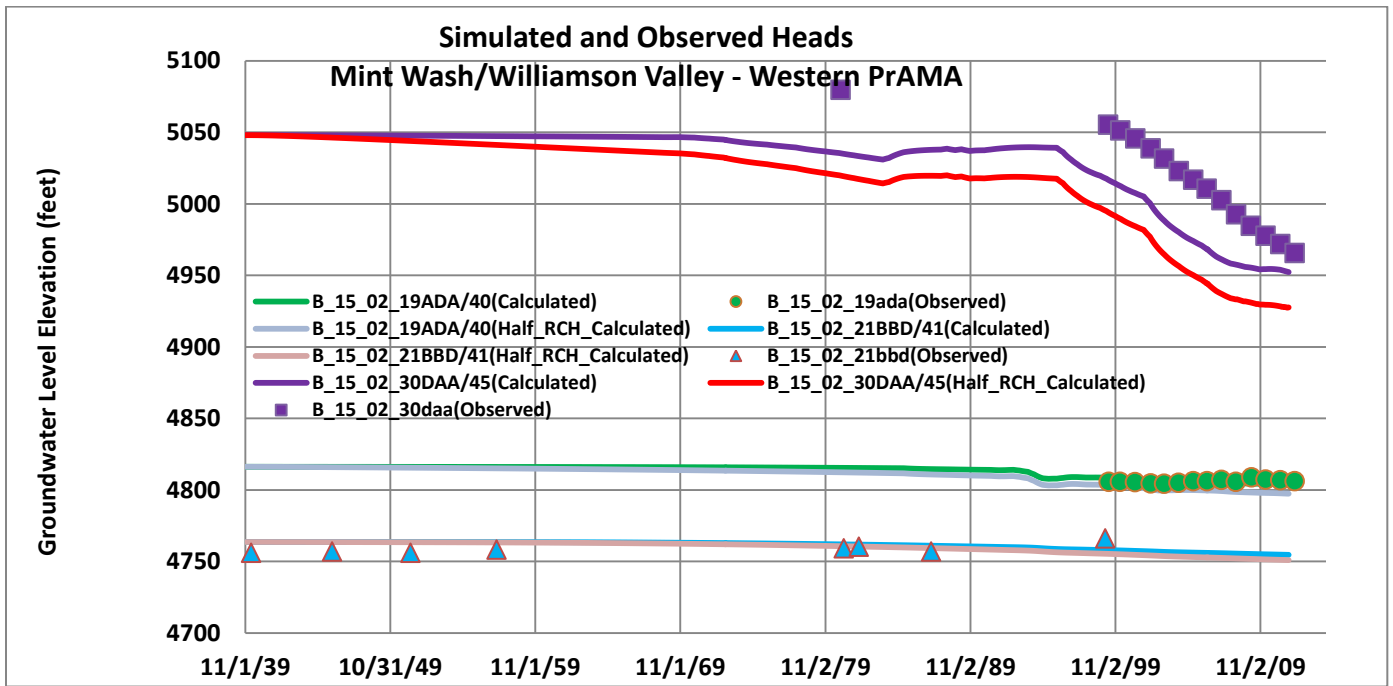


FIGURE C.15. Simulated and Observed Heads Near UAF/LIC Sub-basin Divide

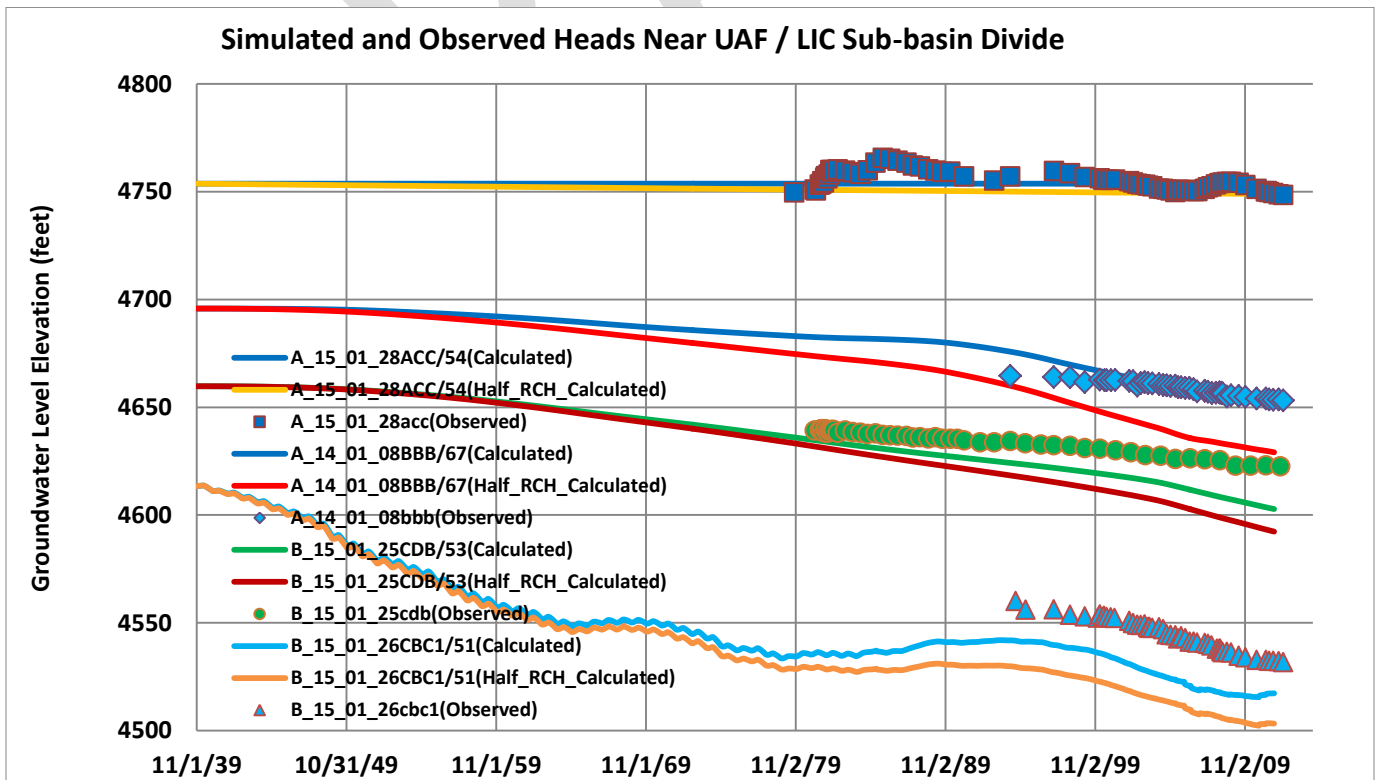


FIGURE C.16. Simulated and Observed Heads, UAF/LIC Sub-basin Divide (2)

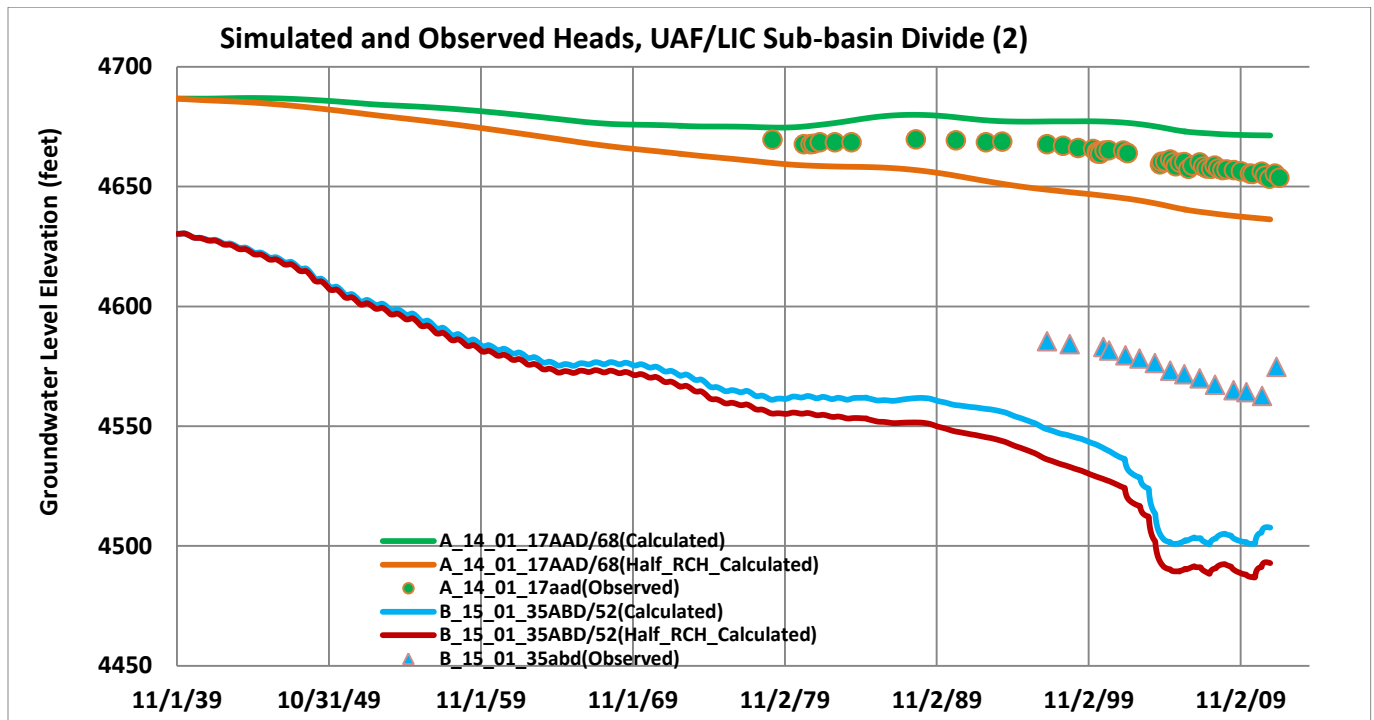


FIGURE C.17. Simulated and Observed Heads PV's Upper Well Field, UAF Sub-basin

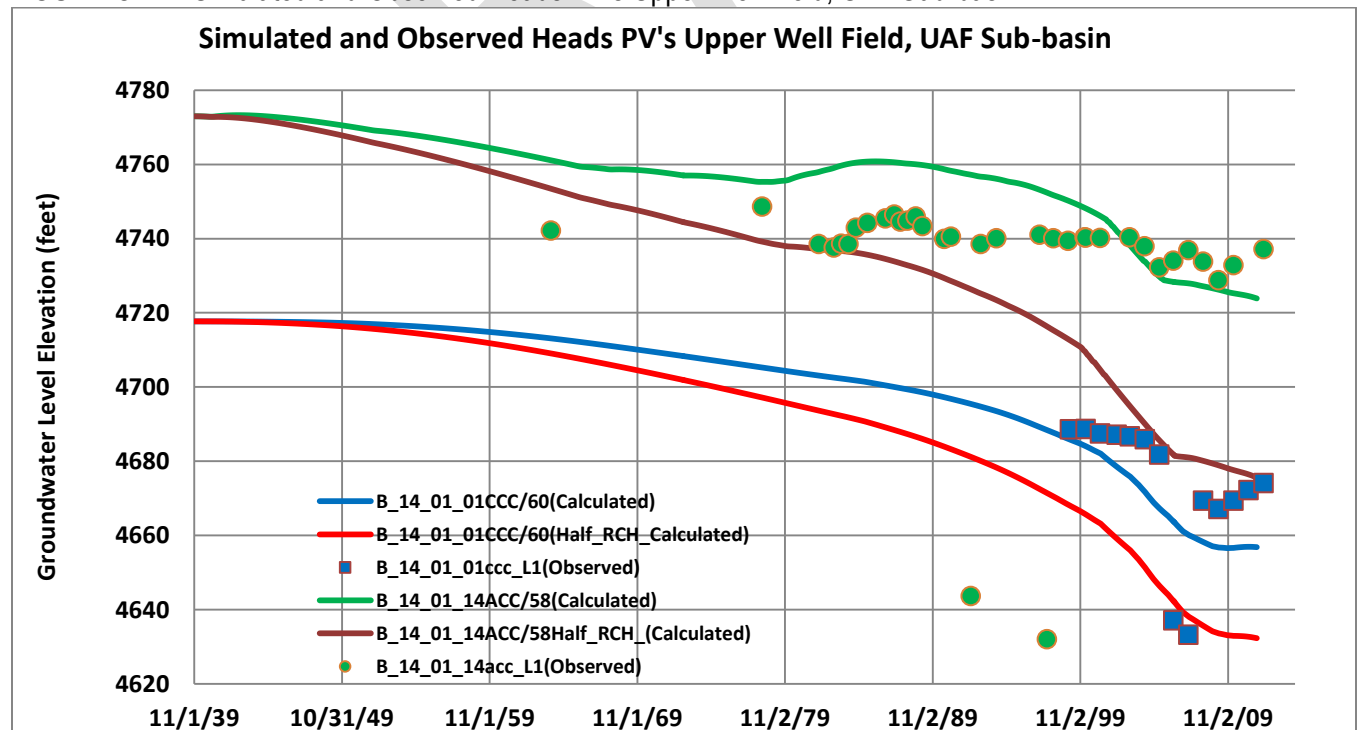


FIGURE C.18. Simulated and Observed Heads PV's Upper Well Field, UAF Sub-basin

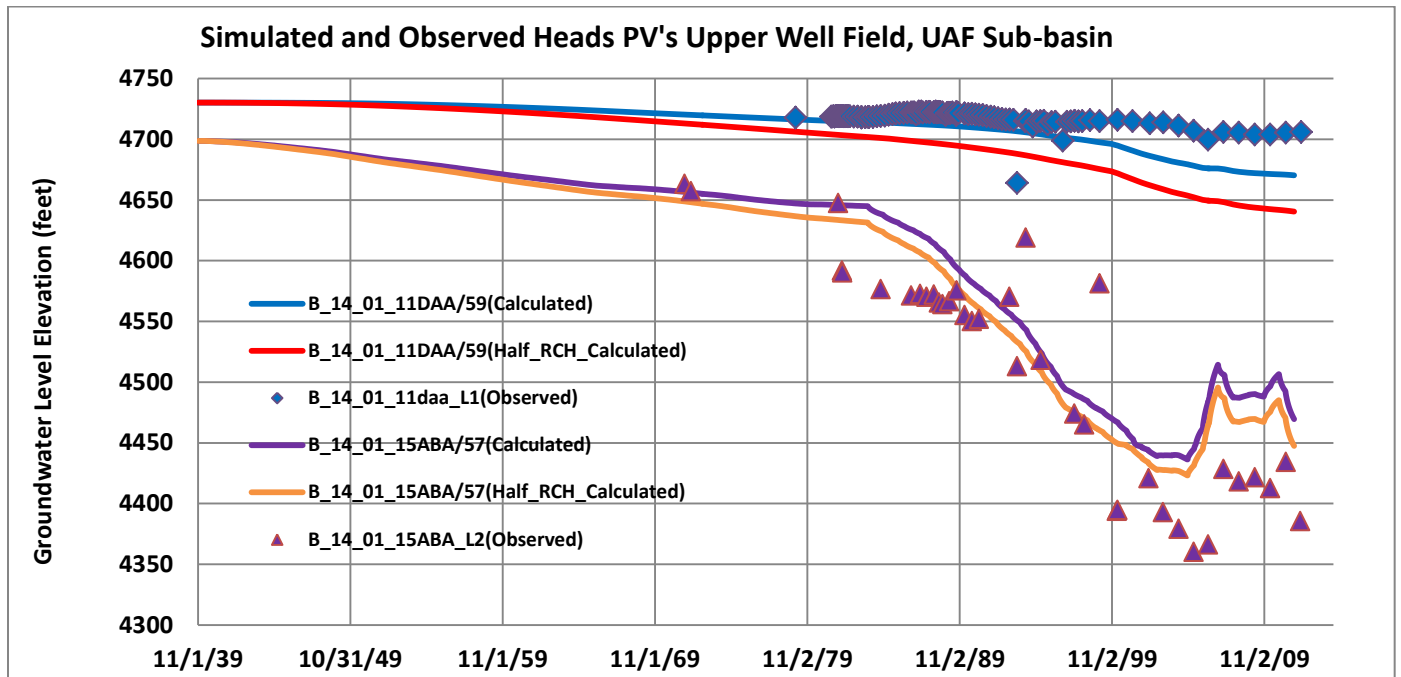


FIGURE C.19. Simulated and Observed Heads Near Lynx Creek, UAF Sub-basin

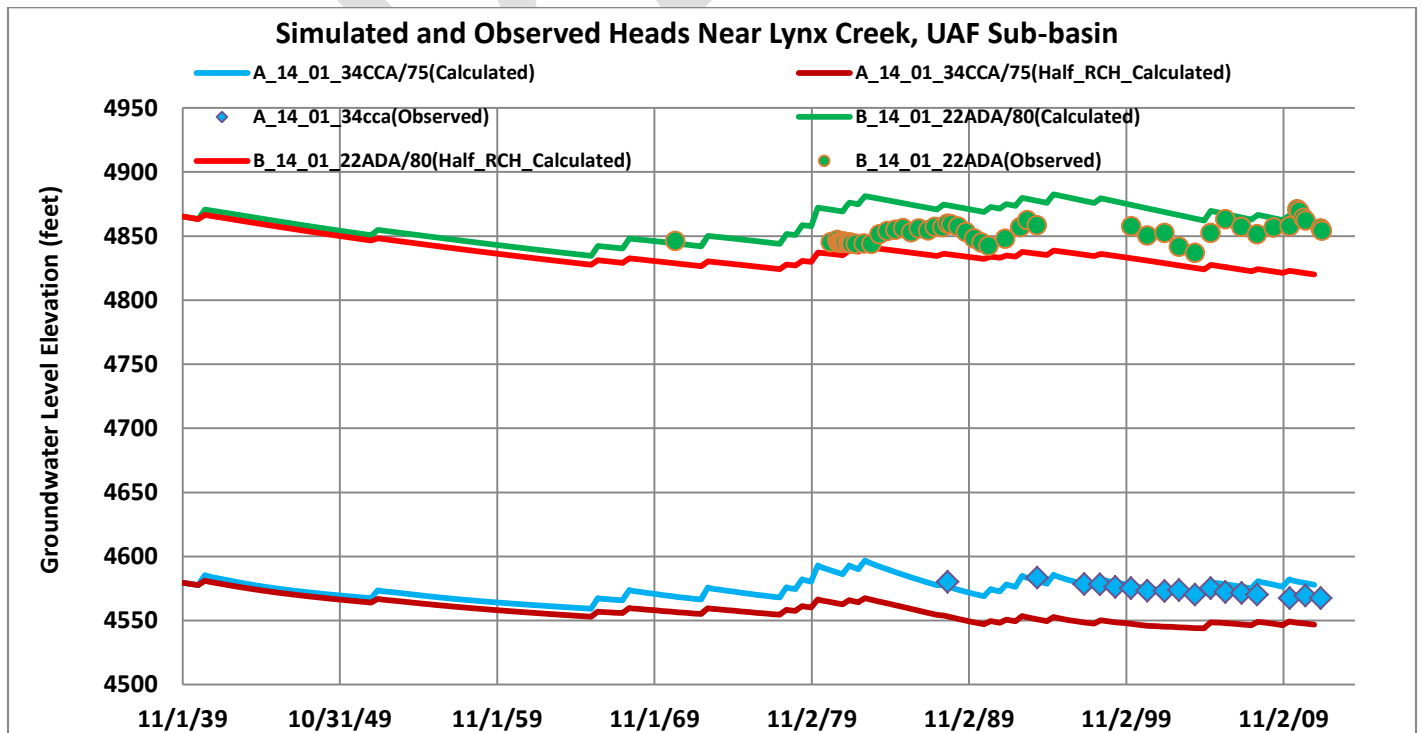


FIGURE C.20. Simulated and Observed Heads Near Lynx Creek, UAF Sub-basin

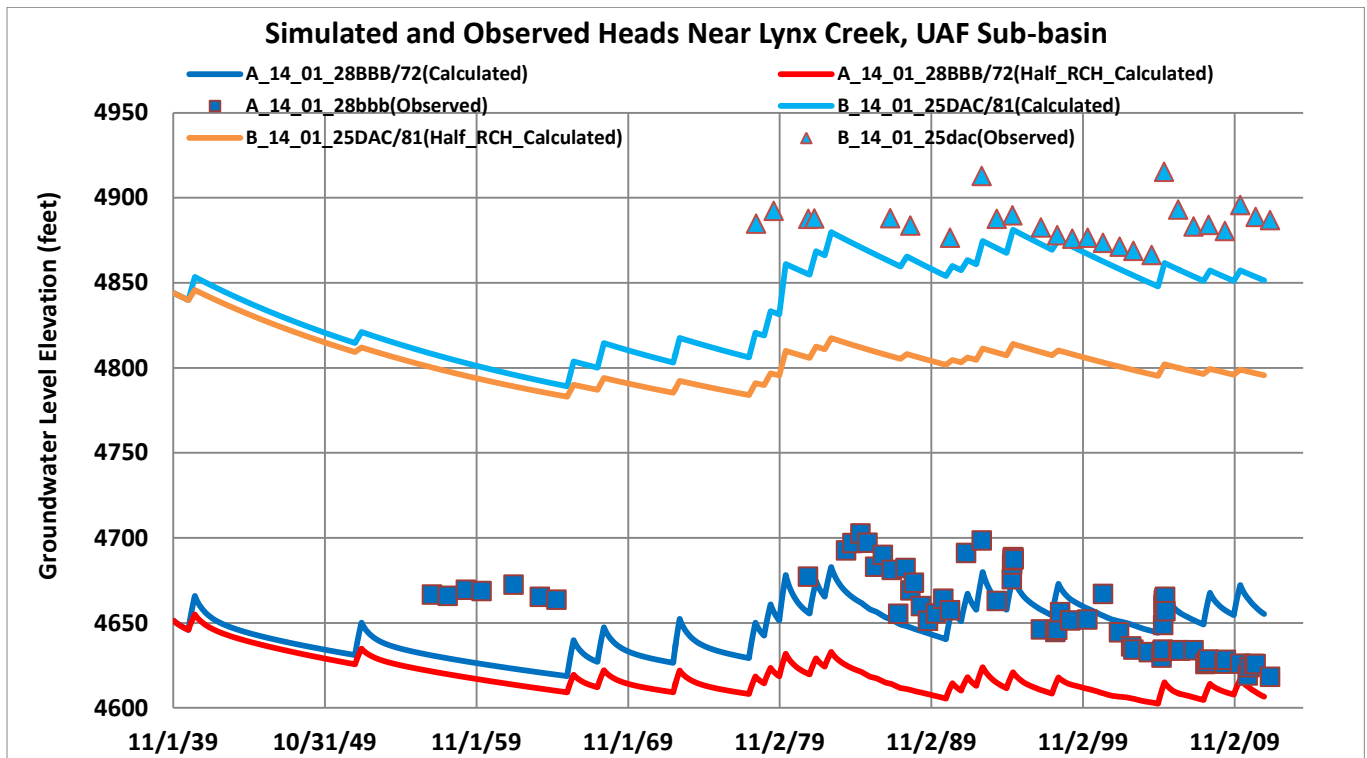


FIGURE C.21. Simulated and Observed Heads Lower UAF Sub-basin

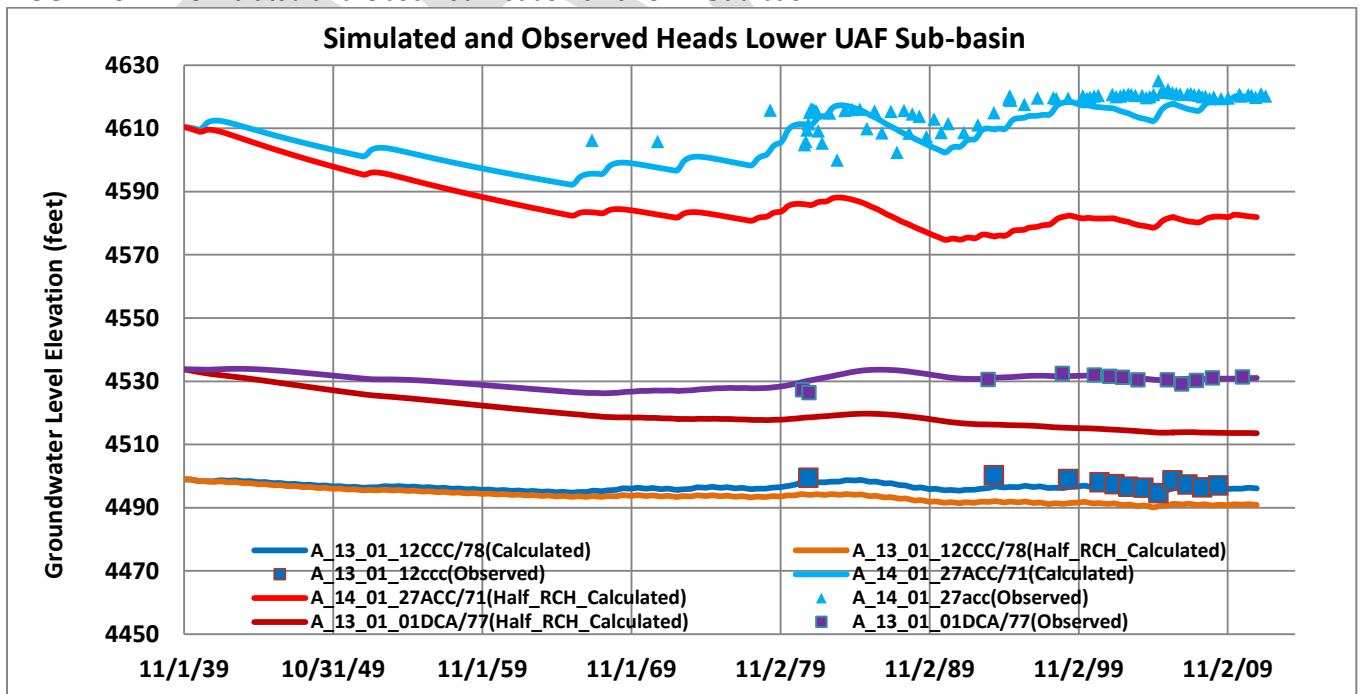
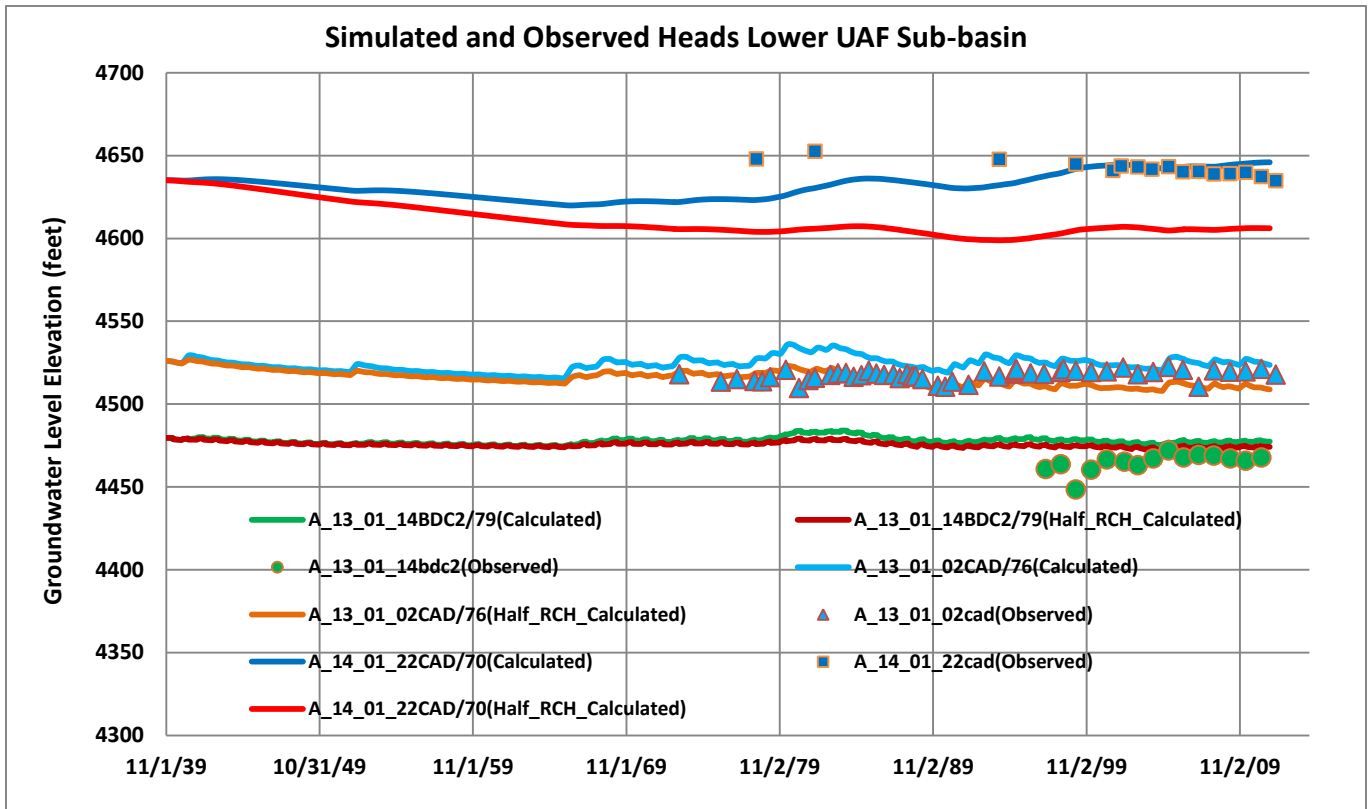


Figure C.22. Simulated and Observed Heads Lower UAF Sub-basin

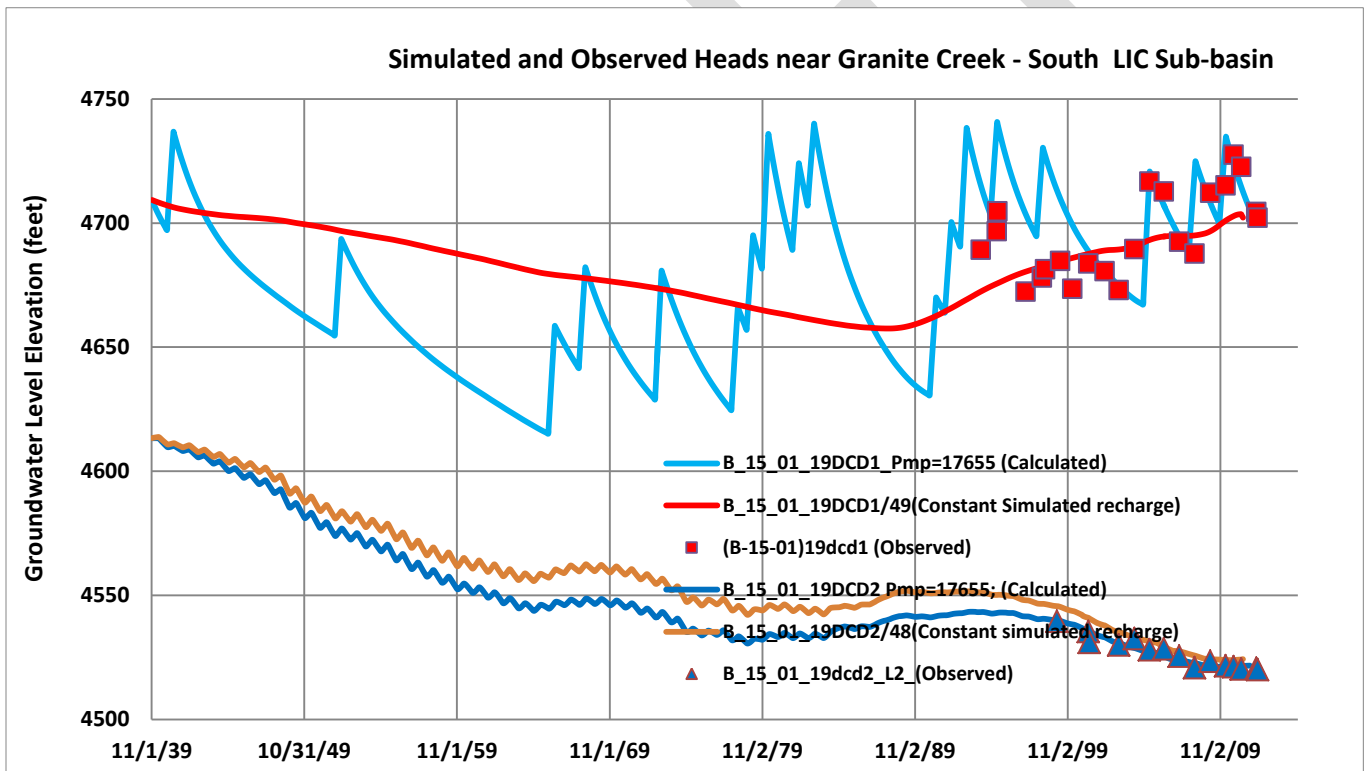


Results of Selected Alternative Conceptual Models (ACM's)

Selected results from a few ACM's are presented below. For brevity, only figures accentuating the ACM characteristics and/or important differences with respect to the base model are presented. A succinct yet effective way to evaluate model error and bias is to 1) compare observed and simulate groundwater discharge representing Del Rio Springs and baseflow along the Agua Fria River; 2) evaluate observed and transient-simulated head mean residuals (either as X-Y plots or histograms), as shown in Figures C.1, C.2, C.27, C.28, C.31 and F.6; and 3) or 3) evaluate steady and transient objection function error. Also see Appendix D for ACM result summary.

ACM 1: Assuming constant (non-variable) natural recharge was assigned during the transient period simulation (1939-2011), as Base-model rates ($\approx 10,000$ AF/yr). Hydrograph C.23. below, shows results when 1) natural recharge is simulated *when* recharge events occur (cool colors, blue lines) for the Base model; and 2) when natural recharge along major tributaries is simulated at long-term constant rates, consistent with *long-term averaged* periodic rates (warm colors, red lines). This is a plausible solution, however applying natural recharge when events occurs result in less model bias.

FIGURE C.23. Simulated and Observed Heads Near Granite Creek- South LIC Sub-basin



ACM 2: PEST optimized K and boundary fluxes, with natural recharge fixed at 5,100 AF/yr. ACM solution in red. Resulting solution showed good simulated head separation between layers 1 and 2 through central portion of model domain. However, lower long-term natural recharge rates resulted in under-simulated groundwater discharge, making this ACM not plausible.

FIGURE C.24. Simulated and Observed Groundwater Discharge, Del Rio Springs Base Model and ACM constraining Natural Recharge at 5,100 AF/yr

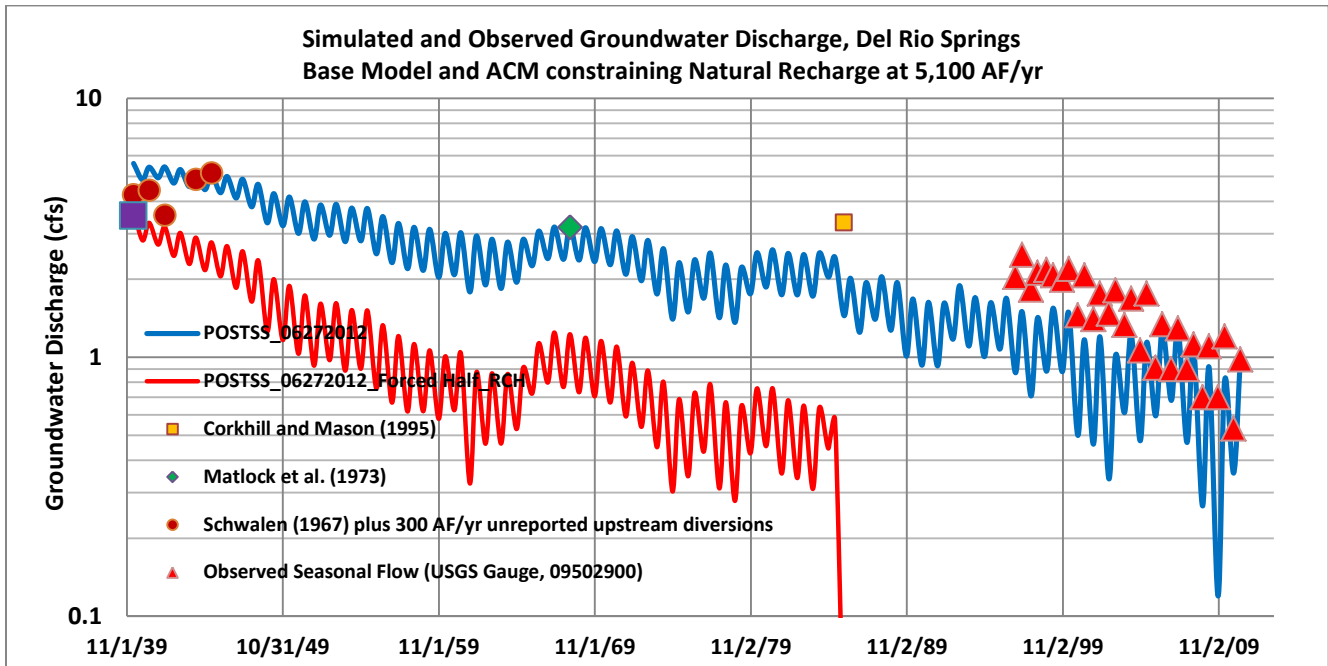
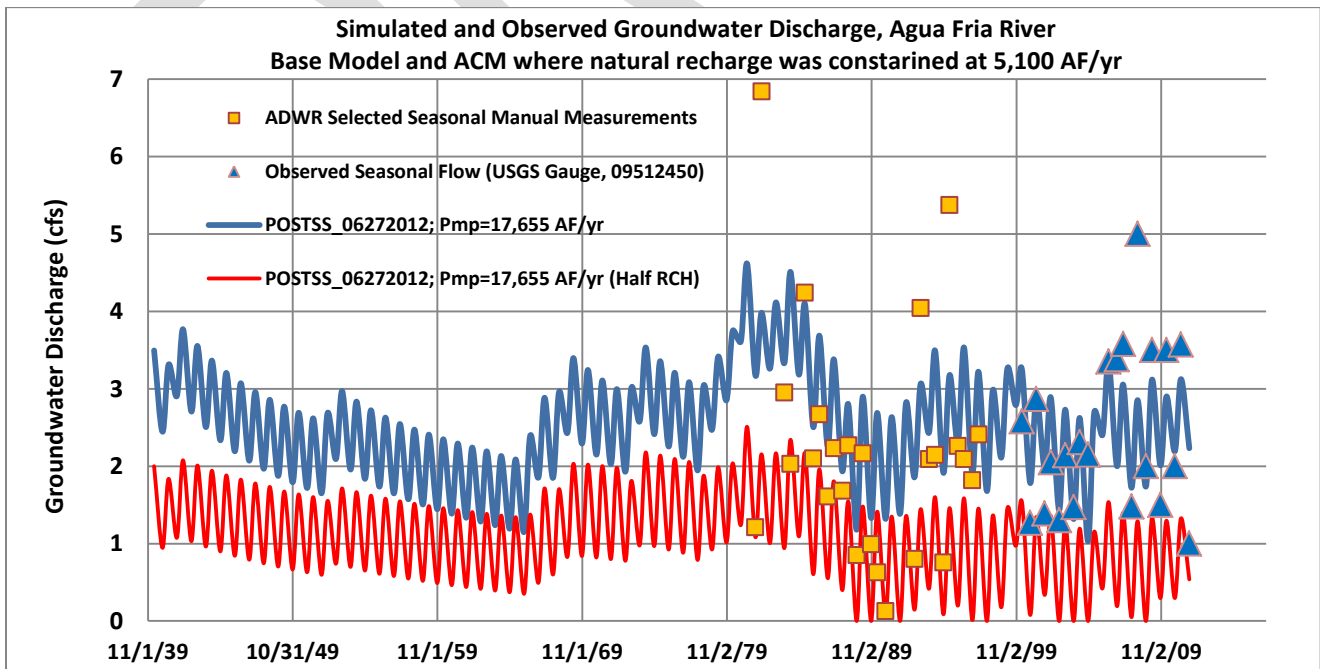


Figure C.25. Simulated and Observed Groundwater Discharge, Agua Fria River Base Model and ACM where natural recharge was constrained at 5,100 AF/yr



ACM 3: Assuming no underflow out of the UAF Sub-basin, but otherwise solution was optimized by PEST, resulted in lower long-term annualized natural recharge of 8,590 AF/yr. Observed and simulated groundwater discharge at Del Rio and Agua Fria River: 1) Base model (blue) and 2) an ACM. [Also see Appendices F and G]. Solution provides a plausible - but less likely- solution, due to under simulated flow bias representing Del Rio Springs and the over simulated flow bias representing the Agua Fria River.

FIGURE C.26. Simulated and Observed Groundwater Discharge, Del Rio Spring Base and ACM assuming no underflow from UAF Sub-basin

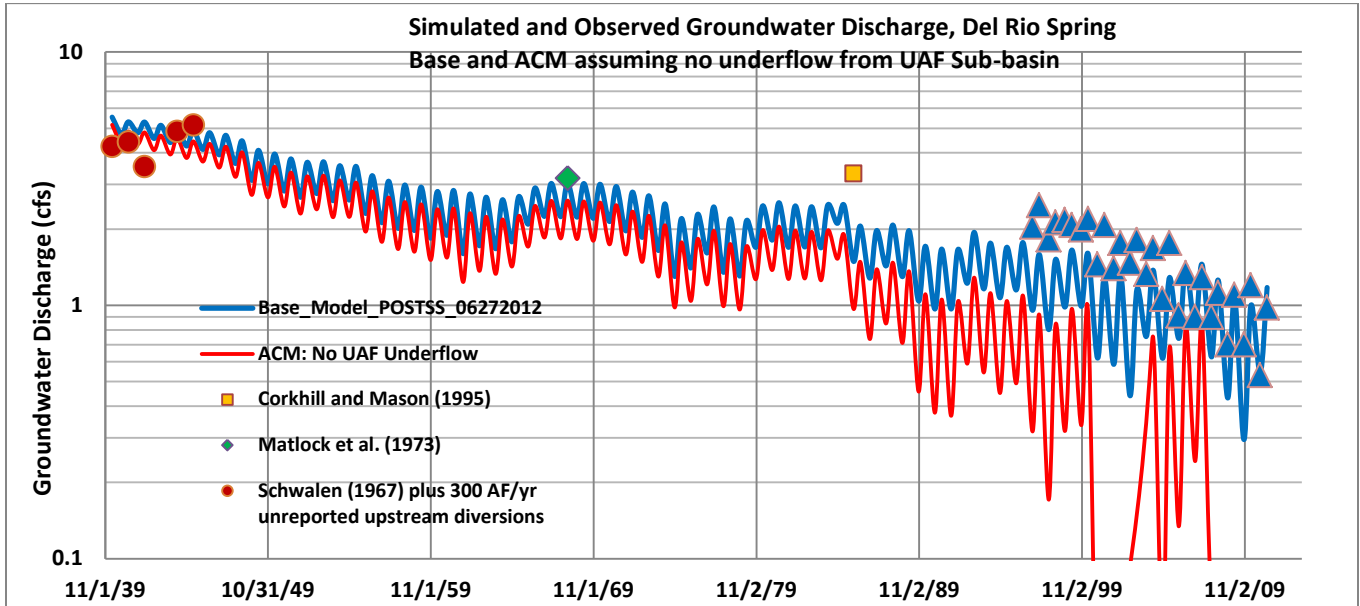


FIGURE C.27. Simulated and Observed Groundwater Discharge, Agua Fria River Base and ACM assuming no underflow from UAF Sub-basin

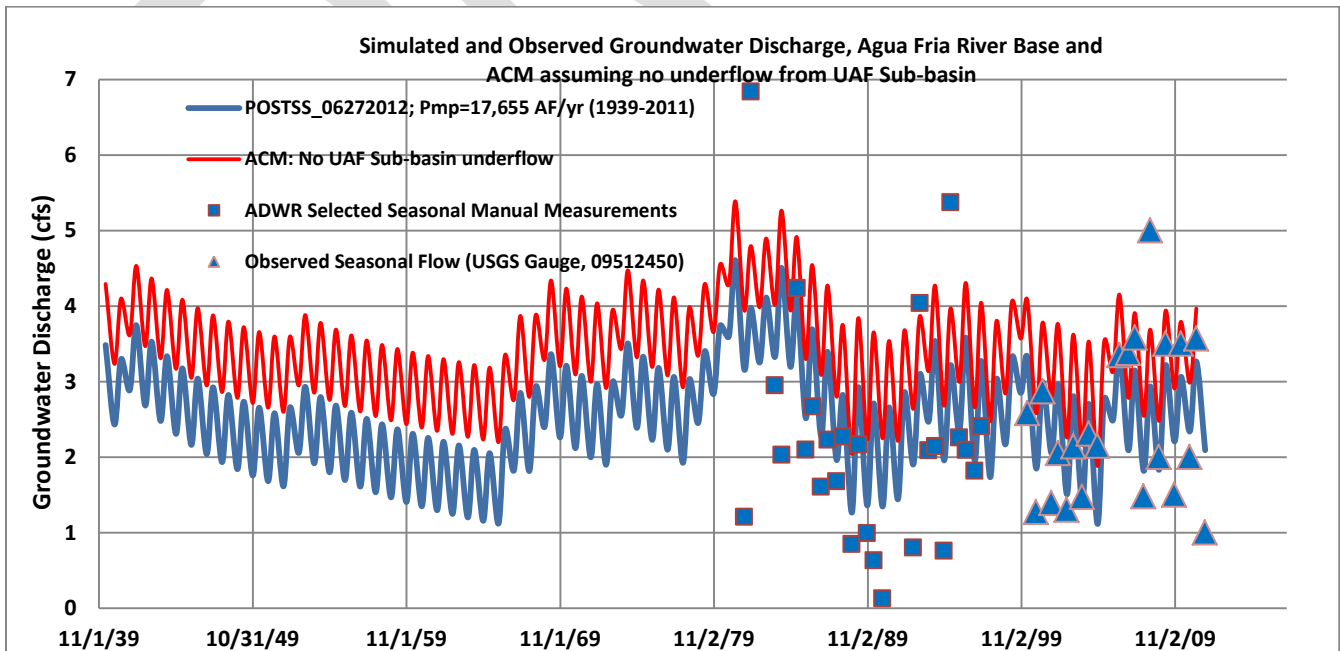


FIGURE C.28. Base Model: Simulated minus observed residual plots

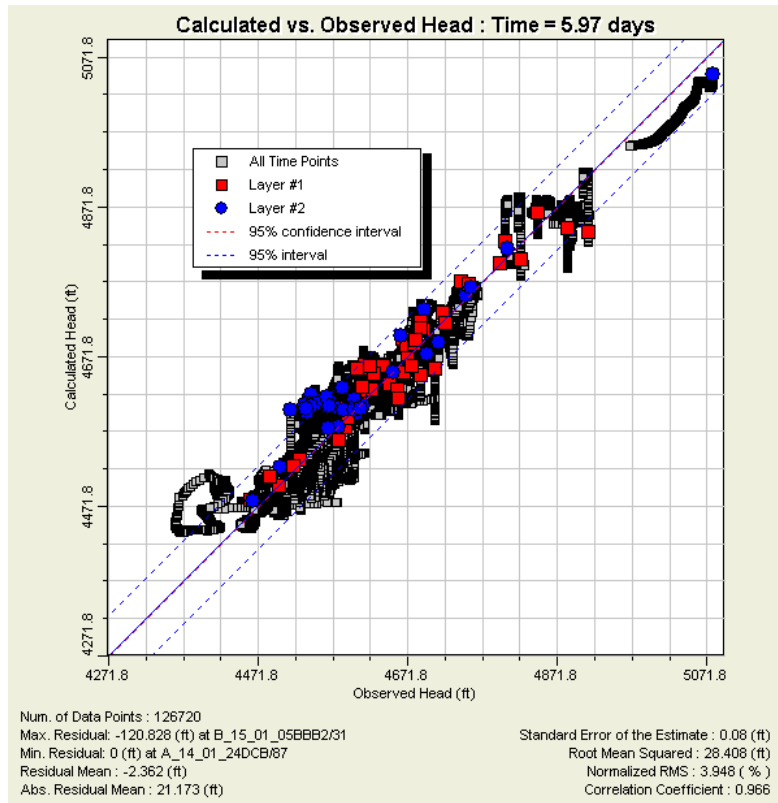
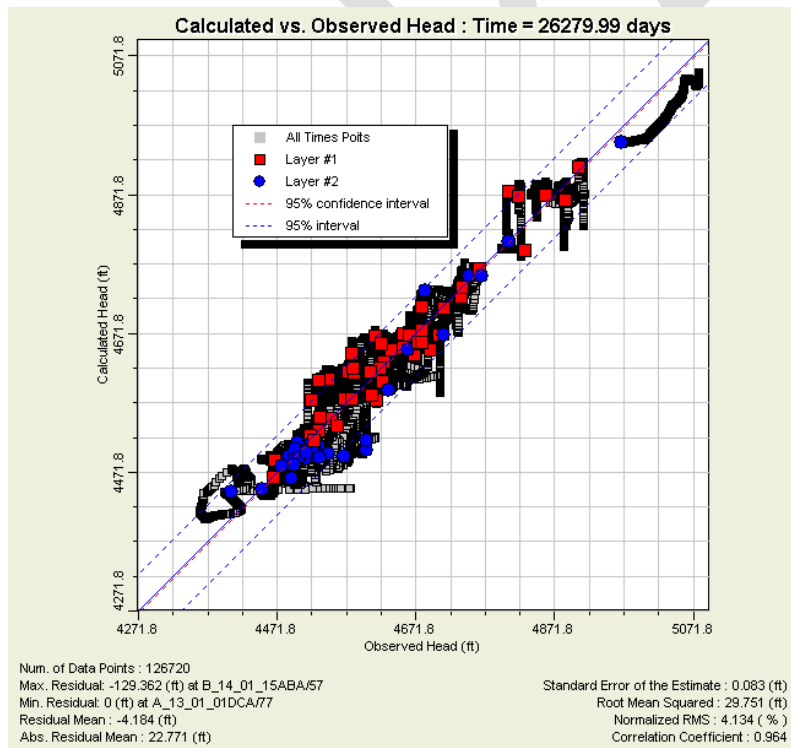


FIGURE C.29. ACM 3: No underflow from UAF Sub-basin



ACM 4: (PreSS): Initialization based on assumption of no pumpage and no incidental agricultural-related recharge circa 1939, as posed by Corkhill and Mason (1995). Long-term natural recharge rate =11,120 AF/yr. In general, this ACM was one of the least biased model solutions evaluated over transient conditions. Plausible solution.

FIGURE C.30. Simulated and Observed Groundwater Discharge, Del Rio Springs

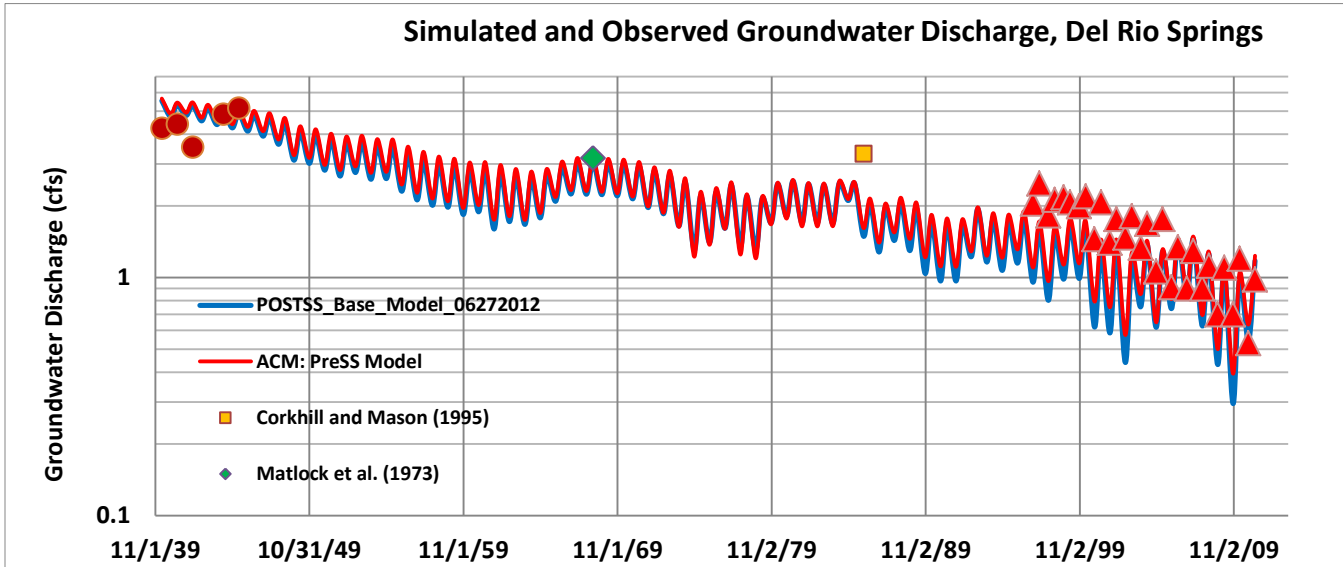


FIGURE C.31. Simulated and Observed Groundwater Discharge, Agua Fria Base and Base Model and ACM assuming true pre-development steady conditions

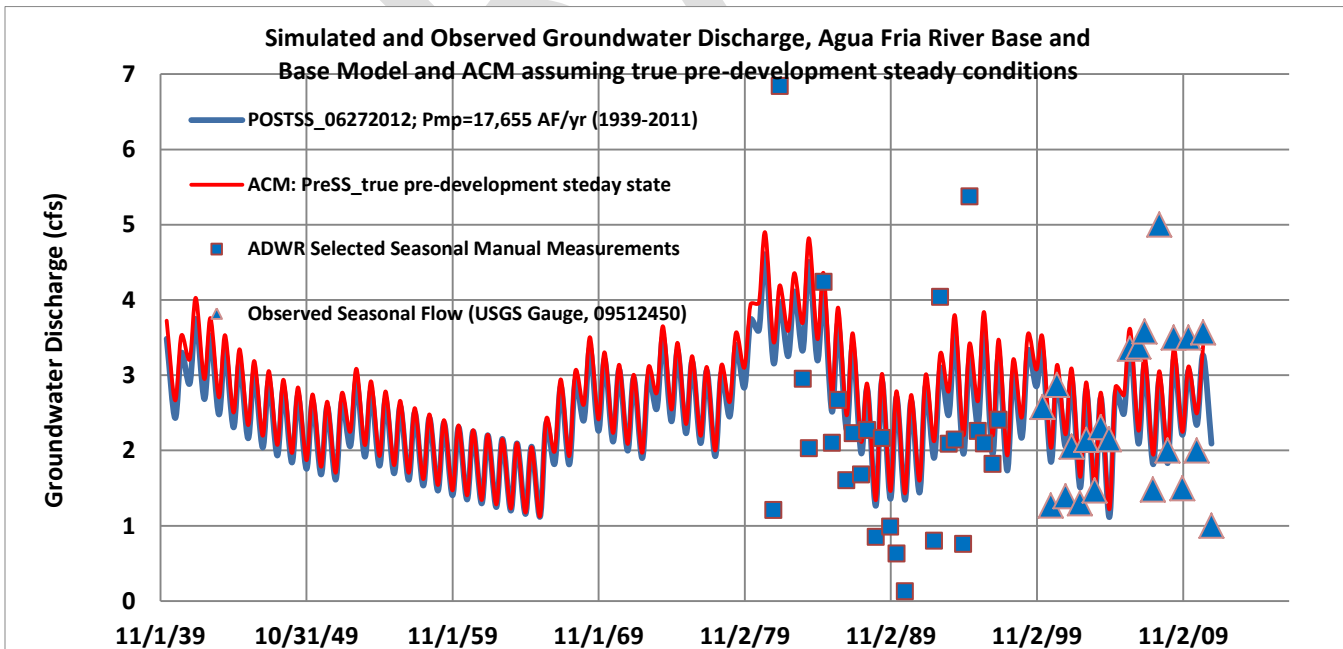
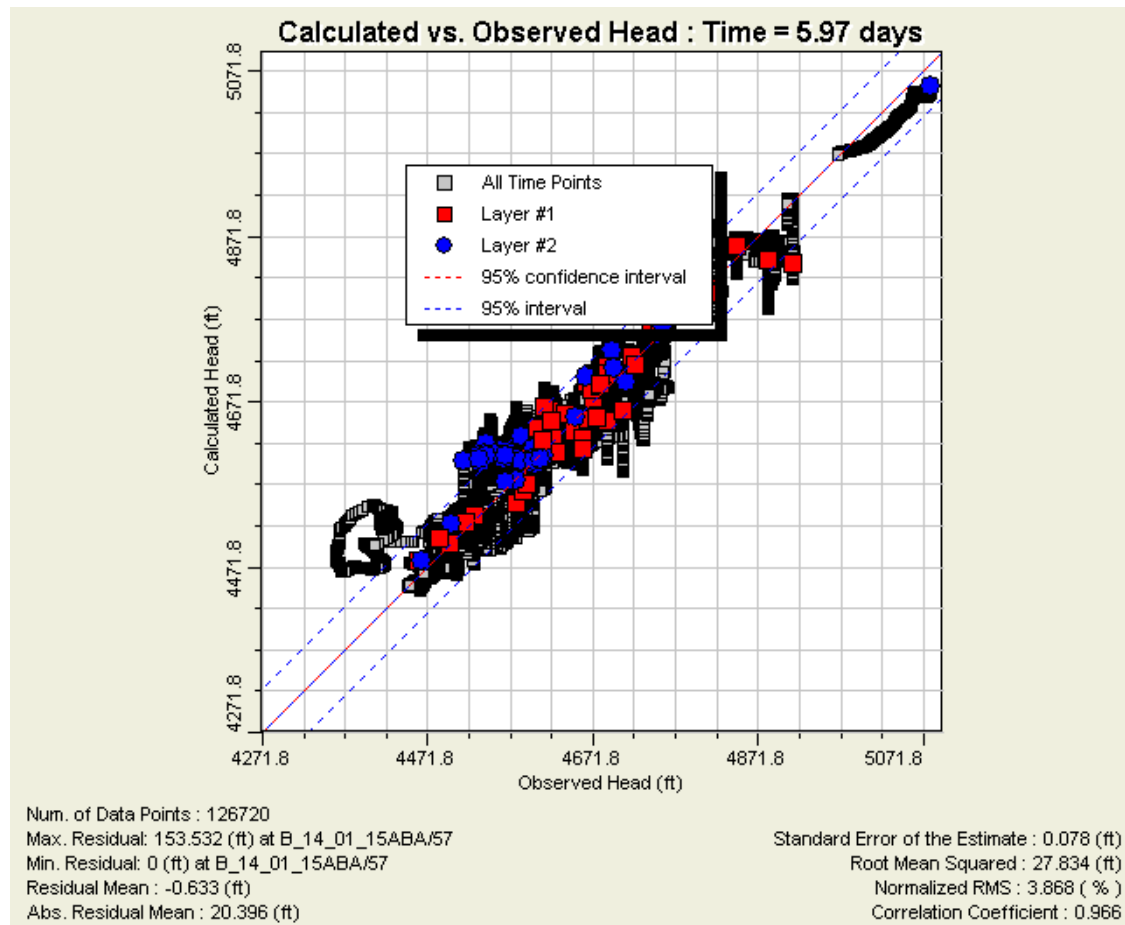


FIGURE C.32. Transient head residuals for AMC 4 assuming true pre-development conditions for initialization



ACM 5: Lower prior information weighting (long-term natural recharge rate = 10,610 AF/yr). Initialization based on using lower values of prior information, assigned to three LVU K zones (K23, K25 and K26). Plausible solution; best simulated flow of Del Rio Springs.

FIGURE C.33. Simulated and Observed Groundwater Discharge, Del Rio Springs

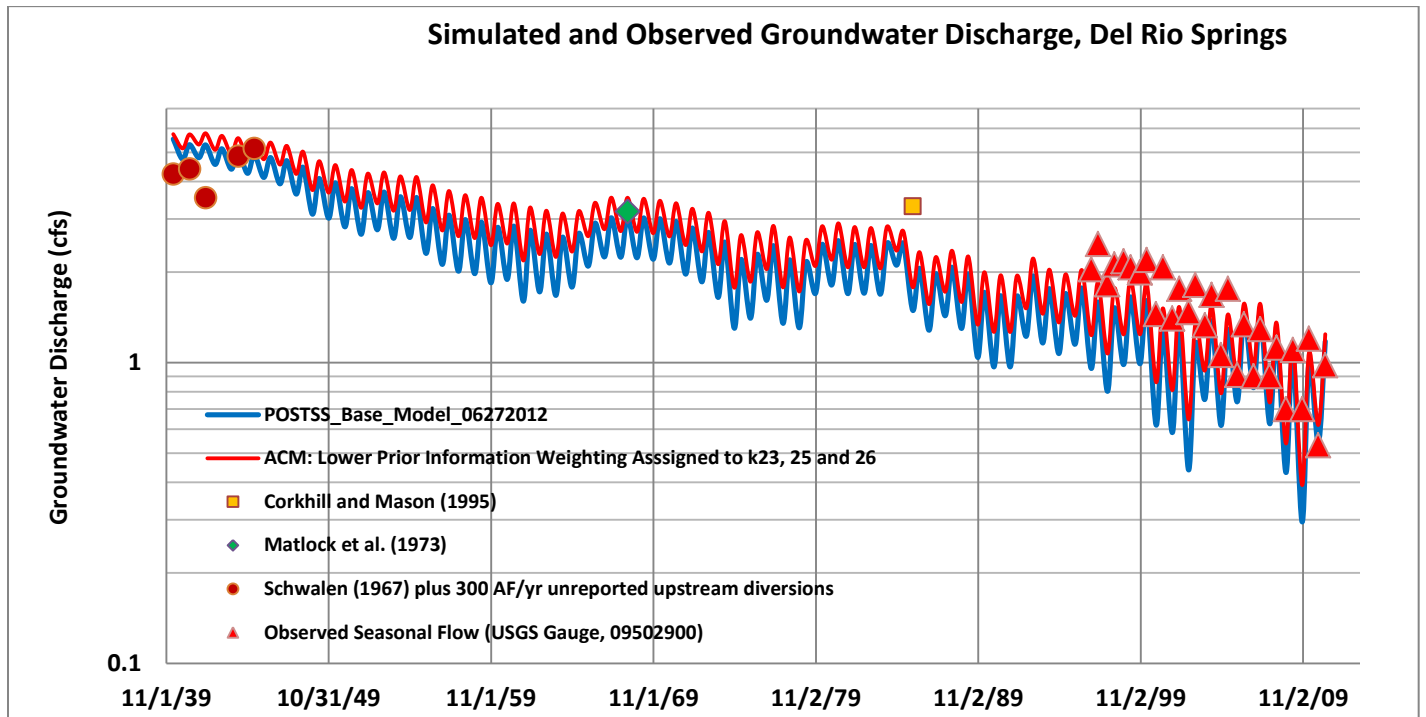


FIGURE C.34. Simulated and Observed Groundwater Discharge, Agua Fria River Base and Base Model and ACM assuming true pre-development steady conditions

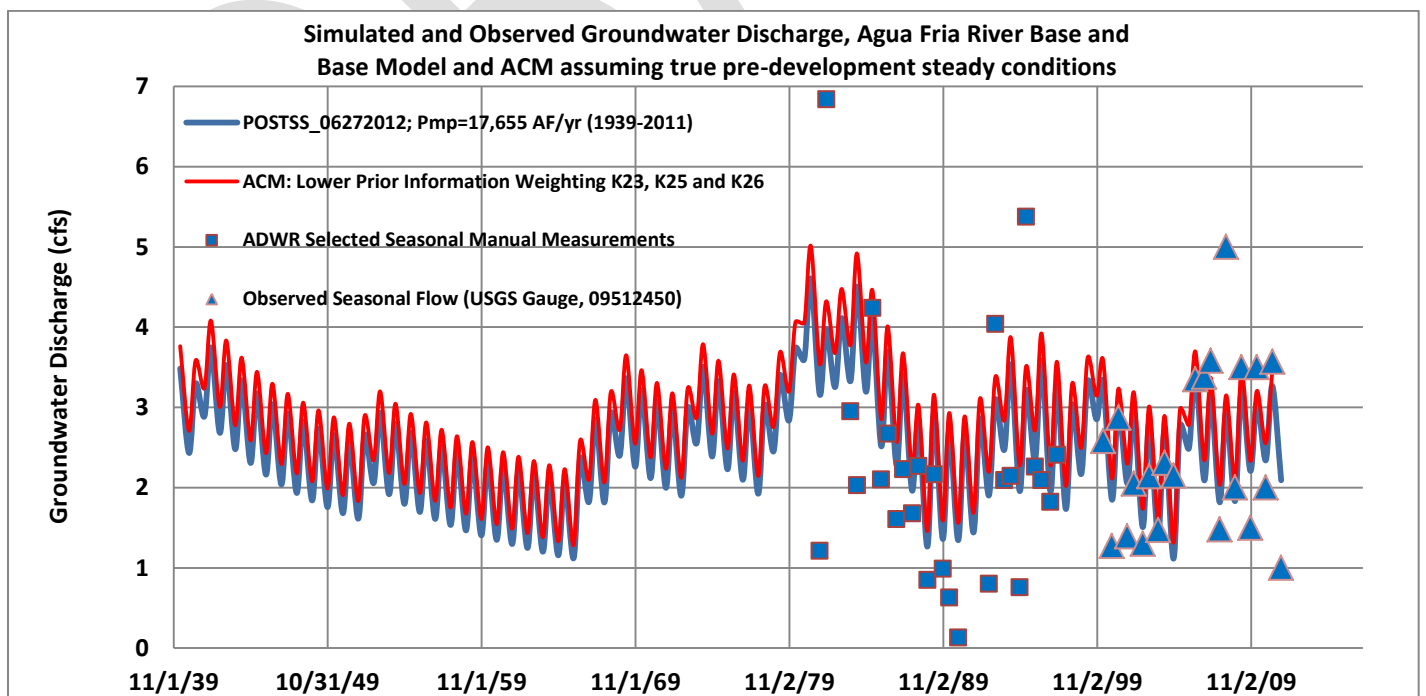
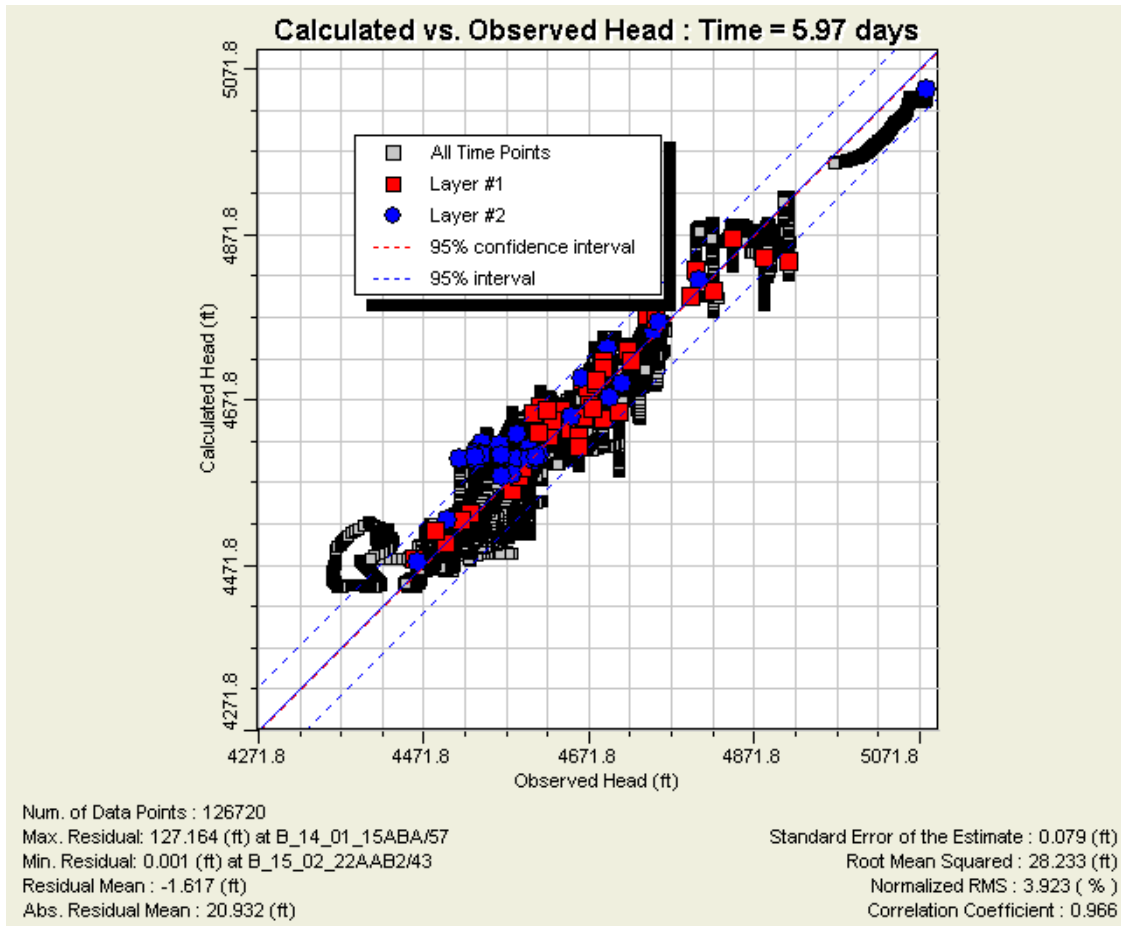


FIGURE C.35. ACM 5



APPENDIX D:

Information about Model Calibration and Alternative Conceptual Models

DRAFT

Appendix D

Information about Model Calibration and ACM's

The steady state calibration and portions of the transient calibration were optimized using the inverse modeling tool, PEST. Because of high CPU demands associated with PEST in the transient-simulation mode, it was more practical to estimate most model parameters (for numerous ACM's) over steady flow conditions and evaluate the quality of each tested ACM over transient conditions using forward (traditional) modeling techniques. Nonetheless, inversion statistics including parameter sensitivity were obtained for both steady and transient flow conditions. [Note that parameters estimated in the transient mode include storage, natural recharge, boundary conditions; note that K-zones were activated in the non-linear regression process in order to obtain information about parameter sensitivity, parameter covariance and parameter correlation.] See sections below.

It should be noted that most of the fundamental model parameters are more sensitive over steady state conditions with respect to (exclusively) transient simulations conditions, even though the transient period is 72 years; these results thus indicate the importance of initialization and parameter conditioning for the subsequent transient simulation. Unless otherwise noted, high model error, as defined by the objective function (Φ) quantified in the steady solution, is generally associated with higher levels of model error and bias in the transient solution. A notable exception is the ACM assuming true pre-development initialization, as posed by Corkhill and Mason (1995), where although the steady state error was relatively high (185), transient-based model error and bias was low.

Note that not all steady ACM solutions were fully evaluated, for statistical purposes, over transient conditions. Nonetheless, many different ACM's were evaluated over steady flow conditions including ; 1) alternative initializations; 2) alternative spatial recharge distributions and constraints; 3) alternative boundary conditions, alternative treatment of prior-information included within the inverse model process and alternative model layering elevations. Alternative K-distributions were also evaluated in combination with alternative recharge distribution area. Due to varying degrees of parameter dependence between K and recharge, it is necessary to evaluate combinations of K and recharge distribution. While minor variations of the K-distributions shown in Figures E.1, E.2 and E.3 were not acutely sensitive, more significant alterations of K-distributions shown in Figures E.1, E.2 and E.3 may yield significant differences. Based on available data and the ACM tested herein, the distributions shown in Figures E.1 through E.3 yield relatively low model error and bias, given the assigned distribution and magnitude of natural recharge. Note that there may be untested, alternative K-distributions in combination with alternative natural recharge distributions that yield lower model error and bias, with respect to observation data. In addition, there may be data collected in the future that provide model solutions with lower model error and bias.

TABLE D.1. Relation between Estimated Recharge and Model Error, Steady State PHI

ACM / Nat RCH Model All models applied recharge (RCH cells) along portions of Granite & Lynx Creek and Agua Fria River Blue = Solution plausible; Green = Plausible solution, but less likely; Red = Solution much less unlikely	Steady State Annualized Natural recharge using both stream cells and recharge cell	
	Total rate of simulated natural recharge AF/yr Steady State	PEST Φ Steady State
Base Model	9,167	175.7
ACM 5: Lower prior info weighting on 3 LVU K zones ^b	9,910	173
ACM: No prior information	10,770	171.2
ACM 6: Underflow into model assigned near Watson Lake	9,474	174.3
ACM 4: Initialization assumes true pre-development ^a	10,613	185
ACM 9: Same initial stresses applied in USGS NARGFM	8,340	175.5
ACM: Same as Base except Layer 2 thickness=250 feet	8,600	182.4
ACM: "Base except Layer 2 thickness=250 feet; lower prior ^b	10,000	175.8
ACM: Same as Base except Layer 2 thickness=400 feet	9,050	177.3
ACM: "Base except Layer 2 thickness=400; lower prior ^b	11,160	172.6
ACM: Same as Base except Layer 1 lowered by 15 feet	8,840	182.1
ACM: " Base except Layer 1 lowered by 15 feet; lower prior ^b	10,460	178.3
ACM: "Same as Base except Layer 1 increased by 15 feet	9,890	170.7
ACM: "Base except Layer 1 increased by 15 feet; lower prior ^b	10,090	169.3
ACM 3b: Assumed steady state baseflow mean = 3cfs	9,336	170.5
ACM 3: No underflow in UAF Sub-basin* 12 parameter	7,780	178
ACM 3a: No underflow in UAF Sub-basin 13 parameter	8,080	177
ACM 2: Natural recharge PEST constrained to ~5,000 AF/yr	5,000	201
ACM 8: MFR-to-stream recharge constrained to 1:1	5,200	241
ACM 10: Constrained PEST to Lowest Possible Nat RCH	4,310	224
ACM 11: Limit LIC Sub-Basin Underflow to 100 AF/yr	5710	189

Φ =Objective function, sum of weighted square residuals. For steady state layer 1 head weights based on $\sigma = 20$ ft.; steady state layer 2 head weights based on $\sigma = 10$ ft.; steady flow at Del Rio based on $\sigma = 0.5$ cfs; steady flow at Agua Fria groundwater discharge based on $\sigma = 1.0$ cfs; Used consistent head and flow weighting Testing of other, alternative, weighting factors were found to be moderately insensitive about the weights assigned/applied herein. *Although steady flow error is similar to base model error, the transient objection function error is 28% greater than base model error. ^aSteady state ACM assumes no groundwater pumpage or AG-related incidental recharge; although steady Φ is relatively high, higher natural recharge and underflow rates yield low transient model error and bias. ^bPrior information on K23, K25 and K26 (log-transformed) lowered from 6, 3.33 and 6 to 2,1 and 2, respectively. ACM 8 results in significant model error and bias when half of all natural recharge is applied along peripheral model areas; this result further demonstrates that most natural recharge occurs along major streams and tributaries. ACM 9 represents only the stresses the USGS NARGFM applied for initialization; that is, no pumping was assigned, and 2,041 AF/yr of incidental agricultural recharge was applied in the LIC Sub-basin. The K distributions, layering and recharge distributions associated with AMC 9 are not consistent with the USGS NARGFM. ACM 3b solution results in relatively high rate of underflow from UAF Sub-basin; represents seasonal low baseflow rates with best accuracy of any ACM, but with sustained underflow bias along Agua Fria River. Thus, the ACM 3b solution is plausible- but less likely - with respect to Base Model due to under-simulated flows; possible increases in transient recharge may improve solution. See Appendix G. Base model layer 2 thickness generally assigned at 300 feet.

Transient State (1939-2011) Solutions

Measures of transient model error include the mean residual error and the absolute mean residual error, as presented below in Table D.3. for a few ACM's below. In the case presented below, the residual (Resid) errors represent *simulated minus observed heads*, which were then interpolated with respect to model time-step using the observed indexed-target wells (126,720 head residual samples): Note that a negative residual mean value indicates that the model heads are below the observed heads (i.e., under simulated).

TABLE D.2. Relation between Estimated Recharge and Model Error, Transient State Mean Residual Error

ACM / Nat RCH Model All models applied variable recharge (stream and RCH cells) along portions of Granite & Lynx Creek and Agua Fria River unless otherwise noted. Blue = Solution plausible; Green= plausible solution, but less likely; Red = Solution not likely	Transient State Long-term average (μ) annualized natural recharge rate (72 years)	
	Natural Recharge AF/yr	Resid μ (ft); abs Resid μ (ft)
Base Model	9,920	-2.36 21
ACM 5: Lower prior information weighting on 3 LVU K-zones	10,610	-1.62 21
ACM 6: Underflow into model assigned near Watson Lake	10,220	-1.41 21
ACM 4: Initialization based in true pre-development ^a	11,120	-0.633 20
ACM 3: No underflow in UAF Sub-basin(12 parameter) ¹	8,590	-4.18 23
ACM 3a: No underflow in UAF Sub-basin(13 parameter) ²	8,780	-5.36 23
ACM 7: Base model except reduced general Sy from 9% to 7% and reduced Sy (Lynx Creek) from 16% to 13%.	9,920	-8.62 25
ACM 1: Base with all constant rate of natural recharge**	9,352	+4.01 21
ACM: Base model but Natural recharge reduced by half	~5,100	-13.3 26
ACM 2: Natural recharge PEST constrained to ~5,000 AF/yr*	~5,100	-8.57 27

Transient raw head residual (simulated minus observed). A negative residual (resid) indicates under-simulated heads (i.e., simulated head are below observed target). 126,720 head targets used in the transient analysis including 88 indexed observation wells interpolated to time-steps. *Under simulated groundwater discharge. See Appendix C. **Note that a uniform distribution of recharge over time (72 years) resulted in a small positive model bias. This result is different than, effectively, all other ACM's, which applied natural recharge at long-term annualized rates of less than 10,000 AF/yr. Applying natural recharge at a constant rate over time resulted in more early time recharge and thus less early-time simulated drawdown. It is interesting how the "front-loading" of natural recharge resulted in sustaining layer 2 heads, and that the relatively high rate of recharge imposed in the variable recharge models between 1973 and 1995, has in effect, "lagged behind", at least with respect to available target data and the residual calculations. ¹Over simulation of groundwater discharge at Agua Fria River, under-simulation of groundwater discharge at Del Rio; see Appendix C above. ²Decreased natural recharge in UAF sub-basin increased recharge in LIC sub-basin led to improved simulation of groundwater discharge at Agua Fria River and simulation of groundwater discharge at Del Rio, but led to an overall, increased head error; see Appendix F. ^aThe original Prescott model was initialized with no assigned pumpage or incidental ag-related recharge (Corkhill and Mason, 1995).

Another measure of transient model error, consistent with steady state model error, includes evaluation of the objective function Φ . For transient-based PEST simulations it was generally more difficult for PEST to optimally-estimate solutions having minimal error, in part, because of initial conditions provided by the steady solution. Also see sensitivity analysis in Appendix E. In some cases, the transient-based PEST process was terminated prior to optimization because of indeterminate Φ , oscillatory or unstable conditions towards Φ minimization; also see WinPEST (2002). Nonetheless, the transient-based objective function magnitude provides yet another measure of model error and bias quantification. In addition inversion statistics were available from the inversion process.

TABLE D.3. Relation between Estimated Recharge and Model Error, Transient State PEST Objective Function

ACM / Nat RCH Model All models applied variable recharge (RCH cells) along portions of Granite & Lynx Creek and Agua Fria River unless otherwise noted Blue = Solution plausible; Green=Plausible solution, but less likely Red = Solution not likely	Transient State Annualized Natural recharge RCH cells only	
	Annualized Rate of Simulated long-term natural recharge AF/yr	PEST Φ Transient
Base Model variation–variable natural recharge using only recharge cells	9,352	4,080
Base Model variation–variable natural recharge rate fixed at higher rate	10,287	4,045
ACM 6: Underflow into model assigned near Watson Lake	9,659	3,876
ACM 1 Base with all constant natural recharge	9,352	4,518
ACM 3: No underflow UAF Sub-basin–variable natural recharge rate	7,950	5,235
ACM 7 Base Model variation with lower natural recharge set to 7,482	7,482	4,903
ACM 2: PEST Constrained natural recharge ~5,000 AF/yr	5,100	7,300
ACM 8: MFR-to-stream recharge constrained to 1:1	5,200	7,948
ACM 10: Constrained PEST to Lowest Possible Nat RCH	4,310	16,969
ACM 11: Limit LIC Sub-Basin Underflow to 100 AF/yr	5710	7,370

Φ =Objective function, sum of weighted square residuals. For transient state weighting for layers 1 and 2 head weights based on $\sigma = 20$ ft; transient state flow weighting at Del Rio Springs and Agua Fria River based on weighting $\sigma = 1.0$ cfs. Used consistent head and flow weighting Testing of other, alternative, weighting factors were found to be moderately insensitive about the weights assigned/applied herein. Total number transient PEST residuals = 3,147; (86 index wells 3,107 heads) and 40 flow targets at Del Rio and the Agua Fria River.

APPENDIX E:

Information about Model Calibration and Inversion Statistics

DRAFT

APPENDIX E

INFORMATION ABOUT MODEL CALIBRATION AND INVERSION STATISTICS

For the distribution of hydraulic conductivity (K) in Layers 1 and 2, see Figures E.1–3.

FIGURE E.1. K Distribution Layer 1

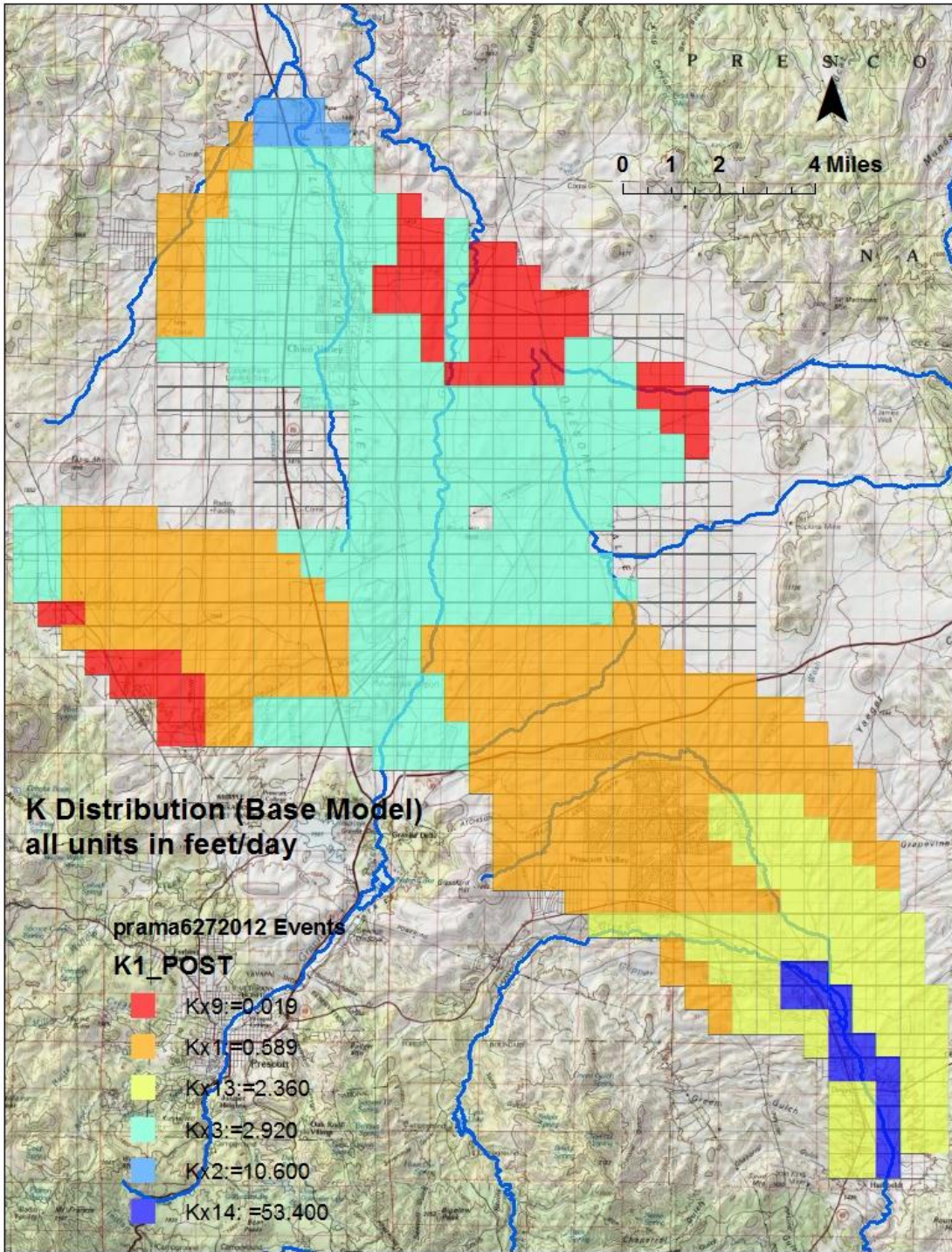


FIGURE E.2. Distribution Layer 2

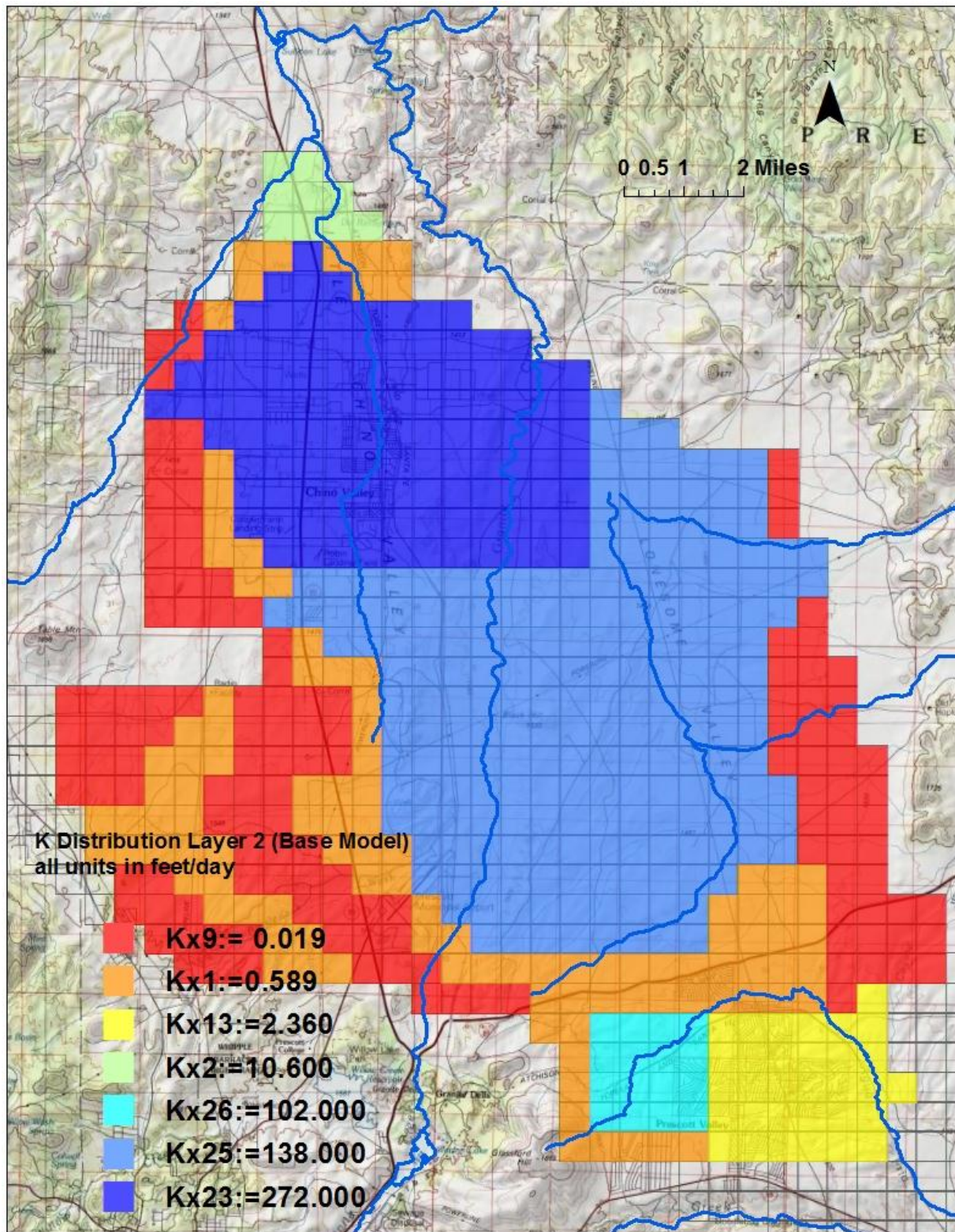
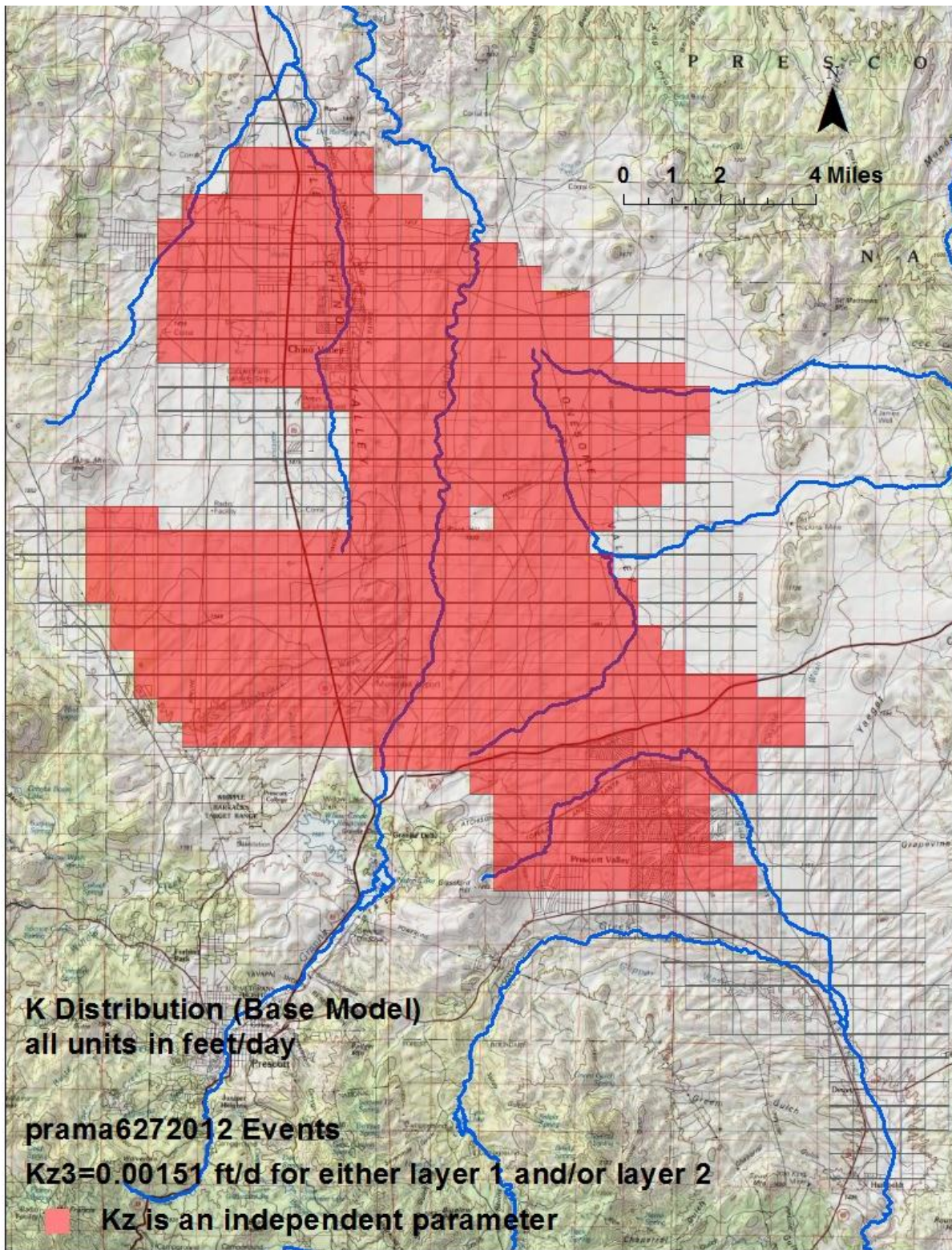


FIGURE E.3. Distribution of aquitard (restriction of vertical flow due to fine-grain materials); areas shown in red have the potential to simulate vertical gradients.



Steady State OPTIMISATION RESULTS from PEST (Base steady state model)

The base model inversion statistics indicate that one standard deviation about the optimal natural recharge rate ranges from 6,600 AF/yr to 11,700 AF/yr; adding induced recharge during transient period (1939-2011) results in a long-term natural recharge rate range of about 7,500 AF/yr to 12,000 AF/yr. Note that the 95% confidence interval for steady natural recharge plus transient-period induced recharge ranges from about 5,000 AF/yr to 15,000 AF/yr.

Adjustable parameters ----->

Parameter	Estimated value	95% percent confidence limits	
		lower limit	upper limit
kx_13	2.36102	1.23034	4.53080
kx_14	53.3762	28.1219	101.310
kx_1	0.589013	0.335697	1.03348
kx_23	271.577	117.960	625.247
kx_25	137.712	37.4156	506.865
kx_26	101.502	36.1578	284.937
kx_2	10.5771	6.15460	18.1773
kx_3	2.91677	1.32867	6.40305
kz_3	1.507271E-03	7.477174E-04	3.038400E-03
kx_9	1.878777E-02	1.077578E-02	3.275684E-02
Underflow UAF	1,135 AF/y	-2604 AF/yr	3,739 AF/yr
Underflow LIC	2,315 AF/yr	-322 AF/yr	4,952 AF/yr
Nat Recharge	9,167 AF/yr	4,109 AF/yr	14,224 AF/yr

Note: confidence limits provide only an indication of parameter uncertainty.

They rely on a linearity assumption which may not extend as far in parameter space as the confidence limits themselves - see PEST manual.

See file C:\PRESCOTT\PRESCOTT_07_17_2012\POSTSS06272012.SEN for parameter sensitivities.

Tied parameters ----->

Parameter	Estimated value
ky_13	2.36102
kz_13	0.236102
ky_14	53.3762
kz_14	5.33762
ky_1	0.589013
kz_1	1.507271E-03
ky_23	271.577
kz_23	1.507271E-03
ky_25	137.712
kz_25	1.37712
ky_26	101.502
kz_26	1.015021E-06
ky_2	10.5771
kz_2	4.48838
ky_3	2.91677
ky_9	1.878777E-02
kz_9	1.507271E-03
par009	0.954647
par010	0.954647
par002	0.954647
par003	0.954647
par004	0.954647
par005	0.954647
par006	0.954647
par007	0.954647
par008	0.954647

See file C:\PRESCOTT\PRESCOTT_MODEL_REPORT_2012\POSTSS06272012.SEN for parameter sensitivities.

Observations ----->

Observation	Measured value	Calculated value	Residual	Weight	Group
of000001	4530.00	4557.37	-27.3670	5.0000E-02	hds.11
of000002	4526.00	4538.42	-12.4170	5.0000E-02	hds.11
of000003	4517.00	4526.14	-9.14000	5.0000E-02	hds.11
of000004	4567.00	4541.07	25.9260	5.0000E-02	hds.11

of000005	4669.00	4645.79	23.2080	5.0000E-02	hds.11
of000006	4481.00	4499.44	-18.4420	5.0000E-02	hds.11
of000007	4508.00	4515.77	-7.77200	5.0000E-02	hds.11
of000008	4500.00	4498.45	1.55300	5.0000E-02	hds.11
of000009	4473.00	4487.31	-14.3070	5.0000E-02	hds.11
of000010	4460.00	4479.63	-19.6260	5.0000E-02	hds.11
of000011	4665.00	4695.77	-30.7740	5.0000E-02	hds.11
of000012	4671.00	4675.17	-4.17100	5.0000E-02	hds.11
of000013	4669.00	4688.74	-19.7400	5.0000E-02	hds.11
of000014	4700.00	4700.80	-0.800000	5.0000E-02	hds.11
of000015	4680.00	4689.55	-9.54800	5.0000E-02	hds.11
of000016	4647.00	4635.09	11.9120	5.0000E-02	hds.11
of000017	4658.00	4627.88	30.1160	5.0000E-02	hds.11
of000018	4625.00	4629.15	-4.14800	5.0000E-02	hds.11
of000019	4606.00	4610.43	-4.42800	5.0000E-02	hds.11
of000020	4605.00	4615.46	-10.4640	5.0000E-02	hds.11
of000021	4666.00	4651.44	14.5560	5.0000E-02	hds.11
of000022	4630.00	4641.87	-11.8710	5.0000E-02	hds.11
of000023	4600.11	4614.91	-14.8020	5.0000E-02	hds.11
of000024	4607.00	4608.87	-1.86600	5.0000E-02	hds.11
of000025	4630.00	4604.11	25.8880	5.0000E-02	hds.11
of000026	4656.00	4663.69	-7.68600	5.0000E-02	hds.11
of000027	4580.00	4586.85	-6.84600	5.0000E-02	hds.11
of000028	4755.00	4753.70	1.30200	0.1000	hds.12
of000029	4709.00	4724.96	-15.9590	5.0000E-02	hds.11
of000030	4785.00	4730.24	54.7590	5.0000E-02	hds.11
of000031	4802.00	4741.29	60.7060	5.0000E-02	hds.11
of000032	4663.00	4698.67	-35.6690	0.1000	hds.12
of000033	4855.00	4868.13	-13.1290	5.0000E-02	hds.11
of000034	4823.00	4807.50	15.4980	5.0000E-02	hds.11
of000035	4884.00	4847.81	36.1890	5.0000E-02	hds.11
of000036	4648.00	4656.34	-8.33600	5.0000E-02	hds.11
of000037	4643.00	4661.78	-18.7780	5.0000E-02	hds.11
of000038	4600.00	4613.39	-13.3870	0.1000	hds.12
of000039	4700.00	4704.10	-4.10100	5.0000E-02	hds.11
of000040	4666.01	4659.73	6.28000	5.0000E-02	hds.11
of000041	4754.00	4776.12	-22.1240	0.1000	hds.12
of000042	4805.00	4816.22	-11.2160	0.1000	hds.12
of000043	4756.00	4763.64	-7.64300	0.1000	hds.12
of000044	4700.00	4693.91	6.08700	5.0000E-02	hds.11
of000045	4650.00	4651.16	-1.15700	0.1000	hds.12
of000046	4678.00	4665.75	12.2480	0.1000	hds.12
of000047	4713.00	4686.05	26.9550	0.1000	hds.12
of000048	5042.00	5030.16	11.8440	5.0000E-02	hds.11
of000049	5090.66	5083.60	7.05500	5.0000E-02	hds.11
of000050	5080.00	5091.64	-11.6410	5.0000E-02	hds.11
of000051	4795.00	4803.56	-8.55700	5.0000E-02	hds.11
of000052	5000.00	4946.95	53.0460	5.0000E-02	hds.11
of000053	4875.00	4883.63	-8.62700	0.1000	hds.12
of000054	5025.00	4948.20	76.8040	5.0000E-02	hds.11
of000055	5033.00	5038.06	-5.06200	5.0000E-02	hds.11
of000056	5035.00	5011.36	23.6370	5.0000E-02	hds.11
of000057	4608.00	4601.63	6.36700	0.1000	hds.12
of000058	4613.00	4606.23	6.77400	0.1000	hds.12
of000059	4621.00	4659.77	-38.7700	5.0000E-02	hds.11
of000060	4600.00	4603.83	-3.83200	0.1000	hds.12
of000061	4730.00	4717.01	12.9930	5.0000E-02	hds.11
of000062	4609.00	4619.68	-10.6770	5.0000E-02	hds.11
of000063	4600.99	4608.52	-7.53500	0.1000	hds.12
of000064	4611.00	4631.59	-20.5940	5.0000E-02	hds.11
of000065	4605.00	4594.69	10.3150	0.1000	hds.12
of000066	4577.00	4578.06	-1.06200	0.1000	hds.12
of000067	4606.00	4584.52	21.4760	0.1000	hds.12
of000068	4599.00	4594.45	4.55100	0.1000	hds.12
of000069	4596.00	4594.68	1.31900	0.1000	hds.12
of000070	4596.00	4590.72	5.28000	0.1000	hds.12
of000071	4595.00	4595.94	-0.939000	0.1000	hds.12
of000072	4600.00	4589.16	10.8360	5.0000E-02	hds.11
of000073	4600.00	4565.33	34.6710	5.0000E-02	hds.11
of000074	4597.00	4596.81	0.186000	0.1000	hds.12
of000075	4599.00	4596.81	2.18600	0.1000	hds.12
of000076	4592.00	4599.83	-7.83300	0.1000	hds.12
of000077	4605.00	4599.06	5.94400	0.1000	hds.12
of000078	4599.00	4600.41	-1.40800	0.1000	hds.12

of000079	4599.28	4598.96	0.318000	0.1000	hds.l2
of000080	4598.00	4598.33	-0.328000	0.1000	hds.l2
of000081	4603.00	4599.46	3.53600	0.1000	hds.l2
of000082	4550.00	4605.36	-55.3580	0.1000	hds.l2
of000083	4670.00	4660.75	9.25100	5.0000E-02	hds.l1
of000084	4595.00	4604.77	-9.76900	0.1000	hds.l2
of000085	4600.00	4615.44	-15.4400	5.0000E-02	hds.l1
of000086	4599.00	4599.63	-0.630000	0.1000	hds.l2
of000087	4602.00	4599.95	2.04800	0.1000	hds.l2
of000088	4609.00	4602.35	6.65400	0.1000	hds.l2
of000089	4604.00	4602.28	1.71500	0.1000	hds.l2
of000090	4455.00	4466.21	-11.2100	0.1000	hds.l2
of000091	4566.00	4557.76	8.24000	0.1000	hds.l2
of000092	4522.00	4506.35	15.6500	0.1000	hds.l2
of000093	4490.00	4502.44	-12.4430	5.0000E-02	hds.l1
of000094	4537.00	4518.88	18.1200	0.1000	hds.l2
of000095	4493.00	4518.88	-25.8800	0.1000	hds.l2
of000096	4576.00	4577.76	-1.75500	0.1000	hds.l2
of000097	4465.00	4478.19	-13.1880	0.1000	hds.l2
of000098	4630.00	4624.97	5.03400	5.0000E-02	hds.l1
of000099	4650.00	4622.18	27.8240	5.0000E-02	hds.l1
of000100	4624.00	4638.87	-14.8720	5.0000E-02	hds.l1
of000101	4630.00	4612.03	17.9720	0.1000	hds.l2
of000102	4600.00	4565.39	34.6120	5.0000E-02	hds.l1
of000103	4505.00	4526.07	-21.0740	5.0000E-02	hds.l1
of000104	4545.00	4548.09	-3.89100	5.0000E-02	hds.l1
ob000001	-518400.	-483680.	-34720.0	2.3148E-05	bud.u1
ob000002	-345600.	-309970.	-35630.0	1.1570E-05	bud.u2

Prior information ----->

Prior information	Provided value	Calculated value	Residual	Weight	Group
k23	2.22000	2.43389	-0.213893	6.000	pr_info
k25	2.00000	2.13897	-0.138972	3.330	pr_info
k26	2.00000	2.00647	-6.474994E-03	6.000	pr_info

See file C:\PRESCOTT\PRESCOTT_07_17_2012\POSTSS06272012.RES for more details of residuals in graph-ready format.

See file C:\PRESCOTT\PRESCOTT_07_17_2012\POSTSS06272012.SEO for composite observation sensitivities.

Objective function ----->

Sum of squared weighted residuals (ie phi) = 175.7
 Contribution to phi from observation group "bud.u1" = 0.6459
 Contribution to phi from observation group "bud.u2" = 0.1699
 Contribution to phi from observation group "hds.l1" = 81.85
 Contribution to phi from observation group "hds.l2" = 91.22
 Contribution to phi from ungrouped prior information = 1.863

Correlation Coefficient ----->

Correlation coefficient = 1.000

Analysis of residuals ----->

All residuals:-

Number of residuals with non-zero weight = 109
 Mean value of non-zero weighted residuals = -1.0119E-02
 Maximum weighted residual [observation "of000054"] = 3.840
 Minimum weighted residual [observation "of000082"] = -5.536
 Standard variance of weighted residuals = 1.831
 Standard error of weighted residuals = 1.353
 Note: the above variance was obtained by dividing the objective function by the number of system degrees of freedom (ie. number of observations with non-zero weight plus number of prior information articles with non-zero weight minus the number of adjustable parameters.)
 If the degrees of freedom is negative the divisor becomes the number of observations with non-zero weight plus the number of prior information items with non-zero weight.

Residuals for observation group "bud.u1":-

Number of residuals with non-zero weight = 1
 Mean value of non-zero weighted residuals = -0.8037
 Maximum weighted residual [observation "ob000001"] = -0.8037
 Minimum weighted residual [observation "ob000001"] = -0.8037
 "Variance" of weighted residuals = 0.6459
 "Standard error" of weighted residuals = 0.8037
 Note: the above "variance" was obtained by dividing the sum of squared residuals by the number of items with non-zero weight.

Residuals for observation group "bud.u2":-

Number of residuals with non-zero weight = 1
 Mean value of non-zero weighted residuals = -0.4122
 Maximum weighted residual [observation "ob000002"] = -0.4122

```

Minimum weighted residual [observation "ob000002"] = -0.4122
"Variance" of weighted residuals = 0.1699
"Standard error" of weighted residuals = 0.4122
Note: the above "variance" was obtained by dividing the sum of squared
residuals by the number of items with non-zero weight.
Residuals for observation group "hds.l1":-
Number of residuals with non-zero weight = 61
Mean value of non-zero weighted residuals = 0.1318
Maximum weighted residual [observation "of000054"] = 3.840
Minimum weighted residual [observation "of000059"] = -1.939
"Variance" of weighted residuals = 1.342
"Standard error" of weighted residuals = 1.158
Note: the above "variance" was obtained by dividing the sum of squared
residuals by the number of items with non-zero weight.
Residuals for observation group "hds.l2":-
Number of residuals with non-zero weight = 43
Mean value of non-zero weighted residuals = -0.1428
Maximum weighted residual [observation "of000047"] = 2.695
Minimum weighted residual [observation "of000082"] = -5.536
"Variance" of weighted residuals = 2.121
"Standard error" of weighted residuals = 1.456
Note: the above "variance" was obtained by dividing the sum of squared
residuals by the number of items with non-zero weight.
Ungrouped prior information residuals:-
Number of residuals with non-zero weight = 3
Mean value of non-zero weighted residuals = -0.5950
Maximum weighted residual [observation "k26"] = -3.8850E-02
Minimum weighted residual [observation "k23"] = -1.283
"Variance" of weighted residuals = 0.6209
"Standard error" of weighted residuals = 0.7880
Note: the above "variance" was obtained by dividing the sum of squared
residuals by the number of items with non-zero weight.

```

Parameter covariance matrix ----->

	kx_13	kx_14	kx__1	kx_23	kx_25	kx_26	kx__2
kx__3							
	kz__3	kx__9	par011	par012	par001		
kx_13 3.7510E-03	2.0275E-02	9.1346E-03	1.2744E-02	8.8483E-03	4.7670E-03	-5.9401E-05	1.1741E-02
	1.4974E-02	1.3145E-02	0.1195	4.8328E-02	3.0551E-02		
kx_14 1.3467E-03	9.1346E-03	1.9598E-02	1.4260E-02	9.8537E-03	7.6904E-03	6.6460E-05	1.3104E-02
	1.5204E-02	1.3576E-02	0.1081	5.2386E-02	3.1621E-02		
kx__1 1.0244E-03	1.2744E-02	1.4260E-02	1.5086E-02	9.5638E-03	5.7905E-03	1.3167E-05	1.2704E-02
	1.4007E-02	1.3059E-02	0.1140	5.1101E-02	3.1109E-02		
kx_23 1.3990E-04	8.8483E-03	9.8537E-03	9.5638E-03	3.3187E-02	-7.0054E-03	-2.2138E-06	4.4754E-03
	9.0764E-03	9.3591E-03	7.9015E-02	3.9757E-02	2.1559E-02		
kx_25 4.6301E-04	4.7670E-03	7.6904E-03	5.7905E-03	-7.0054E-03	8.1036E-02	-9.8014E-05	8.5272E-03
	1.9643E-03	7.7732E-03	5.6239E-02	2.7383E-02	1.6354E-02		
kx_26 5.6603E-06	-5.9401E-05	6.6460E-05	1.3167E-05	-2.2138E-06	-9.8014E-05	5.0846E-02	3.0971E-05
	1.0505E-04	4.5735E-05	1.7183E-04	5.9024E-05	9.2404E-05		
kx__2 -3.3670E-03	1.1741E-02	1.3104E-02	1.2704E-02	4.4754E-03	8.5272E-03	3.0971E-05	1.3993E-02
	1.5091E-02	1.2188E-02	0.1048	4.4117E-02	2.8566E-02		
kx__3 2.9506E-02	3.7510E-03	1.3467E-03	1.0244E-03	1.3990E-04	4.6301E-04	5.6603E-06	-3.3670E-03
	-5.1764E-03	2.0962E-03	1.8536E-02	4.4435E-03	4.1915E-03		
kz__3 -5.1764E-03	1.4974E-02	1.5204E-02	1.4007E-02	9.0764E-03	1.9643E-03	1.0505E-04	1.5091E-02
	2.3454E-02	1.3956E-02	0.1256	5.5623E-02	3.3822E-02		

kx__9 2.0962E-03	1.3145E-02	1.3576E-02	1.3059E-02	9.3591E-03	7.7732E-03	4.5735E-05	1.2188E-02
	1.3956E-02	1.4748E-02	0.1117	4.9167E-02	3.0137E-02		
par011 1.8536E-02	0.1195	0.1081	0.1140	7.9015E-02	5.6239E-02	1.7183E-04	0.1048
	0.1256	0.1117	1.837	0.4232	0.2598		
par012 4.4435E-03	4.8328E-02	5.2386E-02	5.1101E-02	3.9757E-02	2.7383E-02	5.9024E-05	4.4117E-02
	5.5623E-02	4.9167E-02	0.4232	0.2063	0.1149		
par001 4.1915E-03	3.0551E-02	3.1621E-02	3.1109E-02	2.1559E-02	1.6354E-02	9.2404E-05	2.8566E-02
	3.3822E-02	3.0137E-02	0.2598	0.1149	7.0190E-02		

Parameter correlation coefficient matrix ----->

	kx__3	kx__13	kx__14	kx__1	kx__23	kx__25	kx__26	kx__2
kx__3								
	kz__3	kx__9	par011	par012	par001			
kx__13 0.1534	1.000	0.4582	0.7287	0.3411	0.1176	-1.8501E-03	0.6971	
	0.6867	0.7601	0.6192	0.7472	0.8099			
kx__14 5.6005E-02	0.4582	1.000	0.8294	0.3864	0.1930	2.1054E-03	0.7913	
	0.7092	0.7985	0.5696	0.8239	0.8526			
kx__1 4.8552E-02	0.7287	0.8294	1.000	0.4274	0.1656	4.7541E-04	0.8744	
	0.7447	0.8755	0.6848	0.9160	0.9560			
kx__23 4.4709E-03	0.3411	0.3864	0.4274	1.000	-0.1351	-5.3892E-05	0.2077	
	0.3253	0.4230	0.3200	0.4805	0.4467			
kx__25 9.4689E-03	0.1176	0.1930	0.1656	-0.1351	1.000	-1.5269E-03	0.2532	
	4.5056E-02	0.2248	0.1458	0.2118	0.2168			
kx__26 1.4614E-04	-1.8501E-03	2.1054E-03	4.7541E-04	-5.3892E-05	-1.5269E-03	1.000	1.1611E-03	
	3.0420E-03	1.6701E-03	5.6228E-04	5.7629E-04	1.5468E-03			
kx__2 -0.1657	0.6971	0.7913	0.8744	0.2077	0.2532	1.1611E-03	1.000	
	0.8330	0.8484	0.6536	0.8211	0.9115			
kx__3 1.000	0.1534	5.6005E-02	4.8552E-02	4.4709E-03	9.4689E-03	1.4614E-04	-0.1657	
	-0.1968	0.1005	7.9624E-02	5.6952E-02	9.2104E-02			
kz__3 -0.1968	0.6867	0.7092	0.7447	0.3253	4.5056E-02	3.0420E-03	0.8330	
	1.000	0.7504	0.6050	0.7996	0.8336			
kx__9 0.1005	0.7601	0.7985	0.8755	0.4230	0.2248	1.6701E-03	0.8484	
	0.7504	1.000	0.6787	0.8913	0.9367			
par011 7.9624E-02	0.6192	0.5696	0.6848	0.3200	0.1458	5.6228E-04	0.6536	
	0.6050	0.6787	1.000	0.6875	0.7234			
par012 5.6952E-02	0.7472	0.8239	0.9160	0.4805	0.2118	5.7629E-04	0.8211	
	0.7996	0.8913	0.6875	1.000	0.9552			
par001 9.2104E-02	0.8099	0.8526	0.9560	0.4467	0.2168	1.5468E-03	0.9115	
	0.8336	0.9367	0.7234	0.9552	1.000			

Miscellaneous comments: For details on parameter covariance and parameter correlation see WinPEST (2003) and Hill (1998). Modestly-high parameter correlation is calculated between hydraulic conductivity (K) variables and natural recharge. However, this parameter correlation is not extreme and was further evaluated and tested for uniqueness in that different starting parameter values (i.e., K; recharge) tended toward consistent solutions in the non-linear regression process. Furthermore, when natural recharge (par001) was divided into three independent variables/parameters including: par001 = MFR; par007 = Lynx Creek/Agua Fria River and Bradshaw Foothills; and par011 = Granite Creek recharge, parameter correlation between all hydraulic conductivity (K) variables and natural recharge par007 and par011 was lower (not shown herein) than the values presented above. It is also of interest to note that for ACM 3 (i.e., ACM assuming no underflow from the UAF sub-basin), parameter correlation between K and natural recharge (not shown herein) was calculated to be slightly lower than with respect to the Base model, because the singular groundwater discharge target removed - to an extent - parameter interdependence.

Normalized eigenvectors of parameter covariance matrix ----->

	Vector_1	Vector_2	Vector_3	Vector_4	Vector_5	Vector_6	Vector_7
Vector_8	Vector_9	Vector_10	Vector_11	Vector_12	Vector_13		
kx_13 -0.1278	-0.1557	-6.7017E-02	0.5420	4.1768E-02	-0.1171	3.8680E-02	0.7802
	9.1003E-02	-2.1422E-03	-4.2418E-02	0.1452	6.6225E-02		
kx_14 -4.0761E-02	-0.1067	-8.1659E-02	0.6717	-9.1648E-03	4.2122E-02	-0.4689	-0.5136
	-8.1192E-03	1.0675E-03	-1.5059E-02	0.1987	6.1594E-02		
kx_1 -5.7393E-02	-0.2974	-0.6434	-0.2918	0.4426	-0.3906	-0.1554	-3.5404E-02
	-1.5999E-04	-3.5101E-04	-3.3802E-02	0.1732	6.4038E-02		
kx_23 0.9093	-9.3712E-02	6.9526E-02	-4.9783E-02	3.6881E-02	6.6333E-02	-0.2084	0.1341
	9.2888E-02	-2.7580E-03	-0.2398	0.1472	4.5140E-02		
kx_25 0.2010	-1.9926E-02	-3.3668E-02	-6.6857E-03	2.5377E-02	7.6725E-02	-3.8138E-02	6.2252E-02
	4.3823E-03	3.0755E-03	0.9592	0.1578	3.2771E-02		
kx_26 2.0519E-03	-6.0113E-04	3.7892E-05	8.0943E-04	4.3139E-04	-1.2472E-03	1.7364E-03	1.6516E-03
	1.4672E-03	1.000	-3.6686E-03	4.0735E-04	1.0066E-04		
kx_2 -0.1921	-0.5233	0.6557	-0.2351	8.1459E-02	-0.1886	-0.3210	5.5391E-02
	-0.1717	7.0470E-04	2.1490E-02	0.1496	5.8571E-02		
kx_3 -0.1544	-0.1289	5.8882E-02	-0.1235	4.4681E-02	0.2094	-0.1085	-3.3934E-02
	0.9391	-5.2333E-04	7.7295E-03	-9.2011E-03	9.5592E-03		
kz_3 -0.1760	-0.1120	-0.2128	-0.1891	4.1041E-02	0.8236	-0.2181	0.1780
	-0.2583	1.5001E-03	-9.3735E-02	0.1889	7.0526E-02		
kx_9 -4.6177E-02	-9.5853E-02	-0.2504	-0.1937	-0.8764	-0.1940	-0.2106	7.3865E-02
	3.3828E-02	4.3448E-04	-6.7201E-03	0.1671	6.2673E-02		
par011 1.6531E-02	-1.0095E-03	-8.2682E-04	3.6582E-03	-7.7196E-04	3.0842E-03	1.0070E-02	-1.7718E-02
	-9.9750E-03	9.9943E-05	1.9005E-02	-0.3246	0.9452		
par012 -5.9829E-03	-8.4547E-02	8.5078E-02	1.3116E-02	-2.7943E-02	3.3280E-02	0.5936	-0.2073
	4.4165E-02	-1.3982E-03	-8.9427E-02	0.7216	0.2398		
par001 -0.1313	0.7399	0.1424	-0.1529	0.1456	-0.1586	-0.3878	0.1406
	4.2281E-02	6.3905E-04	-3.7943E-02	0.3882	0.1457		

Eigenvalues ----->

	7.7622E-05	6.7271E-04	1.3482E-03	1.8151E-03	4.5189E-03	8.5341E-03	1.0868E-02
2.4209E-02							

3.2189E-02 5.0846E-02 8.0115E-02 0.1633 2.036

Miscellaneous comments: For details on parameter covariance and normalized eigenvectors of the parameter covariance matrices see WinPEST (2003) and Hill (1998). The principal components associated with the recharge variable are expressed - to a large extent (90%) - through eigenvectors 1, 2, 6, 12 and 13. Other parameters important to the estimation of recharge (par001) include Kx2, underflow from the LIC sub-basin (par012) and underflow from the UAF sub-basin (par011). These relations generally hold for other ACM's.

DRAFT

Sensitivity Analysis

A sensitivity analysis provides a good indication of what model parameters are important (or “sensitive”) in calibrating the model. As a byproduct of the non-linear regression process, both model parameters and observation target sensitivities can be evaluated. The presentation of model parameter sensitivities will be based, to a large extent, on inversion statistics. This includes scaled and un-scaled composite sensitivities from steady state and transient simulations, as well as discussion about parameter inter-relations (parameter correlation or lack thereof) that may impact the calibration. Results from the inverse model are also used to determine calibration target sensitivity.

Because of parameter inter-relations, a practical yet effective method of understanding the model parameter sensitivity and/or coordinated-parameter sensitivity is to examine composite parameter sensitivity. The composite sensitivity of each parameter is the normalized (with respect to the number of observations) magnitude of the column of the Jacobian matrix pertaining to that parameter, with each element of that column multiplied by the weight pertaining to the respective observation. One can think of the Jacobian matrix as a (typically-rectangular) sensitivity matrix where each column represents a parameter and each row represents a simulated response with respect to observed data (location). Thus written in matrix form, the composite sensitivity (s_i) is: $S = (J^T Q J)^{-1/2} / m$, where J is the Jacobian matrix, Q is the cofactor matrix (i.e., weight matrix), m is the number of observations, i is the parameter and t is the transpose operator (WinPEST, 2002). In other words, J is the matrix of M composed of m rows (one for each observation) and n elements of each row being the derivative of one particular (weighted) observation with respect to each estimated parameter, or $J_{ij} = \Delta \text{observation}_j / \Delta \text{parameter}_i$.

Both scaled and un-scaled composite sensitivities will be presented because some parameters were log-transformed (i.e., K) during the non-linear regression process while others were not (i.e., recharge; underflow; S_y). For more information about composite parameter sensitivities, see Hill (1998) and WinPEST (2002). Furthermore the 95% confidence intervals, shown above, also provide a good indication of parameter reliability, notwithstanding the linearity assumptions. For distribution of model parameters and recharge distribution see Appendix C and Figure 1.

Model Weights

Weights are important factors in the non-linear regression process (Hill, 1998; WinPEST, 2003). However the assignment of weights were not acutely sensitive about the final values assigned herein. That is, relatively minor changes in weighting did not significantly impact the parameter estimation results or inversion statistics. Evaluation of the standard error statistic was also used as a guide for weight assignment; also see Hill (1998); WinPEST (2002) for more details.

Weights used herein were assigned on a categorical basis: Steady state head weights assigned to layer 1 and layer 2 were based on standard deviations (σ) of 20 feet and 10 feet, respectively. High reliability was assigned in layer 2 because more steady period head data was available for layer 2, and in particular the LVU aquifer, with respect to layer 1. Many areas of the model domain lacked head data during steady state conditions. In the non-linear regression, only layer one head targets not impacted by groundwater development (or assumed to be not impacted by groundwater development) were assigned as calibration targets. Inspection of post-1940 UAU aquifer head data in the ADWR GWSI database was used to infer groundwater level trends over time (i.e., long-term dynamic equilibrium, etc.); thus, inferences were made about steady state layer 1 head targets and associated head-weighting. Nonetheless, more certainty exists for layer 2 (i.e., LVU aquifer heads), and is thus reflected in the weighting.

Transient state head weights assigned to layer 1 and layer 2 were based on a σ of 20 feet. The transient-assigned weights for layer 2 heads was reduced, with respect to steady state conditions, because of; 1) the inherent resulting differences between heads associated with, and about, model-assigned pumping (stress-period intervals) verses real-world pumping timing (diurnal; weekly, etc.); 2) “built-in” steady state models errors associated with the initial conditions and 3) adjustment of weighting to better reflect the standard error statistic, and “natural” weighting magnitude g ; see WinPEST, 2003; and Hill (1998). Steady state flow weights assigned to represent groundwater discharge at Del Rio Springs and baseflow along the Agua Fria River near Humboldt were based on a σ equal to 0.5 cfs and 1 cfs, respectively. Transient state flow weights assigned to represent groundwater discharge at Del Rio Springs and baseflow along the Agua Fria River near Humboldt were based on a σ equal to 1 cfs. For the base model the steady state standard error of weighted residuals was 1.353, while the transient state standard error of weighted residuals was 1.351; both are close to the target standard error of 1.0, as defined by Hill 1998.

Factors influencing head weights include: 1) measurement error; 2) well head elevation error; 3) comparison of statistic measured (unknowingly) during recovery period (or the converse); 4) simulated head interpolation error (i.e., adjacent cells having significantly different [contrasting] K values in combination with significant head differences); 5) incorrect location of observation well with respect to cell center; 6) head elevation accuracy representing average head in referenced aquifer/layer; 7) for steady state -- difference in head elevation representing “long-term” steady state tendency of the system; and finally 8) model error, which may include 3-7 above or combinations of 3-7 above, as well as: 8a) model scaling factor; 8b) influence of externally-assigned boundary conditions; 8c) mismatch of real-world pumping times and the assignment of simulated pumping; 8d) real-world pumping location constrained in model to cell center. It is further assumed that the model error has a mean of zero.

Primary factors influencing flow weights include: 1) measurement error; 2) baseflow separation error from high-flow - flood - event (potentially a larger problem/uncertainty for Agua Fria baseflow); 3) incorrect seasonal adjustment; 4) possible incidental runoff or other non-groundwater discharge signal impacting observed baseflow target (potentially a larger problem/uncertainty for Agua Fria baseflow); 5) imperfect spatial match between observed and model-cell assigned groundwater discharge; 6) groundwater discharge target representing “long-term” steady state condition (potentially a larger problem/uncertainty for Agua Fria River baseflow; and 7) model error, which may include 3-6 above or combinations of 3-6 above, as well as: 8a) model scaling factor; 8b) influence of externally-assigned boundary conditions; 8c) mismatch of real-world pump times and the assignment of simulated pumping impacted groundwater discharge.

For most ACM's explored herein, including the base model, prior information was added to three LVU K aquifer zones to moderate estimated K values. (Without prior information, estimates of K tended to be *significantly* larger than previous model versions. The weighting was based on aquifer test data, as well as, past calibrated values. Thus, prior information as well as head and flow target data provided the non-linear regression constraints for the three LVU K zones. All estimated K zones were log-transformed in the non-linear regression. For information on weighting see Table E.1; for additional background regarding log-normal transformations see Hill (1998).

TABLE E. 1. Prior Information Assigned in Non-Linear Regression for Three LVU Aquifer K-Zones, Base Model

A-Priori K Zone	Target K (ft/d)	Approximate a-priori, 95 % CI (ft/d)*
LVU Zone 23 (North LIC)	166	75 – 370
LVU Zone 25 (Central LIC)	100	25 – 390
LVU Zone 26 (Northwest UAF)	100	45 – 215

*Log-normal distribution based on available aquifer test data and previous model-calibrated values. These statistics were used as criteria to assign prior information weights. Note that without the assignment of prior information “anchoring” the LVU K’s, inverse model estimates of the LVU K’s were higher and more uncertain than the posterior estimates provided below. No other K zones employed prior information in the regression.

Note that even if all head and flow measurement error was eliminated, model-error would still be prevalent and weighting would still be required. Furthermore, the inclusion of prior information (also known as a “penalty” in WinPEST, 2002) in most of the tested ACM’s (added to moderate the LVU K zones) including the base model, implies that model error or conceptual model error exists.

Sensitivity Analysis Results

Most of the model parameters were sensitive, and important for calibration purposes. The 95% confidence intervals, as shown above, also provide a general indication of parameter sensitivity; that is the more sensitive (and/or less correlation between parameters) parameters tend to have narrower confidence intervals.

TABLE E.2. Composite Scaled and Un-scaled Sensitivity Analysis, Estimated Parameters

Composite Parameter Sensitivity from PEST (15 Parameter Solution)				
Parameter (15-P)	Steady scaled	Steady unscaled	Transient scaled	Transient unscaled
Kx13	0.320	0.312	0.022	0.022
Kx14	0.292	0.0126	0.031	0.0031
Kx1	0.526	2.05	0.171	0.67
Kx23	0.186*	0.00157*	0.159	0.0013
Kx25	0.0589*	0.000983*	0.157	0.0026
Kx26	0.055*	0.00124*	0.0071	0.00016
Kx2	0.685	0.149	0.150	0.033
Kx3	0.237	0.187	0.158	0.125
Kz3*	0.247	377	0.156	238
Kx9	0.324	39.7	0.149	18
Underflow UAF	0.153	0.153	0.0027	0.0027
Underflow LIC	0.0134	0.0134	0.069	0.069
MFR	0.276	0.276	0.069	0.069
Gran Crk RCH	0.535	0.535	0.025	0.025
Lynx AF RCH	0.493	0.493	0.064	0.064
S (all Sy and Ss)	N/A	N/A	3.74	3.74

All Kx=Ky. Kxy13 and Kxy14 fixed at Kxy:Kz ratio of 10:1. Kz1, Kz9, Kz25 are tied to Kz3. Kx2:Kz2=2.36. **Note that Kz3 is the primary aquitard feature.*Includes Base prior information for K23, K25 and K26. No other parameters including the other K zones, recharge, underflow or S included prior information.

On average, the steady state scaled sensitivity was 3.2 times greater than transient based sensitivity (72-year simulation). On average, the steady state unscaled sensitivity was nearly 1.6 times greater than the unscaled transient state simulation (72-year simulation).

Statistics from the inverse model were used to better understand the relative significance of the calibration targets including heads, flow and for steady state, prior information. The averaged sensitivity of observations, as grouped by layer 1 heads, layer 2 heads, flow at Del Rio, flow at Agua Fria River and prior information for steady flow conditions, are presented in Table E.4. for the Base Model. Although there are significantly fewer flow targets than head targets, and flow components comprise a relatively small part of the objective function, flow targets are sensitive in constraining model parameter estimates. As with parameter sensitivity, observation target sensitivity was disproportionately sensitive over steady state conditions, with respect to transient state conditions, despite fewer steady period sample targets. This further underscores the importance of model initialization.

TABLE E.3. Scaled Sensitivity Analysis of Observation Targets

Observation Target Group	Steady State (number of targets)		Transient (number of targets)	
	Sensitivity	Relative sensitivity	Sensitivity	Relative sensitivity
Del Rio Springs	2.44	2.35 (1)	0.54	0.69 (38)*
Agua Fria Baseflow	0.694	0.68 (1)	0.19	0.20 (30)*
Layer 1 heads	0.31	0.35 (61)	0.21	0.30 (1,413)**
Layer 2 heads	0.54	0.58 (43)	0.026	0.042 (1,775)**
Prior info	0.39	0.87 (3)	N/A	N/A

For details on PEST sensitivities and relative sensitivities see WinPEST, 2003. For details on weighting see section above.

APPENDIX F:

Upper Agua Fria Sub-basin Information

DRAFT

APPENDIX F

UPPER AGUA FRIA SUB-BASIN INFORMATION

When the provisional Prescott AMA groundwater flow is constrained to available head and flow data, less model error and bias result when underflow is simulated from the UAF sub-basin, with respect to ACM 3, which assumes *no* underflow from UAF sub-basin, estimated rates of simulated underflow from the UAF sub-basin for most ACM's are typically about 1,000 AF/yr. Although UAF sub-basin underflow pathway(s) have not been positively identified, faults and linear features, consistent with the general direction of groundwater flow, exist in the area and *may* have the potential to facilitate underflow, (Barnett et al, 2009). Faults shown in http://pubs.usgs.gov/sim/2996/downloads/pdf/2996_map.pdf include Brushy Wash Fault, the Shylock Fault (Barnett et al, 2009) and an unnamed fault west of Brushy Wash Fault.

In addition to groundwater discharge to baseflow, a significant riparian habitat supported by shallow water tables (see Figures F.1a and F.1b and Barnett et al, 2007), as well as agricultural-related pumpage and historical diversions (Barnett, 2007), may provide a groundwater discharge (“drain”) mechanism for underflow out of the UAF sub-basin. Wilson (1988) conducted a “synoptic” study of the Agua Fria River baseflow during the “dry” winter of 1980/1981. In addition, there are many productive groundwater wells near the Upper Agua Fria Sub-basin terminus; see Figure F.1c. Thus, the combination of productive wells, stable groundwater levels and a sub-regional hydraulic gradient (towards the south) imply that there is the potential for subsurface flow. The evaluation of groundwater level elevations - and in particular groundwater discharge - over time, will help to better understand groundwater flow conditions. It is thus recommended that 1) additional groundwater level measurements (survey grade) and synoptic baseflow measurements be conducted along the Agua Fria River between Dewey and near Mayer. In addition, aquifer testing near the UAF Sub-basin terminus (near Humboldt) may provide additional information about subsurface flow conditions.

FIGURE F.1a. Agua Fria River, Riparian Corridor and Linear Features



FIGURE F.1b. Baseflow along Agua Fria River and Riparian Corridor about 4.5 miles southeast of Humboldt between USGS 09512450 and 09512500. Geologic structure controlling streamflow and possible underflow



FIGURE F.2. Map of UAF Sub-basin/Prescott Area; faults shown as red lines, registered wells as black triangles. Source map http://pubs.usgs.gov/sim/2996/downloads/pdf/2996_map.pdf

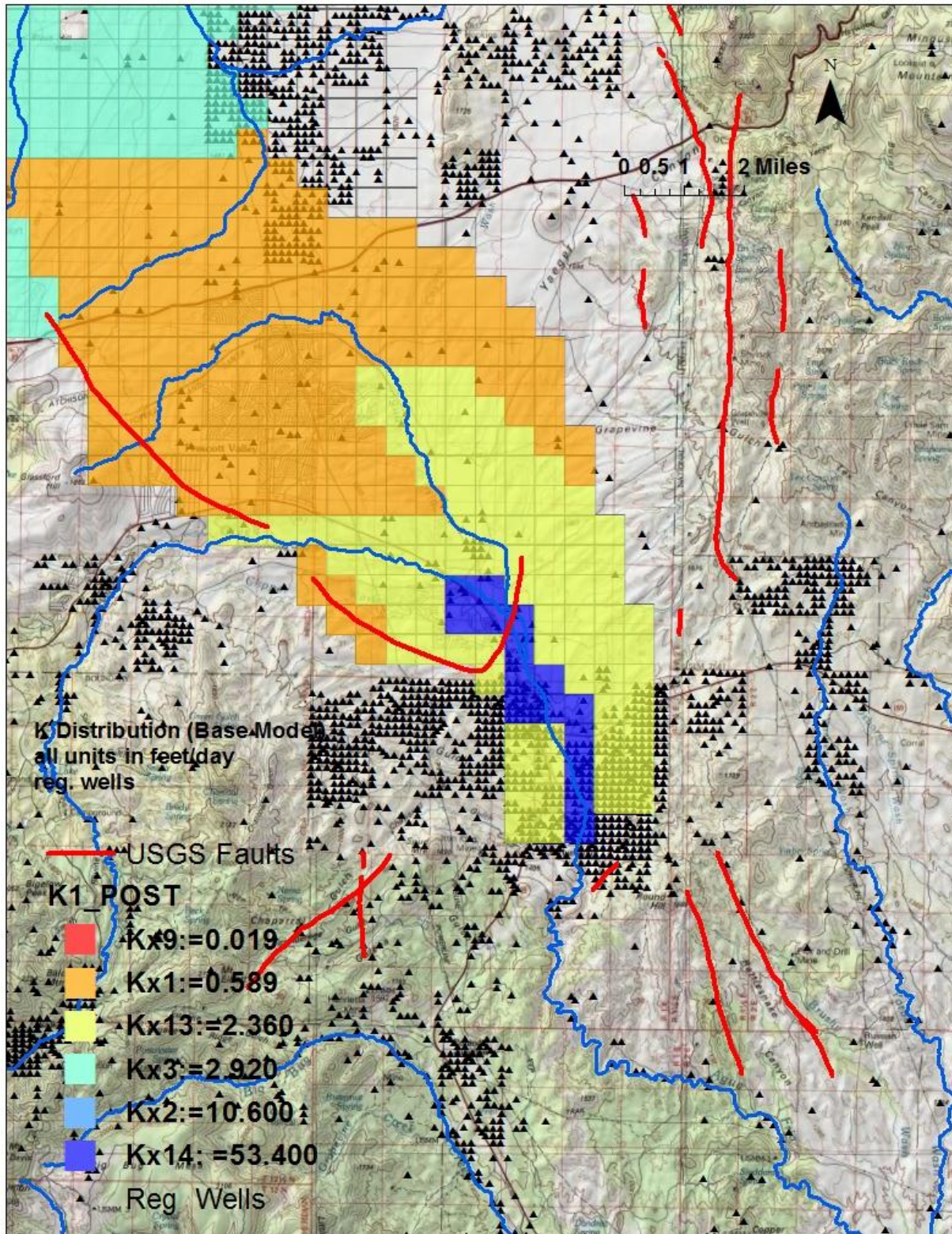


FIGURE F.3a. Lower Portion of UAF Sub-basin

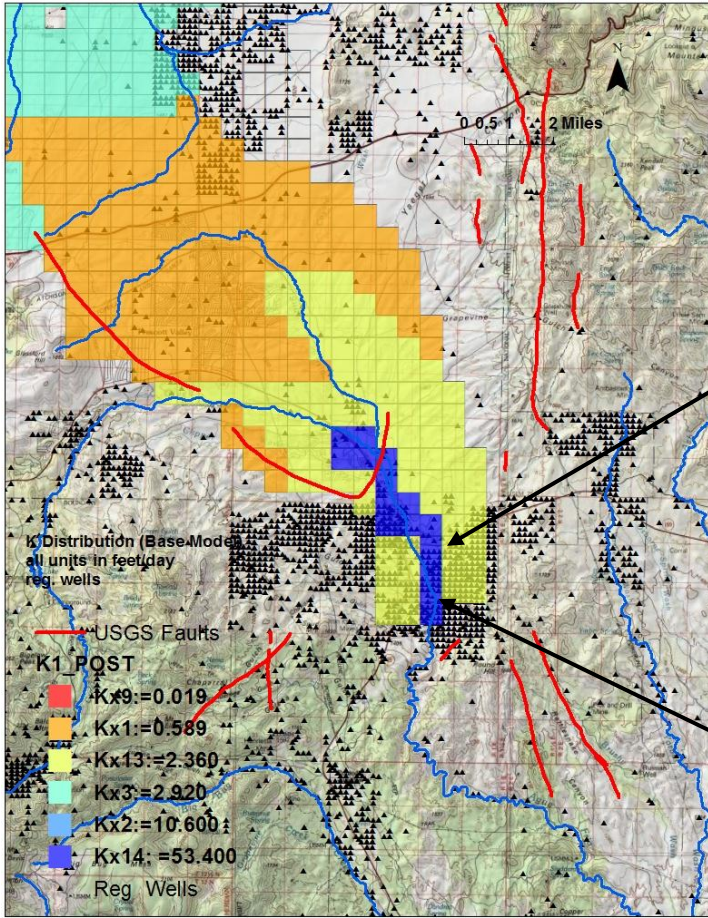


FIGURE F.3b Hydrograph for (A-13-01)02cad

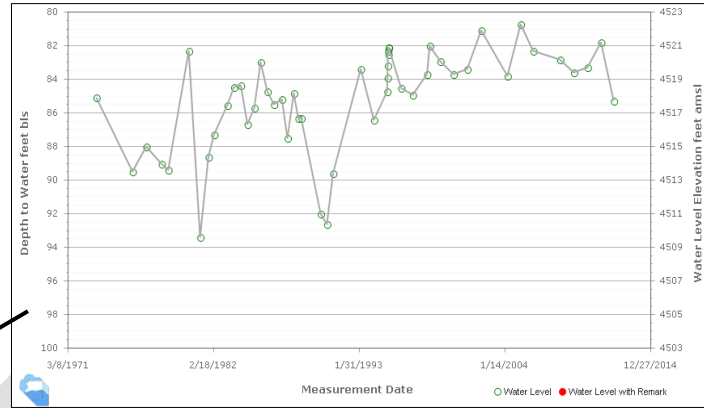
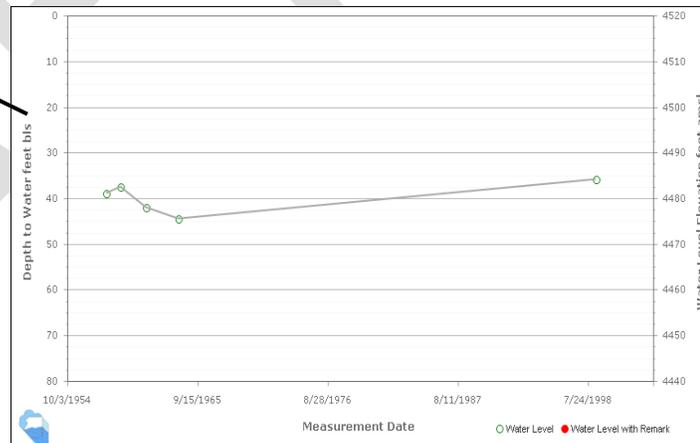


FIGURE F.3c Hydrograph for (A-13-01)cdb showing long-term stable groundwater level trends



In an attempt to better optimize model solutions assuming no underflow from the UAF Sub-basin, ACM 3a, was developed with the assumption of underflow from the UAF sub-basin *while* independently optimizing natural recharge exclusively in the UAF Sub-basin; thus an independent natural recharge variable (par007) was assigned in the non-linear regression. Par007 represents/estimates natural recharge in Lynx Creek, Agua Fria River and Bradshaw Mountain foothills); note that the existing natural recharge variable (par001) includes the other natural recharge components associated with Granite Creek and MFR areas. Result: Phi Φ = 176.5. However, as with all other ACM's tested assuming no underflow from the UAF sub-basin, increased transient model bias and error manifest when compared to models simulating underflow from the UAF sub-basin. (Simulated hydrographs and residual results for this solution are not shown herein.)

OPTIMISATION RESULTS ACM 3a: Assumption: No UAF sub-basin underflow; included independent natural recharge variable (Par007) for UAF sub-basin; in Base model UAF sub-basin was included in total recharge (par001) see Appendix E.

Adjustable parameters ----->

Parameter	Estimated value	95% percent confidence limits	
		lower limit	upper limit
kx_13	2.38991	1.28558	4.44288
kx_14	49.7901	29.1339	85.0917
kx_1	0.491052	0.320173	0.753131
kx_23	240.522	104.332	554.488
kx_25	123.615	32.4789	470.476
kx_26	101.154	35.9484	284.635
kx_2	8.94208	5.70754	14.0097
kx_3	2.76945	1.31144	5.84844
kz_3	1.234615E-03	6.909560E-04	2.206037E-03
kx_9	1.542518E-02	9.840257E-03	2.417987E-02
par012 LIC Underflow	0.559572 1,623 AF/yr	-6.861E-02 (-200)	1.18783 (3,450)
par001 Granite/MFR	0.790439 4,863 AF/yr	0.454511 (2,070)	1.12637 (6,930)
par007 Lynx/AFR	0.930803 3,212 AF/yr	0.507934 (1,460)	1.35367 (4,670)

Note: confidence limits provide only an indication of parameter uncertainty.

They rely on a linearity assumption which may not extend as far in parameter space as the confidence limits themselves - see PEST manual.

Tied parameters ----->

Parameter	Estimated value
ky_13	2.38991
kz_13	0.238991
ky_14	49.7901
kz_14	4.97901
ky_1	0.491052
kz_1	1.234615E-03
ky_23	240.522
kz_23	1.234615E-03
ky_25	123.615
kz_25	1.23615
ky_26	101.154
kz_26	1.011542E-06
ky_2	8.94208
kz_2	3.79458
ky_3	2.76945
ky_9	1.542518E-02
kz_9	1.234615E-03
par009	0.930803
par010	0.790439
par002	0.790439
par003	0.790439
par004	0.790439
par005	0.790439
par006	0.790439
par008	0.790439

See file C:\PRESCOTT\PRESCOTT_MODEL_REPORT_2012\POSTSS10232012.SEN for parameter sensitivities.

Based on the solution of ACM 3a (assumption that the steady state groundwater discharge target rate equals 3.0 cfs and a weight based on the assumption that $\sigma = 1$ cfs.) additional effort was made to redistribute (re-calibrate) natural recharge in order to increase natural recharge in the LIC sub-basin (to increase simulated groundwater discharge representing Del Rio Springs), while simultaneously decreasing natural recharge in the UAF sub-basin (to reduced simulated groundwater discharge representing the Agua Fria River. Some improvement in simulated groundwater discharge resulted at both Del Rio and the Agua Fria River (but did not remove the bias), but came at the “expense” of increasing head residual bias – see Figures, F.4, F.5, and F.6.

FIGURE F.4. Simulated and Observed Groundwater Discharge, Del Rio Springs

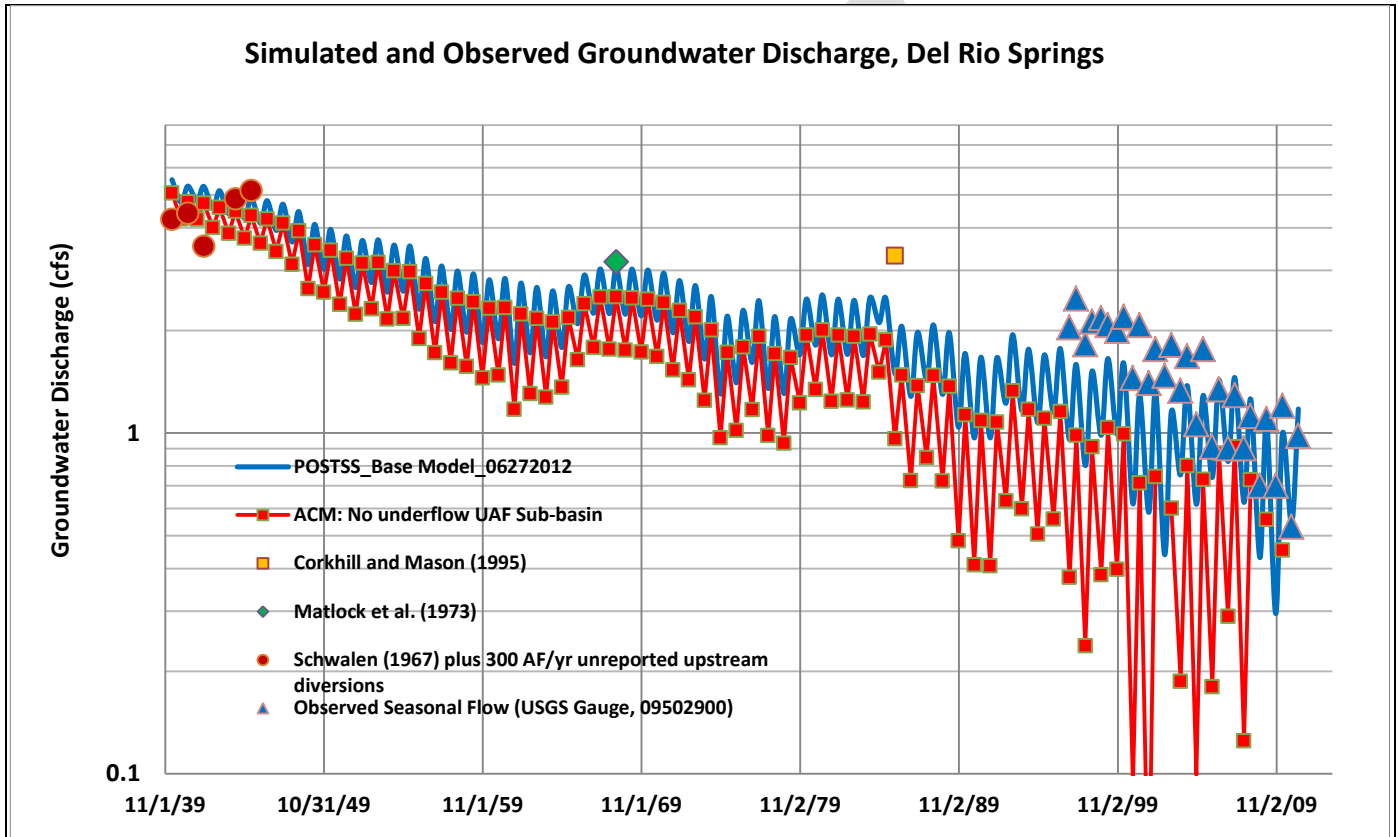


FIGURE F.5. Simulated and Observed Groundwater Discharge, Agua Fria River

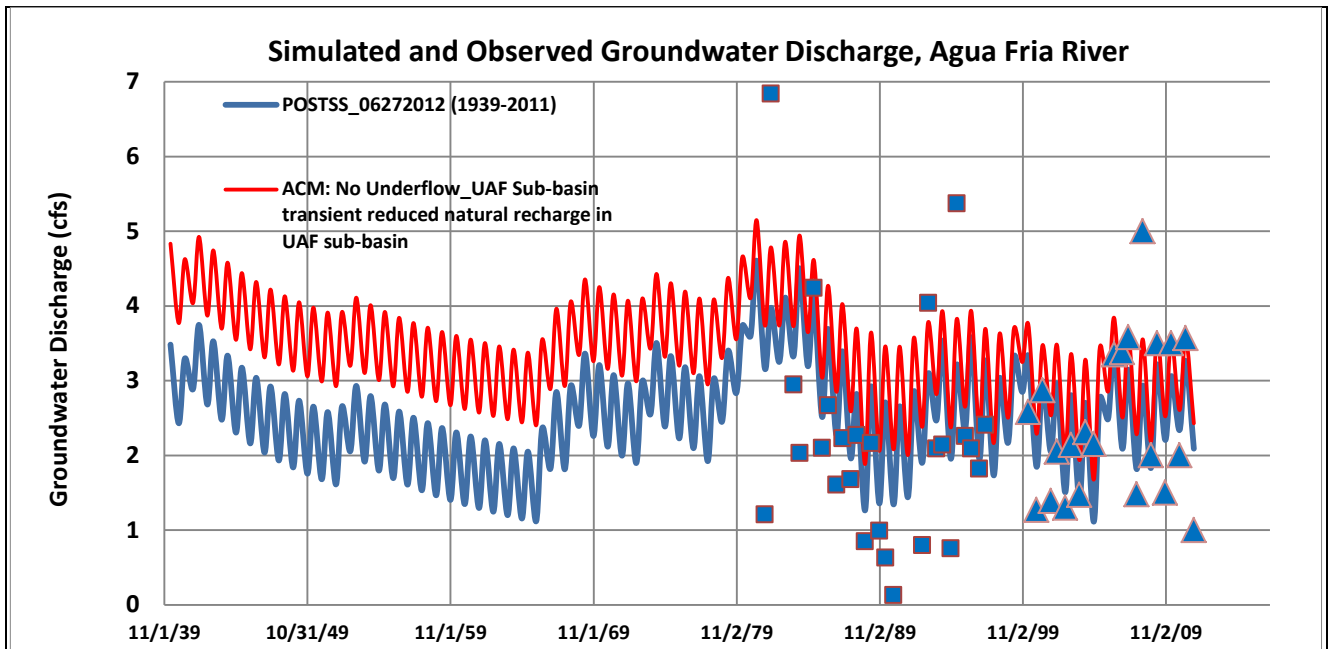
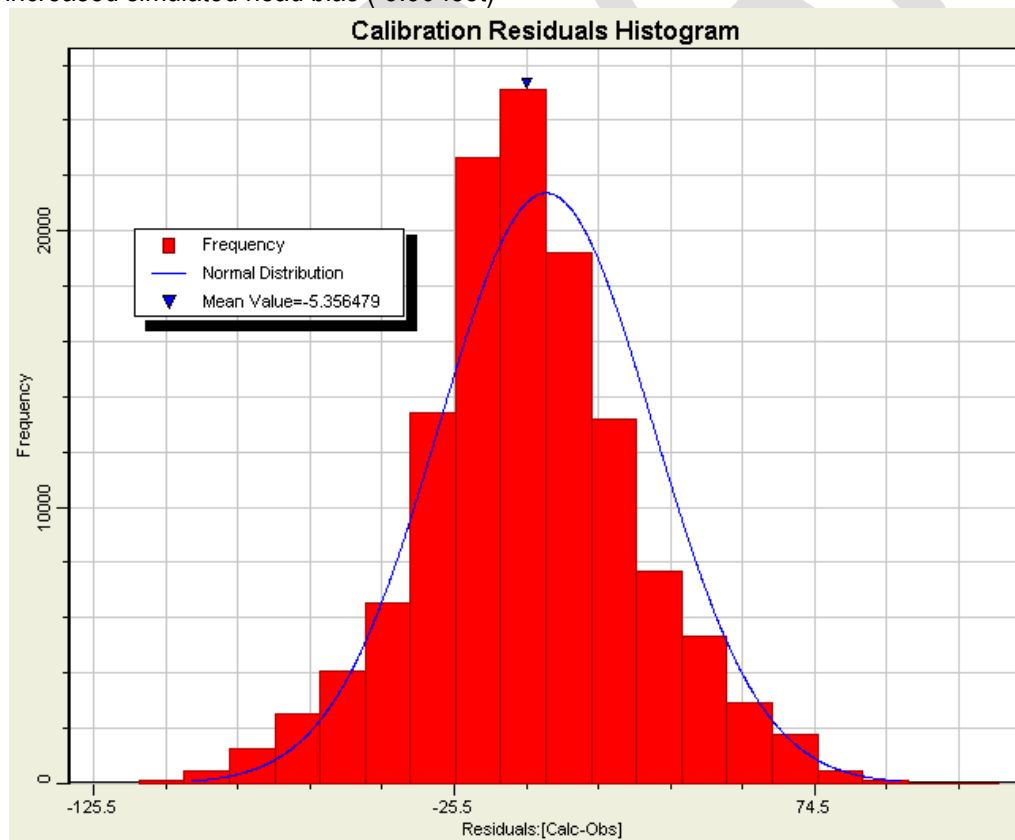


FIGURE F.6. ACM assuming no underflow from UAF sub-basin: Somewhat improved simulated flow resulted in increased simulated head bias (-5.36 feet)



Another ACM was developed and tested to explore the possibility of better simulating low seasonal baseflow along the Agua Fria River (Low AFR Baselow ACM, ACM3b). Assumptions included a mean steady target of 3 cfs ($\sigma=1$ cfs) for the Agua Fria baseflow, and independent parameter for 1) natural recharge for UAF sub-basin (in addition to other natural recharge components), and 2) underflow from the UAF Sub-basin.

OPTIMISATION RESULTS (ACM 3b)

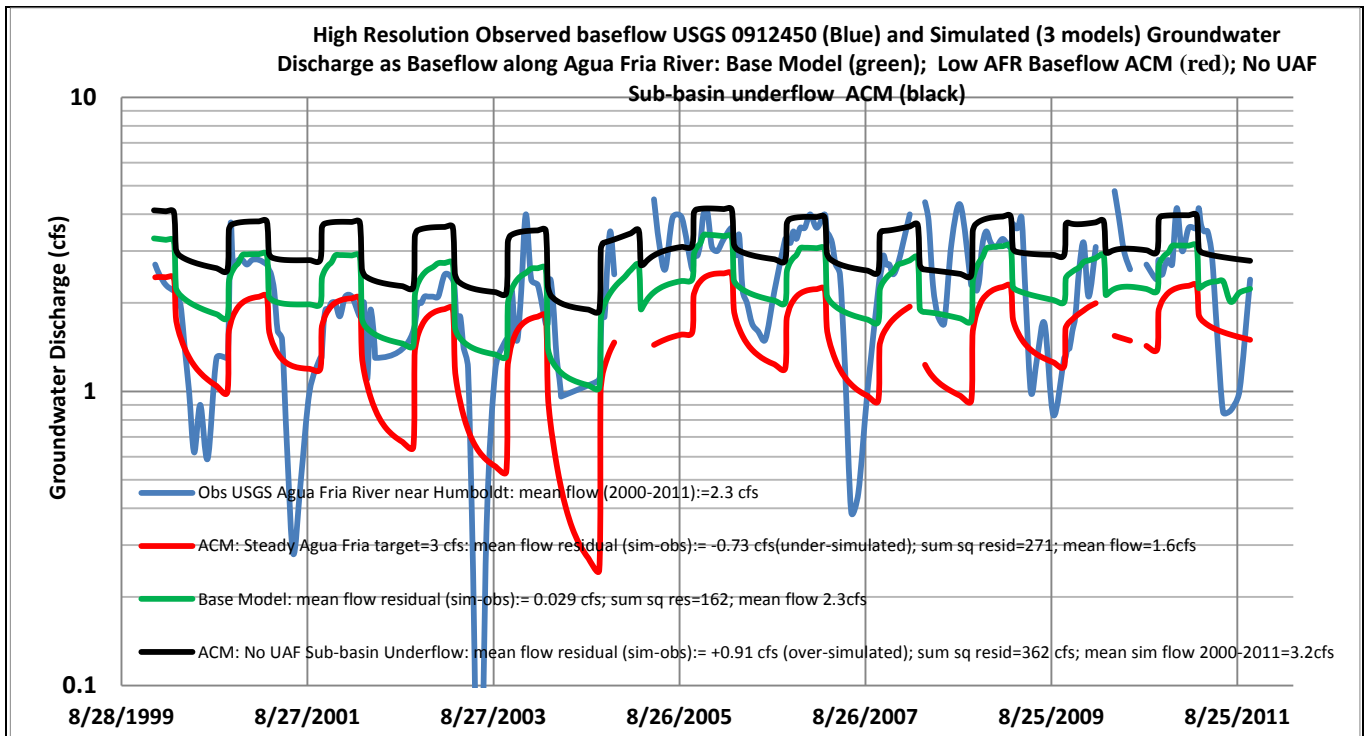
Adjustable parameters ----->

Parameter	Estimated value	95% percent confidence limits	
		lower limit	upper limit
kx_13	2.80936	1.09536	7.20540
kx_14	57.8099	26.1619	127.742
kx_1	0.565705	0.294317	1.08734
kx_23	374.078	75.6749	1849.15
kx_25	126.879	21.4093	751.925
kx_26	106.872	4.98387	2291.73
kx_2	9.82220	5.68232	16.9782
kx_3	2.68378	1.24967	5.76366
kz_3	1.401062E-03	6.507484E-04	3.016486E-03
kx_9	1.761293E-02	9.133583E-03	3.396426E-02
par011 UAF UF	1,705 AF/yr	-1,620	5,030
par012 LIC UF	2,212 AF/yr	-333	4,760
par001 Gran +MFR RCH	5,548 AF/yr	2,116	8,980
par007 UAF RCH	3,788 AF/yr	955	6,621

Note: confidence limits provide only an indication of parameter uncertainty.

Although ACM 3b was able to simulate more accurate low flow summer, seasonal rates than any other ACM tested thus far, it also yielded an overall under-simulated baseflow bias, with respect to observed baseflow at USGS 09512450. In contrast, the No UAF Sub-basin Underflow ACM resulted in a clear over-simulated baseflow bias, while the base model provide the smallest overall groundwater discharge bias along the Agua Fria River. These differences are most sensitive - and best compared - when evaluating high-resolution groundwater discharge observations recorded at the USGS 09512450 gauge, located near Humboldt for the entire record (2000-2011), at model time-step intervals/sample rates. [The residual sample number is 215 counts. Note that this high sample rate was not employed in the transient non-linear regression.] See Figure F.7 below for observed flow (blue), Low AFR Baselow ACM in red (mean residual undersimulation error -0.73 cfs), the No UAF Sub-basin Underflow ACM in black (mean residual oversimulation error +0.91 cfs) and the Base model in green (mean residual error 0.029 cfs).

FIGURE F.7. High Resolution Observed Baseflow



Careful evaluation of numerous ACM's suggest that an underflow component from the UAF Sub-basin is more likely than not, based on constraining the provisional Prescott model to *available head and flow data*. However, there may be other untested ACM's with different K and recharge distributions that yield less model error and bias, when no UAF sub-basin underflow is assumed. In addition there may be data - not currently available - that, in the future, may provide a better understanding and quantification of underflow (or lack-there-of) from the UAF Sub-basin.

APPENDIX G:

Provisional Simulated Water Budget Information for “Base” Model

DRAFT

APPENDIX G

PROVISIONAL SIMULATED WATER BUDGET INFORMATION FOR “BASE” MODEL

To compare the relative magnitude and significance of natural recharge estimates with other simulated groundwater (saturated zone) flow components, simulated water budgets for a few selected periods are presented for the “Base” model. The selected water budget components include: 1) the total 72-year simulation period (1939-2011), Table G.1.; 2) a “dry” 24-year period (1941-1965), Table G.2.; 3) a “wet” 30-year period (1965-1995), Table G.3.; and 4) the most recent 16-year period (1995-2011), Table G.4.

Note that the water budget components provided below - including natural recharge - are provisional and subject to revision. Further, some budget components were rounded, and terms are currently being evaluated with input source terms for consistency and accuracy. In addition, the MODFLOW solver resulted in solutions having small mass-balance errors: accordingly, the inflows \approx outflows.

Also note that other plausible ACM’s having different estimated natural recharge rates result in solutions that yield “adjusted” transient water budget components along head-dependent boundaries; thus the storage terms are also affected: For example ACM’s associated with higher rates of natural recharge will result in modified (higher) natural outflow rates, while ACM’s associated with lower rates of natural recharge will typically result in lower natural outflow rates.

TABLE G.1. Simulated Water Budget, 1939-2011

Simulated Water Budget - Long-term (1939-2011): Annualized Rates in AF/yr for 1939-2011 period (72 years) Long-term (1939-2011) Natural Recharge Rate= 10,000 AF/yr		
Simulated Inflow Component	IN AF/yr	IN AF/yr
Storage		19070
Agricultural-related Recharge	7760	12700
Artificial Recharge	1210	
Natural Recharge (recharge cells)	3700	
Natural Recharge* (stream cells ¹)		6300
Total Inflow		38070
Simulated Outflow Component		Out AF/yr
Storage		13010
Pumping		17700
Evapotranspiration* (saturated zone)		800
Underflow LIC* Sub-basin		1730
Underflow UAF Sub-basin		1140
Groundwater Discharge* ² at Del Rio Springs and Baseflow, Agua Fria River		3630
Total Outflow		38010
Net Change-in-Storage: Long-term (1939-2011) Annualized rate of Water Lost from Storage		6,060
*Head-dependent boundaries.**Specified flux - uniform long-term underflow rates. ¹ This predominately losing reach has a small rate of groundwater discharge out contained in the streamflow out term ² . ² This predominately gaining reach has a small rate of stream inflow contained within the Natural Recharge (stream cells) ² .		

TABLE G.2. Simulated Water Budget, 1941-1965

Simulated Water Budget: Dry Period: 1941-1965; Annualized Rates for 1941-1965 (24-year period) Annualized Natural Recharge Rate (1941-1965) = 4,030 AF/yr – “Dry” period		
Simulated Inflow Component	IN AF/yr	IN AF/yr
Storage		18350
Agricultural-related Recharge	9640	12650
Artificial Recharge	0	
Natural Recharge (recharge cells)	3010	
Natural Recharge* (stream cells ¹)		1020
Total Inflow		32020
Simulated Outflow Component		Out AF/yr
Storage		8600
Pumping		15300
Evapotranspiration* (saturated zone)		800
Underflow LIC* Sub-basin		1940
Underflow UAF** Sub-basin		1140
Groundwater Discharge* ² at Del Rio Springs and Baseflow, Agua Fria River		4170
Total Outflow		31950
Net Change-in-Storage: Annualized (1941-1965) Rate of Water Lost from Storage		9,750
*Head-dependent boundaries. **Specified flux – uniform long-term underflow rates. ¹ This predominately losing reach has a small rate of groundwater discharge out contained in the streamflow out term. ² This predominately gaining reach has a small rate of stream inflow contained within the Natural Recharge (stream cells) ² .		

TABLE G.3. Simulated Water Budget, 1965-1995

Simulated Water Budget: Wet Period: 1965-1995; Annualized Rates for 1965-1995 (30 year period) Annualized Natural recharge Rate (1965-1995) = 14,940 AF/yr – “Wet” period		
Inflow Component	IN AF/yr	IN AF/yr
Storage		19400
Agricultural-related Recharge	9320	14410
Artificial Recharge	550	
Natural Recharge (recharge cells)	4540	
Natural Recharge* (stream cells ¹)		10400
Total Inflow		44210
Outflow Component		Out AF/yr
Storage		18850
Pumping		18400
Evapotranspiration* (saturated zone)		800
Underflow LIC* Sub-basin		1650
Underflow UAF** Sub-basin		1130
Groundwater Discharge* ² at Del Rio Springs and Baseflow, Agua Fria River		3700
Total Outflow		44530
Net Change-in-Storage: Annualized (1965-1995) Rate of Water Lost from Storage		550
*Head-dependent boundaries. **Specified flux – uniform long-term underflow rates. ¹ This predominately losing reach has a small rate of groundwater discharge out contained in the streamflow out term. ² This predominately gaining reach has a small rate of stream inflow contained within the Natural Recharge (stream cells) ² .		

TABLE G.4. Simulated Water Budget, 1995-2011

Simulated Water Budget: 1995-2011 (Annualized Rates for 1995-2011)		
Annualized Natural recharge Rate (1995-2011) = 9,380 AF/yr		
Inflow Component	AF/yr	In Af/yr
Storage		20550
Agricultural-related Recharge	2860	
Artificial Recharge	3900	10260
Natural Recharge (recharge cells)	3500	
Natural Recharge* (stream cells ¹)		5880
Total Inflow		36,690
Outflow Component		Out Af/yr
Storage		8970
Pumping		21650
Evapotranspiration* (saturated zone)		800
Underflow LIC* Sub-basin		1530
Underflow UAF** Sub-basin		1130
Groundwater Discharge* ² at Del Rio Springs and Baseflow, Agua Fria River		2520
Total Outflow		36,600
Net Change-in-Storage: Annualized (1995-2011) Rate of Water Lost from Storage		11,580
<p>*Head-dependent boundaries. **Specified flux – uniform long-term underflow rates. ¹This predominately losing reach has a small rate of groundwater discharge out contained in the streamflow out term. ²This predominately gaining reach has a small rate of stream inflow contained within the Natural Recharge (stream cells)².</p>		